Technical Report

TR-14-28

Flow and pressure response in compacted bentonite due to external fluid pressure

Martin Birgersson, Ola Karnland
Clay Technology AB

September 2015

Svensk Kärnbränslehantering AB
Swedish Nuclear Fuel
and Waste Management Co

Box 250, SE-101 24 Stockholm
Phone +46 8 459 84 00

ISSN 1404-0344
SKB TR-14-28
ID 1464598
September 2015

Flow and pressure response in compacted bentonite due to external fluid pressure

Martin Birgersson, Ola Karnland
Clay Technology AB

Abstract

A large set of pressure and flow response tests in bentonite are reported. The main objective of the study was to gain insight into the process of gas migration in bentonite components. However, because gas pressurization of water saturated bentonite requires consideration of water pressurization, also the latter process was focused upon.

The tests were performed on cylindrical samples of diameter 35 mm and height in the range 2–20 mm, and are divided into three main categories, depending on the externally imposed conditions.

- Externally applied water pressure difference.
- Externally applied air pressure difference.
- Uniformly applied water pressure.

Two main types of injection filter geometries were employed: either the external pressure was applied in a small point-like central filter (type B), or pressurization was performed in a filter covering the full bottom area (type A). The materials tested were mainly MX-80 bentonite, and montmorillonite obtained from purification of MX-80 bentonite.

In the tests, evolution of the pressure exerted by the bentonite was recorded. In tests that involved external pressure difference, also fluid flow evolution was measured. In a few cases, the density response due to applied water pressure differences was measured.

The main results are as follows:

- Externally applied water pressure differences:
  - Sample pressure depends non-linearly on applied water pressure. The type of sample pressure response is also strongly dependent on type of injection filter geometry.
  - For injection filters of type A, the water flow response is linear in the limit of small external water pressure (Darcy's law). Generally, however, the flow response is non-linear, and depends strongly on injection geometry.
  - Water breakthrough events can be induced. In these, he flow completely changes characteristics as compared to "normal" flow; in particular the flow rates increase tremendously (a factor 10^4 or more). The phenomena is very much reminiscent of piping. The necessary (but not sufficient) criteria for inducing water breakthrough events is that injection pressure exceeds sample pressure. The flow path during water breakthrough is preferably at the interface between sample holder and clay body.
  - Density redistribution in samples exposed to water pressure differences.
  - Observations of hysteresis in sample pressure.
- Externally applied air pressure differences:
  - For applied gas pressures below the (initial) sample pressure, there is no response in the latter quantity. This result is independent of injection geometry.
  - For applied gas pressure below sample pressure, the only transport mechanism is diffusion of dissolved gas.
  - For applied gas pressure above (initial) sample pressure, gas breakthrough events can be induced. In these events, the flow changes characteristic drastically – in particular it increases tremendously. A gas breakthrough is analogous to the breakthrough observed in water pressurization. In particular, the flow of gas in a gas breakthrough event preferably occurs at the interface between sample holder and clay body.
  - Rather than inducing a gas breakthrough event when injection pressure exceeds sample pressure, various types of consolidation of the clay body by the gas phase have been demonstrated. In these situations, the increased pressure induces water transport out of the test cell with the result that the volume of the clay body is smaller than the volume of the test cell. The remaining volume is consequently occupied by the gas phase. However, no breakthrough events are induced and gas is only transported through the sample in dissolved form (diffusion).

- In a special test, the pressurizing fluid was kerosene rather than water or air. The response from kerosene pressurization is basically identical to that of air, implying that all types of non-polar fluids have basically the same type of interaction with water saturated bentonite. This interaction is furthermore fundamentally different from the interaction between water and bentonite, demonstrating that gas migration in water saturated bentonite is not a two-phase flow phenomena.
- Uniformly applied water pressure:
  - Hysteresis effects in resulting sample pressure after exposing the sample to pressurization pulses. The trend is that the sample pressure increases after being exposed to water pressurization and the effects seem to be larger in samples of MX-80 bentonite as compared to pure montmorillonite.
  - The response in sample pressure when a uniform external water pressure is applied is always less than the applied pressure. Typically the response is about a factor 0.9 of the applied pressure.

Sammanfattning

I denna rapport redovisas en stor mängd utförda laboratorieförsök rörande tryck- och flödesrespons i bentonit. Huvudsyftet med studien var att ge ökad förståelse för gasmigrationsprocesser i bentonitkomponenter, men fokus låg också på effekter av vattentrycksättning, eftersom sådana effekter alltid måste beaktas när vattenmättad bentonit trycksätts med gas.

Testerna utfördes på cylindriska prover med diameter 35 mm och höjd i intervallet 2–20 mm, och delas in i tre huvudkategorier, beroende på randvillkor:

- Externt pålagd vattentryckskillnad.
- Externt pålagd lufttryckssskillnad.
- Uniformt pålagt vattentryck.

Två huvudtyper av injektionsfilter användes: antingen applicerades trycket i ett punkt-likt, centralt placerat filter (typ B), eller så applicerades trycket i ett filter som täcker hela bottenytan (typ A). De testade materialen var främst MX-80 bentonit och montmorillonit utvunnet ur MX-80 bentonit.

Under testerna mättes bentonitproves tryckutveckling. I de tester som innefattade externt pålagda tryckskillnader mättes även fluidflödet (luft eller vatten) som funktion av tiden. I ett fåtal tester mättes även responsen i densitet som följd av pålagd vattentrycksskillnad.

Studiens huvudresultat är

- Externt pålagd vattentryckskillnad.
  - Bentonitprovens tryck beror icke-linjärt på pålagt vattentryck. Vidare är den resulterande responsen starkt beroende på typ av injektionsgeometri.
  - För injektionsfilter av typ A beror flödet linjärt på pålagt vattentryck i gränsen när de pålagda trycken är låga (Darcys lag). Generellt beror emellertid även flödesresponsen icke-linjärt på pålagt vattentryck, och beror starkt på typ av injektionsgeometri.
  - Vattengenombrott kan induceras. Under sådana genombrott beter sig flödet helt annorlunda än under ”normalt” flöde. Specifikt ökar flödeshastigheten enormt (en faktor 10^4 eller mer). Fenomenet påminner mycket om s.k. piping. Ett nödvändigt (men inte tillräckligt) kriterium för att inducera vattengenombrott är att injektionstrycket överstiger trycket i bentoniten. Flödesvägen under vattengenombrott sker företrädesvis vid gränsytan mellan provhållaren och själva lerprovet.
  - Densitetsomfördelning i bentonitprover som utsätts för vattentryckskillnader.
  - Observationer av hysteres i bentonitens tryck.
- Externt pålagd lufttryckssskillnad.
  - För pålagda gastryck lägre än trycket i bentonitprovet, visar bentonittrycket ingen respons alls. Detta resultat är oberoende av injektionsgeometri.
  - För pålagda gastryck lägre än trycket i bentonitprovet är den enda transportmekanismen diffusion av löst gas.
  - För pålagda tryck högre än (det initiala) trycket i bentoniten kan gasgenombrott induceras. Under gasgenombrott ändrar flödet drastiskt sin karaktär – specifikt så ökar flödet enormt. Ett gasgenombrott är analogt med de genombrott som observerats under vattentrycksättning. I synnerhet sker gasflödet under ett gasgenombrott företrädesvis vid gränsytan mellan provhållaren och själva lerprovet.
  - I stället för att inducera ett gasgenombrott när injektionstrycket överstiger provtrycket, kan olika typer av konsolidering av lerprovet ske. I dessa situationer inducerar det ökade trycket vattentransport ut ur testcellen med resultatet att volymen av leran är mindre än testcellens volym. Den återstående volymen upptas följaktligen av gasfasen. Dock sker inga gasgenombrott i detta tillstånd och gas transporteras genom provet endast i löst form (diffusion).

- I ett speciellt test användes fotogen som trycksättande fluid istället för vatten eller luft. Responsen från trycksättning med fotogen är i princip identisk med den som fås genom trycksättning med luft. Denna observation implicerar att alla typer av icke-polära fluider har liknande interaktion med bentonit. Denna interaktion är dessutom fundamentalt annorlunda från hur vatten och bentonit interagerar, vilket visar att gasmigration i bentonit inte är ett så kallat tvåfasflöde.
- Uniformt pålagt vattentryck.
  - Trycket i bentoniten uppvisar hystereseffekter efter att bentonitproven utsätts för vattentrycks-pulser. Trenden är att bentonittrycket ökar efter att provet blivit utsatt för tryckpulser och effekten verkar vara större i MX-80-prov jämfört med rena montmorillonitprov.
  - Responsen i bentonitens tryck när ett uniformt vattentryck appliceras är alltid lägre än det pålagda trycket. Responsen är typiskt en faktor 0,9 av pålagt tryck.

Contents

1 Introduction

The following report presents pressure and flow response tests made on compacted bentonite (natural and purified) exposed to various external pressure conditions. The investigation was primarily performed in order to gain insight of the process of gas migration in engineered bentonite barriers, which are adopted in many concepts for storage of radioactive waste, including KBS3 (SKB 2011). For such barriers to function properly, they are required to be confined volumetrically while still having access to an external water source. Under such conditions a "swelling pressure" develops, giving the barrier efficient sealing properties.

The relevant boundary condition for studying gas migration in bentonite barriers is thus a system open for both water and gas. This requirement, in turn, have the consequence that response due to gas and water pressure gradients actually are not fully separable. The focus of the present study has therefore been extended to include response both due to water and air pressure gradients.

In addition to giving direct insight of the gas migration process, these tests also gives useful general information on bentonite material properties. The results of are therefore also of value for e.g. validating material models for bentonite.

The work has been performed on the request of the Swedish nuclear fuel and waste management company (SKB) and has received funding from the European Atomic Energy Community's Seventh Framework Programme (FP7/2007-2011) under Grant Agreement no230357, the FORGE project.

1.1 Objective

The objective of the present report is first and foremost to document the vast set of experimental observations made on flow and pressure response in bentonite. These observations naturally forms a foundation for further analysis of active physicochemical processes in the bentonite. However, such an analysis is beyond the scope of the present report.

1.2 Test principles

Bentonite powder was compacted in cylindrical constant-volume steel cells with an inner diameter 35 mm and sample height, h, was varied in the range 2–20 mm. The test cell, schematically pictured in Figure 1-1, permits water to be contacted with the clay via steel filters both in top and bottom. The top part of the cell consists of a piston which allows for measuring the pressure exerted by the clay via a force transducer; the pressure, or actually the average axial stress, is given by dividing by the sample area. The present set-up gives a pressure measurement accuracy of about 0.01 MPa. Water saturation of the samples was simply achieved via the filters by contacting the system with water.

In most of the tests, an external pressure difference was established across the sample by applying a prescribed pressure of a given fluid (air, water, or kerosene) in the bottom channel of the test cell (the injection pressure). The pressure was controlled by a pressure- and volume controlling units from GDS Instruments (in the following referred to as a pressure controlling unit). This unit can both allow for keeping a constant pressure or ramping the pressure (up or down) at a prescribed rate. Figure 1-2 shows a test cell connected to a pressure controlling unit.

To be able to define a swelling pressure it is important to allow the clay to have contact with external water at all times. The top channel (and the circumference channel, in case of filter type C, see below) of the test cells was therefore always kept water filled, regardless of type of pressurizing fluid. Furthermore, in tests where external pressure differences were maintained, the top channel was always kept at approximately atmospheric pressure (here assumed to be 0.1 MPa absolute pressure).

A second type of test was also performed where samples were exposed to uniform external water pressure by pressurizing both the top and bottom channels. In this case no gradients, and consequently no fluxes, were induced.

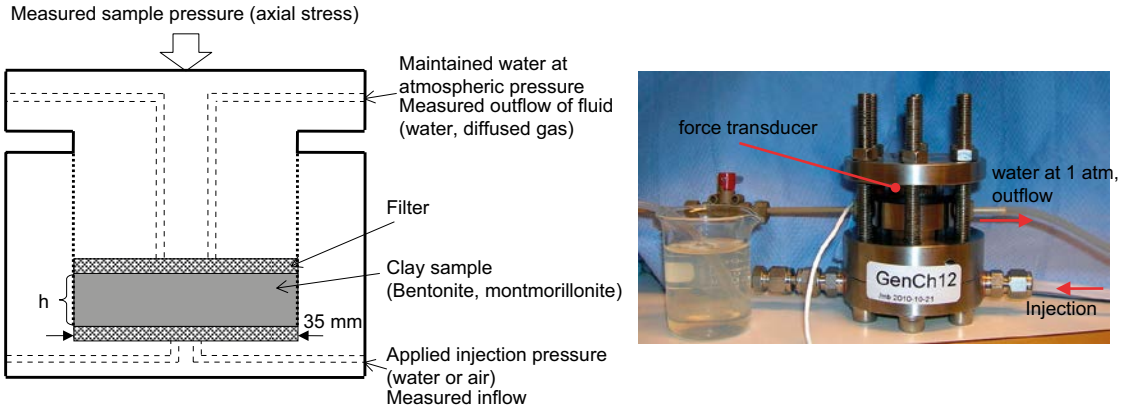

Figure 1-1. *Test cell schematics.*

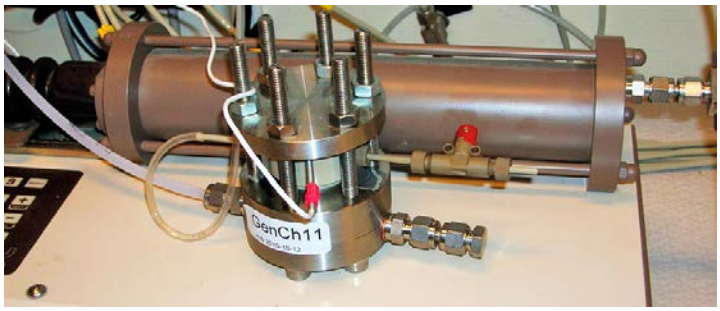

Figure 1-2. *A test cell connected to a pressure controlling unit (white tube in the bottom).*

The main measurements in all tests consisted of sampling pressure evolution of the clay sample. In tests with imposed external pressure gradients, also fluid flow in and out of the system was measured. The volumetric inflow was measured by the pressure controlling unit while outflow was measured manually by connecting a thin tube to the outlet (seen in Figure 1-1 and Figure 1-2) and measuring the water volume in this at different times. The average volumetric flow (q) between two consecutive measurements (at times t_1 and t_2) is given by

$$q = \frac{V(t_2) - V(t_1)}{A \cdot (t_2 - t_1)} \qquad (1\text{-}1)$$

where V(t) denotes reservoir volume at time t and A is the cross section of the sample.

A basic variable which was varied in the performed tests was the geometry of the injection filter. The different bottom plates used are shown in Figure 1-3. Specifically two types of injection filters was considered: one which covered the entire bottom area of the sample (diameter 35 mm) and one which only covered a small part (diameter 5 mm). The first type of geometry allows for a one dimensional flow and is what is conventionally used when e.g. measuring hydraulic conductivity in bentonite. The second type of injection mimics injection in a point.

As it is of interest to identify flow paths in the clay, a third type of geometry also was considered which combines the small central bottom filter with a second circumferential filter. The circumferential filter – in the following referred to as a guard filter – was used as a second outflow channel, isolated from the top channel. Thus, any flow paths *through* the clay could be identified as those flowing out through the top filters, while fluid flowing at the interface between clay and sample holder inevitably "gets caught" at the guard filter.

Throughout this report, basically all pressures and pressure differences are reported as relative to atmospheric pressure (0.1 MPa absolute pressure). When absolute pressures are referred to, this is explicitly stated.

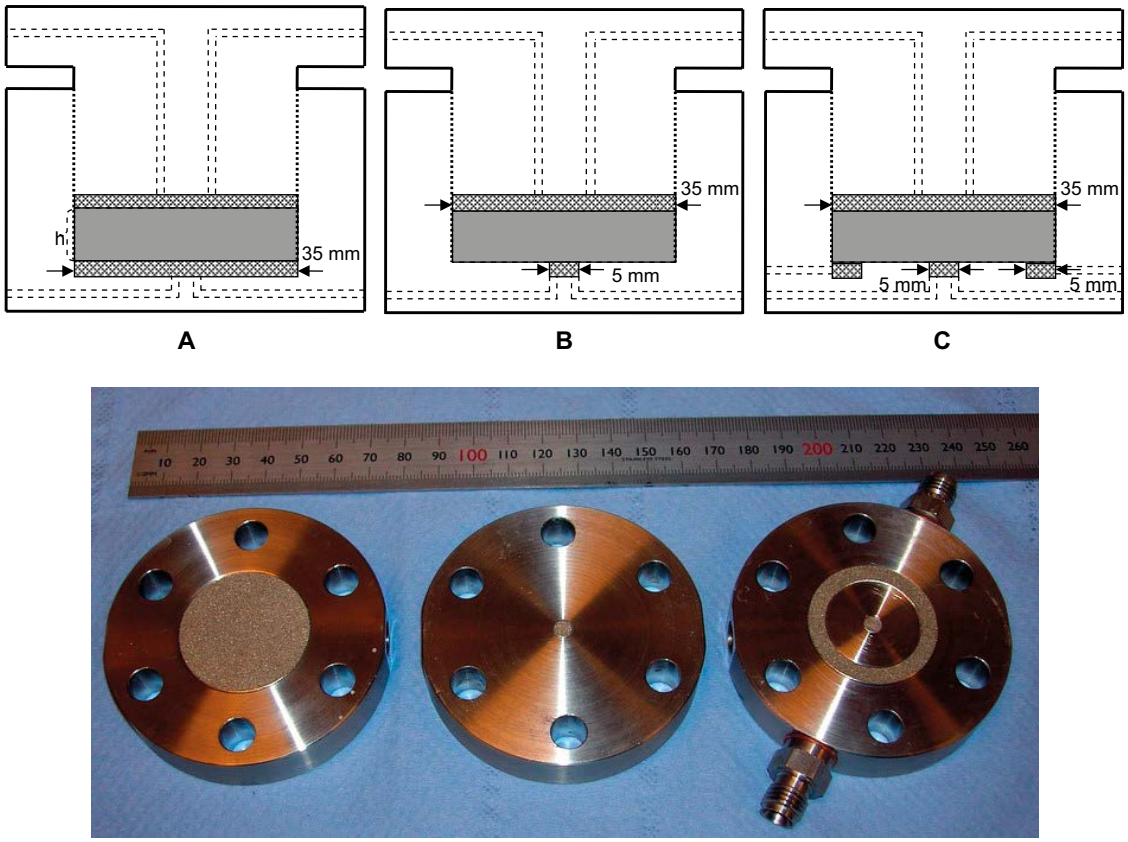

Figure 1-3. *The types of fluid injection geometry adopted. A) Filter in full bottom area B) Small injection filter C) Small injection filter + circumferential outflow filter. The circumferential outflow channel is isolated from the top outflow channel.*

1.3 Sample materials

The main materials used in this study are the commercial bentonite MX-80 from Wyoming, U.S., and homo-ionic sodium and calcium montmorillonite. The latter materials are obtained from the former by purification (sedimentation), washing in salt solutions (NaCl, $CaCl_2$), and dialysis. A detailed description of production methods is found in Karnland et al. (2006), which also contains chemical and mineralogical descriptions of the used materials. Apart from the materials derived from MX-80 bentonite, a few tests were also made on homo-ionic calcium montmorillonite obtained from bentonite from Kutch, India (Ashapura). The materials used are summarized in Table 1-1.

Table 1-1. Test sample materials.

Name	Type	Origin	Exchangeable ions	
			Na	Ca
MX-80	Commercial bentonite	Wyoming, U.S.	70–80%	20–30%
WyNa	Na-montmorillonite	Wyoming, U.S.	100%	0%
WyCa	Ca-montmorillonite	Wyoming, U.S.	0%	100%
KuCa	Ca-montmorillonite	Kutch, India	0%	100%

The distinctive feature of compacted, confined bentonite is that it exerts a swelling pressure when in contact with external water. This pressure is dependent on several quantities, e.g. the type of exchangeable cation, clay density, temperature, and the chemical composition and pressure of the external solution. In the following the label P_s^0 is used to refer to the swelling pressure of a water saturated clay with given set of exchangeable cations and given density, contacted at room

temperature with non-pressurized de-ionized water (i.e. water at 0.1 MPa absolute pressure). For a specific clay (including a specific set of exchangeable cations), P_s^0 is a rather distinct function of density. However, also for a well-defined clay system P_s^0 typically displays hysteresis effects, i.e. its value depends somewhat on the pressurization and hydration history of the sample (such effects have been explored in the tests here reported). Figure 1-4 shows P_s^0 as a function of density in some of the tests performed in this study, as well as values reported in Karnland et al. (2006).

The present study has focused on systems with a value of P_s^0 of approximately 2 MPa or lower. In this pressure regime, there is a substantial difference in density dependence between Na- and Ca-montmorillonite (Figure 1-4). Also, the density dependence of MX-80 bentonite shows more resemblance to Ca-montmorillonite in this pressure range. It should thus be kept in mind that the Na-montmorillonite samples treated in this work generally have lower density than the MX-80 and Ca-montmorillonite samples.

Another aspect to keep in mind is that MX-80 bentonite is produced from mixing naturally occurring soil and contains a certain amount of readily solvable minerals (e.g. gypsum). Hence, although de-ionized water is used as external water source in basically all tests (an exception is presented in Section 3.2.2.1), diffusion of ions into this water will occur, thereby influencing its chemical composition. This effect could have some influence on the resulting sample pressure. Furthermore, MX-80 bentonite contains about 20% of non-swelling material and therefore a density comparison with purified clays should be done with some caution.

The use of de-ionized water as pressurizing fluid imposes a problem for the pure Na-montmorillonite systems; pure Na-montmorillonite at low enough ionic strength appear as a liquid sol rather than a solid gel (Birgersson et al. 2009) which means that colloidal particles (separate montmorillonite layers) may be released and carried away with the flushing water. Consequently, a certain degree of mass loss is experienced in these samples during the course of the tests.

The complete set of tested samples are listed in Table 1-2. After finishing testing a sample, the test cell was dismantled and the water-to-solid mass ratio, *w*, of the clay was determined by weighing before and after drying in oven (> 24 h in 105°C). From *w*, the density and porosity is given by (assuming water saturation)

$$\rho_{dry} = \frac{\rho_s}{w\frac{\rho_s}{\rho_w} + 1} \tag{1-2}$$

$$\phi = \frac{w\rho_s}{w\rho_s + \rho_w} \tag{1-3}$$

where ρ_s and ρ_w are grain density and water density, respectively. In the following the value ρ_s = 2,750 kg/m^3 have been adopted for all samples derived from MX-80 bentonite (MX-80, WyNa, WyCa), while ρ_s = 2,900 kg/m^3 have been used for KuCa (Karnland et al. 2006) For all samples, water density ρ_w = 1,000 kg/m^3 have been used.

The remainder of this report is organized as follows:

- All tests with an imposed external water pressure difference are presented in Chapter 2.
- In Chapter 3 are presented all tests where instead an external air pressure difference was imposed.
- Tests with uniform water pressurization (i.e. no external pressure difference) are presented in Chapter 4.
- A test with an imposed external kerosene pressure difference is presented in Chapter 5.
- Chapter 6 summarizes the most significant observations made in the various types of tests.

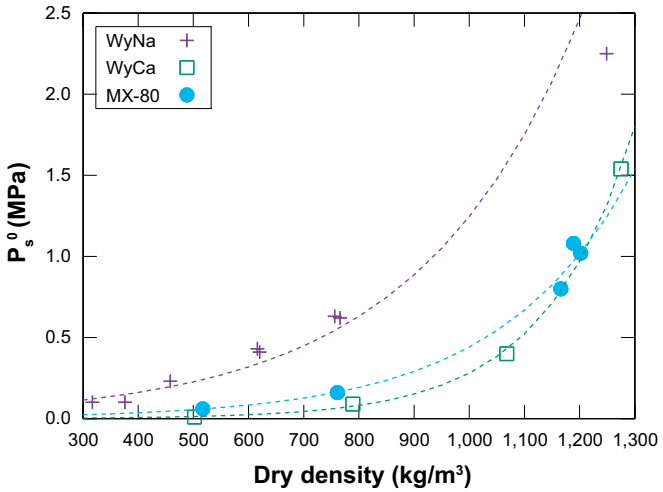

Figure 1-4. *Sample pressure when equilibirated with external non-pressurized pure water (P_s^0) in some of the tests performed in this study. Included are also values from Karnland et al. (2006) (WyNa at densities 458 kg/m³, 766 kg/m³, and 1,249 kg/m³; WyCa at 502 kg/m³, 789 kg/m³, and 1,275 kg/m³; MX-80 at densities 517 kg/m³ and 761kg/m³). The dashed lines corresponds to exponential expressions fitted to the experimental data.*

Table 1-2. All samples on which tests were performed.

	Sample-Id	Material	Nominal dry density (kg/m³)	Dry density (post-analysis) (kg/m³)	Injection filter*	Max. injection pressure (MPa)	Height (mm)
1.	GenCh01	KuCa	1,200	1,130	B (small)**	1.6	5
2.	GenCh02	WyNa	220	126	A (large)	0.25	5
3.	GenCh03	WyNa	440	317	A (large)	2.0	5
4.	GenCh04	WyNa	440	376	B (small)	1.0	5
5.	GenCh05	WyCa	440	–	A (large)	–	5
6.	GenCh06	MX-80	1,166	–	A (large)	5.0	20
7.	GenCh11	MX-80	1,179	1,097	B (small)	3.0	5
8.	GenCh12	WyNa	700	616	A (large)	2.0	5
9.	GenCh13	WyNa	700	620	C (small+guard)	2.0	5
10.	PrefPath01	WyNa	700	–	C (small+guard)	0.5	2
11.	PrefPath02	MX-80	1,179	1,189	C (small+guard)	5.0	2
12.	GenCh21	MX-80	1,166	–	A (large)	5.0	20
13.	GenCh22	WyCa	1,200	1,137	A (large)	5.0	5
14.	GenCh23	WyCa	1,250****)		A (large)	5.0	5–8****
15.	WP3Bench	MX-80	1,179	1,075	A (large)	5.0	5
16.	WyNa(Ca)14***	WyNa	–	756	A (large)	4.5	5
17.	KuCa02***	KuCa	1,095	1,068	A (large)	3.0	5

*) See Figure 1-3.
**) This sample was a prototype for injection type B.
***) These samples were not specifically prepared for the present study. More information is given under the specific sections below.
****) Successively volume expanded, see Section 2.1.3.3.

2 External water pressure difference

This chapter describes all tests made with an imposed external water pressure difference. Each test consists of certain sequences of applied injection pressures (the outlet is kept at atmospheric pressure at all times).

The procedure of maintaining a water pressure difference across a sample resembles a type of hydraulic conductivity measurement. Conventional hydraulic conductivity measurements, however, usually focus on one-dimensional flow and low external water pressures (low in comparison to P_s^0). The present tests, on the contrary, focus on different types of injection geometries and a huge range of injection pressures (up to several times P_s^0) and could therefore be viewed as a type of generalized hydraulic conductivity tests. Moreover, in the present tests special focus was made on response in sample *pressure* as well as on steady-state water flow.

Below follows descriptions of the pressurization history for each specific sample. As the qualitative response characteristics first and foremost are dependent on the type of injection filter, the test descriptions are organized firstly according to injection filter geometry and then according to type of material.

2.1 Injection filter A

2.1.1 Na-montmorillonite

2.1.1.1 Sample GenCh02

This sample represents a very loose system, at the limit of what the test equipment is capable of handling. Its full injection and sample pressure history is displayed in Figure 2-2. Initially the sample exerted a pressure (P_s^0) of about 0.04 MPa. In Figure 2-2 is seen a steady drop in sample pressure with time, which is a consequence of significant erosion in this sample. Due to its low density, the hydraulic conductivity is high relatively, and so are the induced water flows. As the external water is ion free, the Na-montmorillonite of the sample form a sol (a liquid colloidal state) and is being washed away with the flushing water. As P_s^0 lowers with density (Figure 1-4), the erosion explains the observed continuous pressure drop. Judging from the difference between the nominal density and the density determined after the test, approximately half of the sample mass was eroded. The sample pressure is also seen to be negligible at the end of the test (actually, small negative values are recorded, which obviously is a measurement error – the precision of the equipment is in the order of 0.01 MPa). Due to the erosion induced pressure drop, no equilibrium sample pressure vs. injection pressure graph could be constructed for this sample.

Table 2-1. Properties of sample GenCh02.

Material	Nominal density	Post-analysis	Cell type	h
WyNa	ρ_{dry} = 220 kg/m^3 ϕ = 0.920	ρ_{dry} = 126 kg/m^3 ϕ = 0.954	A	5 mm

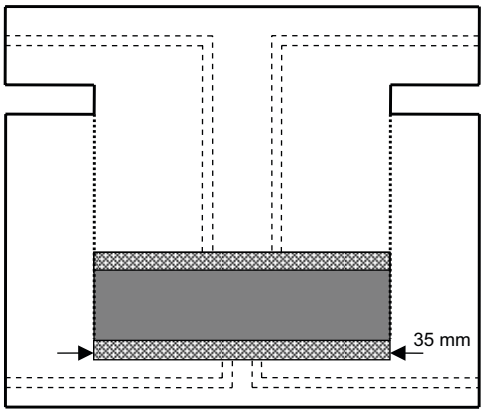

Figure 2-1. *Shematic illustration of injection filter type A.*

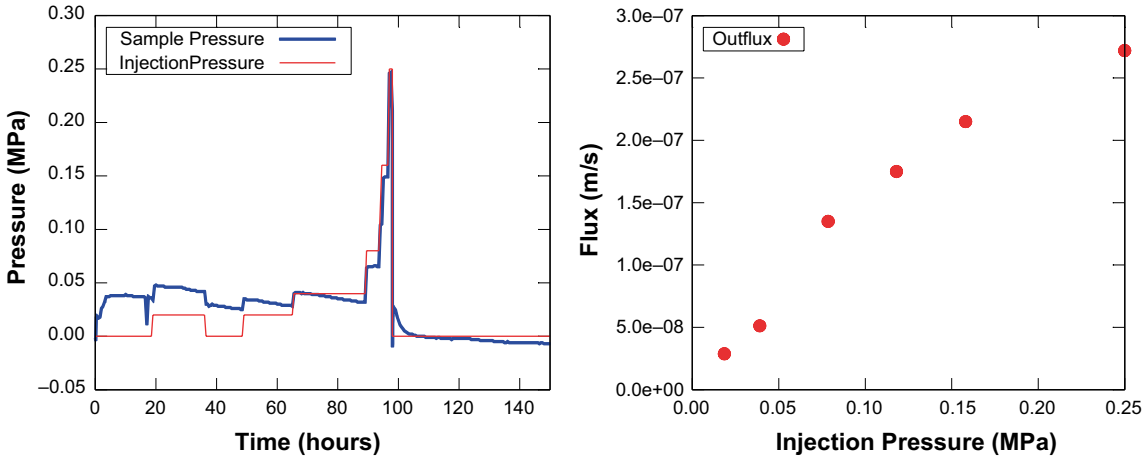

Figure 2-2. *Left: Water injection (red) and sample (blue) pressure history in sample GenCh02. Right: Measured steady-state outflows at different applied injection pressures in GenCh02.*

Despite the problems of achieving a stable sample pressure, a step-up sequence in injection pressure was performed up to 0.25 MPa (i.e. more than six times the initial P_s^0) and fairly stable water flows could be measured (at 50 h – 100 h). These are plotted as a function of injection pressure in Figure 2-2. It is seen that the steady-state flux shows a linear dependence on the applied injection pressure at lower pressures, while it increases less than linear at higher pressures. A linear relationship between steady-state flow and injection pressure (in a one-dimensional set-up) is the well-known Darcy's law and it is seen to be valid up to rather high pressures (considering that P_s^0 is very low in this sample). Another thing to note is the huge response in sample pressure during the injection pressure step-up sequence.

Considering that the sample contains 92–95% water (volume wise), its flow resistance is rather remarkable: the effective hydraulic conductivity at injection pressure 0.25 MPa was $4 \cdot 10^{-11}$ m/s. This extreme sealing ability demonstrates the very special nature of compacted Na-montmorillonite. Figure 2-3 shows a photograph of the sample at the time of termination.

Figure 2-3. *Sample GenCh02 at termination. The sample (right) is covered by the knive used to cut it from the injection filter (left). The loose – almost slurry-like – structure is clearly seen.*

2.1.1.2 GenCh03

This sample contained twice the amount of dry material as compared to sample GenCh02, giving substantially higher P_s^0. Consequently there was no problem in resolving the sample pressure in this test. However, substantial erosion occurred also in this test, which is evident from a drop in P_s^0, measured throughout the test, as well as from the big difference in nominal and post-analysis density. The pressurization history of this sample is presented in Figure 2-4.

In a first sequence (0–40 h), water pressure was increased in steps up to 0.8 MPa. In each step steady-state was achieved. The sample pressure responded strongly to the applied gradients and sample pressure was always larger than injection pressure. The corresponding steady-state flow through the system (Figure 2-5) showed non-linear dependence on applied water pressure (increasing less than linearly). It could be noted, however, that the linear regime (i.e. Darcy's law) is valid up to approximately 0.5 MPa, which is around two times P_s^0.

At 40 h the injection pressure was completely released before a second, quicker, step-up sequence in pressure was performed, up to 2.0 MPa (58–65 h). At the injection pressure of 2.0 MPa, sample pressure and injection pressure was basically equal, while the steady-state flow increase was rather minute (changing injection pressure from 1.2 MPa to 2.0 MPa only changed the flow by a factor of 1.1). A quite extreme state was maintained at this stage: a pressure drop of 2.0 MPa – approximately 10 times P_s^0 – occurs over 5 mm of clay which has a nominal average porosity of 0.84, while the effective hydraulic conductivity is ~ 10^{-12} m/s. This is another demonstration of the extreme sealing properties of confined Na-montmorillonite.

A significant drop in P_s^0 (form 0.209 to 0.162 MPa) could be noticed after the pressure again was completely released (at 65 h). This drop is most probably an effect of lowered sample density due to erosion.

A third step-up sequence in pressure was performed between 81 h – 92 h, this time up to 1.2 MPa. The system response was qualitatively the same as in the previous sequence, but a significant decrease of the steady-state flow could be noticed as compared with the previous step-up sequences (Figure 2-5). Instead of releasing the pressure completely after the highest pressure was reached, the inlet was closed at this stage. This means that the external water pressure on the injection side slowly fell off as water was transported through the system (this pressure drop was not recorded and is not indicated by the red graph in Figure 2-4).

Table 2-2. Properties of sample GenCh03.

Material	Nominal density	Post-analysis	Cell type	H
WyNa	ρ_{dry} = 440 kg/m^3 ϕ = 0.840	ρ_{dry} = 317 kg/m^3 ϕ = 0.885	A	5 mm

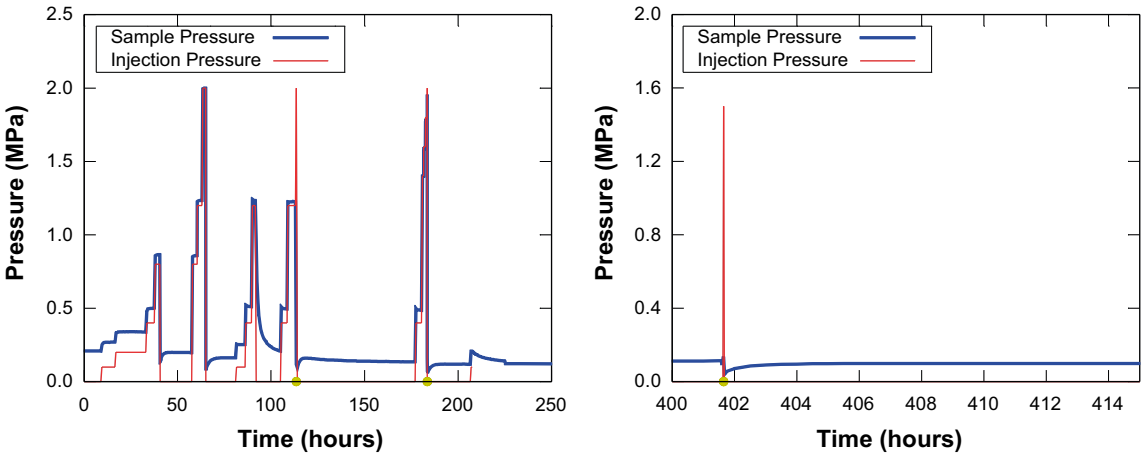

Figure 2-4. *Water injection (red) and sample (blue) pressure history in sample GenCh03. The yellow dots on the time line indicates breakthrough events. During 92 h – 105 h and 208 h – 225 h , the injection was shut off which means that the injection pressure slowly decayed as water flowed through the sample. This pressure decay was not recorded.*

A fourth pressure step-up sequence was performed between 105 h – 114 h. This time a "water breakthrough" event occurred as pressure was increased from 1.2 to 2.0 MPa. During this event the flow increased tremendously (a factor 10^4 or more), making it impossible for the pressure controlling unit to maintain the prescribed pressure. Apparently, the clay can be strained in a high enough water pressure gradient to such an extent that it "breaks". During the water breakthrough, quite a lot of water flushed through the cell as the pressure controlling unit was emptied (and lost its pressure), resulting in enhanced erosion of the sample.

After quite a long period of relaxation which revealed a lower P_s^0 (0.135 MPa), a new quick step-up sequence was performed (177–184 h), resulting in a second water breakthrough event when the pressure was increased from 1.8 MPa to 2.0 MPa (184 h). The steady-state flows were larger than before for the highest pressurized states in this step-up sequence. This is probably an effect due to erosion (i.e. decreased density which implies increased hydraulic conductivity).

At 210 h the system was pressurized with 0.1 MPa and then the inlet was closed, giving a pressure fall off as water continued to flow through the sample. The system was then left to relax for over 200 hours before the injection pressure was instantaneously increased to 1.5 MPa, resulting in an immediate water breakthrough event (402 h).

Figure 2-5 show the steady-state sample pressure at different injection pressures in the conducted pressure step-up sequences. It can be noted that the dependence is non-linear: at lower pressures the response in sample pressure is typically half of the applied increase in injection pressure, while at high pressures the sample pressure response corresponds basically to the full increase in injection pressure. Figure 2-5 also show the corresponding steady-state flows and Table 2-3 summarizes the induced breakthrough events.

Table 2-3. Water breakthrough events in sample GenCh03.

Time (h)	Injection pressure (MPa)	Sample pressure (MPa)
110	1.2 → 2.0	1.226
184	1.8 → 2.0	1.954
402	0.0 → 1.5	0.129

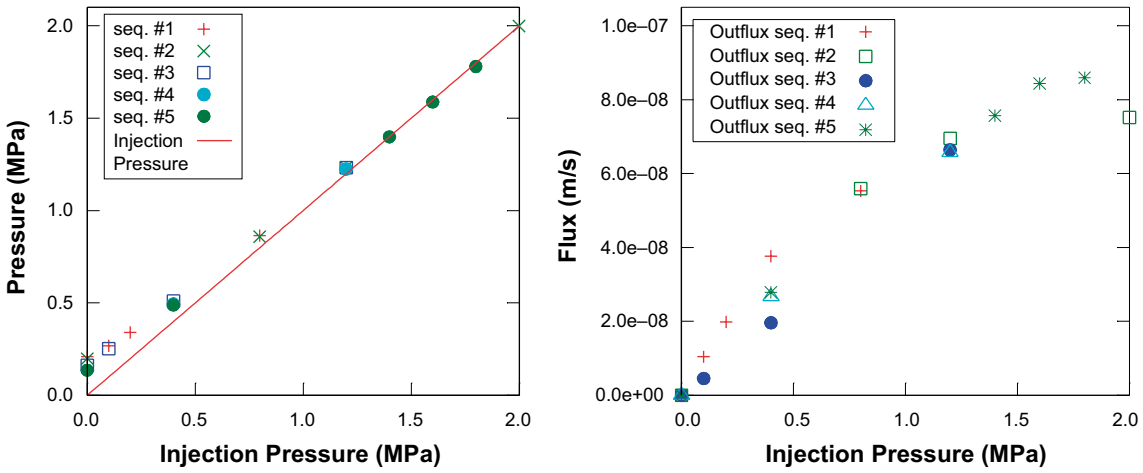

Figure 2-5. *Steady-state sample pressure (left) and in- and outflows (right) at different applied injection pressures in sample GenCh03.*

2.1.1.3 GenCh12

This sample represents a denser Na-montmorillonite system as compared to samples GenCh02 and GenCh03. The pressurization history of the sample is found in Figure 2-6.

In this sample only one step-up sequence in injection pressure was performed, up to a maximum of 2.0 MPa. The time between each pressure increase was rather long (1–3 days) which allowed for checking the stability of the steady-state. The steady-state sample pressures at different injection pressures are plotted in Figure 2-7, which also shows corresponding steady-state in- and outflow. The same types of non-linearities as seen in the previous samples are also seen here.

The applied water pressure was released momentarily to 0 MPa from the 2.0 MPa state. No significant hysteresis was observed in P_s^0 when coming back to the non-pressurized state.

As only one step-up sequence was performed, any hysteretic behavior of the steady-state fluxes was not investigated. No water breakthrough events were induced during the test.

Table 2-4. Properties of sample GenCh12.

Material	Nominal density	Post-analysis	Cell type	h
WyNa	ρ_{dry} = 700 kg/m^3 ϕ = 0.745	ρ_{dry} = 616 kg/m^3 ϕ = 0.776	A	5 mm

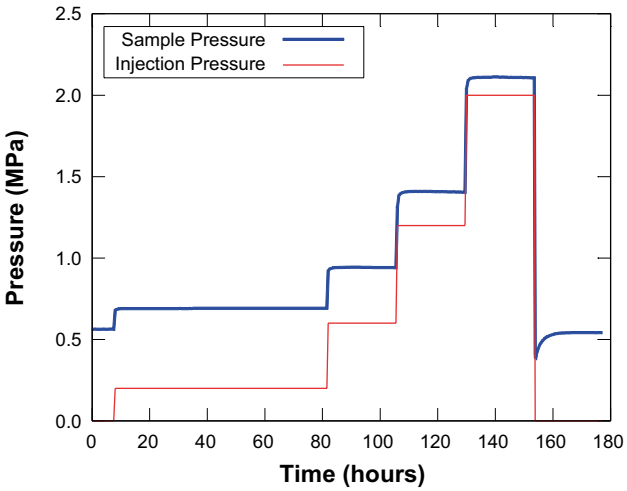

Figure 2-6. Water injection (red) and sample (blue) pressure history in sample GenCh12.

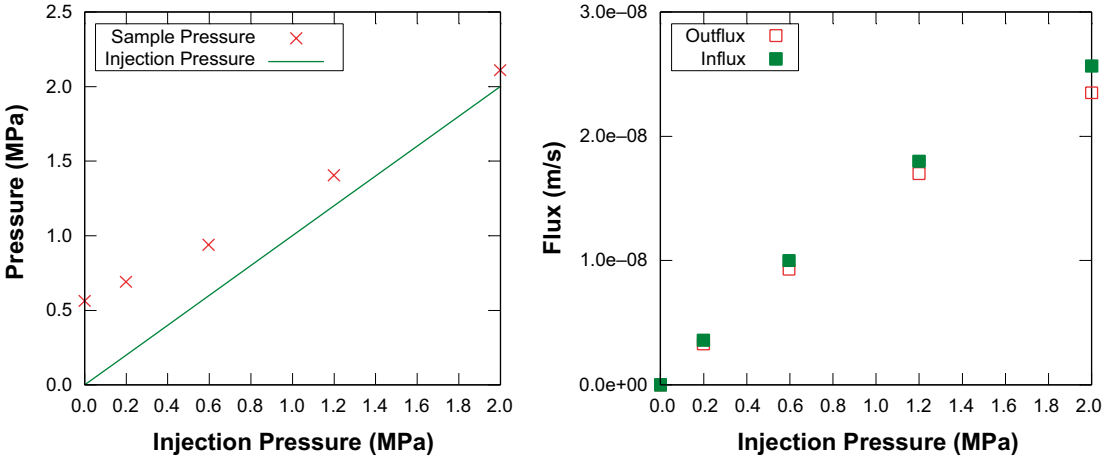

Figure 2-7. Steady-state sample pressure (left) and in- and outflows (right) at different applied injection pressures in sample GenCh12.

2.1.1.4 WyNa(Ca)14

This sample actually belonged to a different set of experiments, and have had quite a different history compared to the samples prepared specifically for tests within the FORGE project. Specifically, this sample had been water saturated for almost 2 years before the generalized hydraulic conductivity test was performed. The sample had furthermore been exposed to an ion exchange from sodium to calcium and back to sodium, as well as being exposed to different temperatures in the range 0–40°C. All of these manipulations induced pressure responses in the sample. The comparison of the response to applied water pressure gradients in this sample with others performed in the same type of cell is therefore an opportunity for checking the influence of sample preparation history.

The test was performed in one single pressure step-up sequence to a maximum applied water pressure of 4.5 MPa which corresponds to more than 7 times P_s^0. No water breakthrough events were induced in the sample. The pressurization history is found in Figure 2-8.

When the sample was pressurized with 4.5 MPa, the coupling between the pressure controlling unit and the test cell unfortunately broke (the set-up was not designed for these injection pressures). A full pressure release was performed the following morning (1,115 h).

The steady-state sample pressures and corresponding steady-state flows are plotted in Figure 2-9. Similar to the previous samples, both the pressure and flow response showed non-linearity at higher pressures. At low water pressure, the increase in sample pressure was approximately half of the increase in water pressure, and the flow response was linear, while at high water pressure the increase in sample pressure approximately equaled the increase in water pressure. Looking at flow response it seen that Darcy's law is valid up to an injection pressure of approximately 1.5 MPa. This corresponds roughly to 2 times P_s^0, and is in accordance with what has been observed in the other samples.

It is interesting to note that no significant hysteresis in P_s^0 (increase) was observed before and after the step-up cycle, despite the fact that the applied pressure gradient had been quite extreme. A speculative conclusion from this observation is that the P_s^0-hysteresis seen in other samples, which did not have this long history of being in the water saturated sate (see e.g. GenCh06, Section 2.1.2.1), is a homogenization/water saturation effect.

Table 2-5. Properties of sample WyNa(Ca)14.

Material	Nominal density	Post-analysis	Cell type	h
WyNa	ρ_{dry} = – kg/m^3 ϕ = –	ρ_{dry} = 756 kg/m^3 ϕ = 0.725	A	5 mm

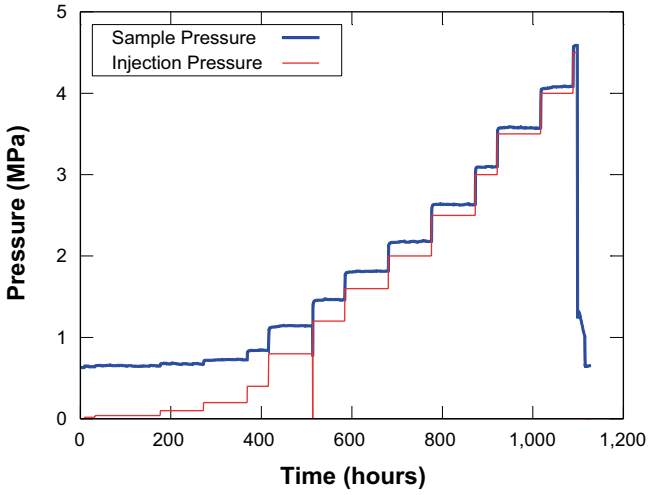

Figure 2-8. *Water injection (red) and sample (blue) pressure history in sample WyNa(Ca)14.*

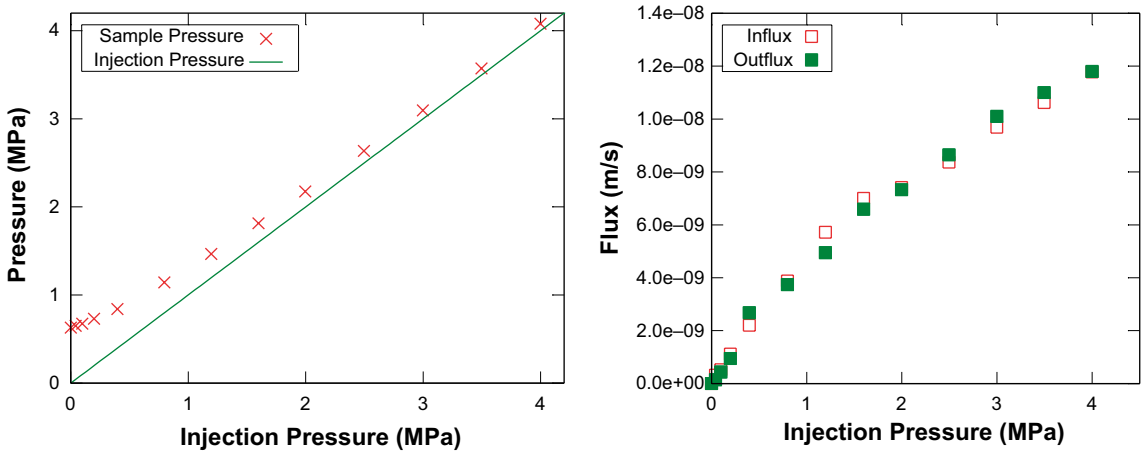

Figure 2-9. *Steady-state sample pressure (left) and in- and outflows (right) at different applied injection pressures in sample WyNa(Ca)14.*

2.1.2 MX-80 Bentonite

2.1.2.1 GenCh06

The pressurization history of sample GenCh06 is plotted in Figure 2-10.

This sample was exposed to two sequences of a stepwise increased water pressure gradient. A pronounced hysteresis effect was noted when the system came back to zero external water pressure: the corresponding swelling pressure (P_s^0) increased by approximately 60%. Also, the flow was considerably lower in the second step-up sequence as compared to the first (Figure 2-11). The reason for this hysteresis was not further investigated but could be due to e.g. homogenization effects (i.e. the initial state was not really at equilibrium), or due to that the sample became somewhat anisotropic when exposed the very high pressure gradients. It might also reflect some more fundamental microscopic aspect of swelling and swelling pressure (see e.g. Dueck 2004). A similar type of hysteresis was observed in water pressurization tests in MX-80 bentonite (Harrington and Horseman 2003). Hysteresis phenomena is further explored in Chapter 4.

Table 2-6. Properties of sample GenCh06.".

Material	Nominal density	Post-analysis	Cell type	h
MX-80	ρ_{dry} = 1,166 kg/m^3 ϕ = 0.576	Sliced and analyzed, see below	A	20 mm

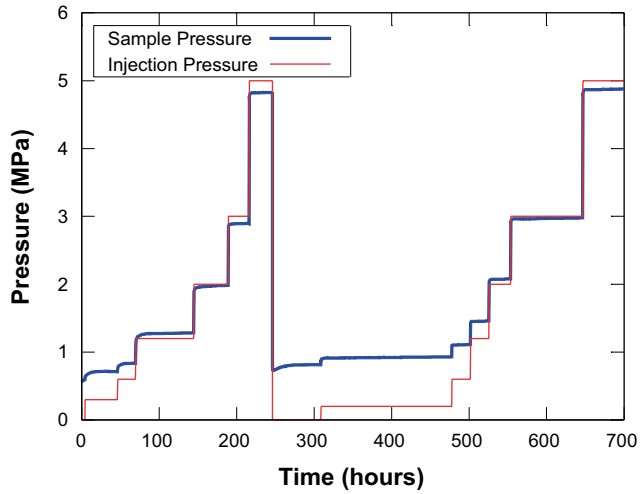

Figure 2-10. *Water injection (red) and sample (blue) pressure history in sample GenCh06.*

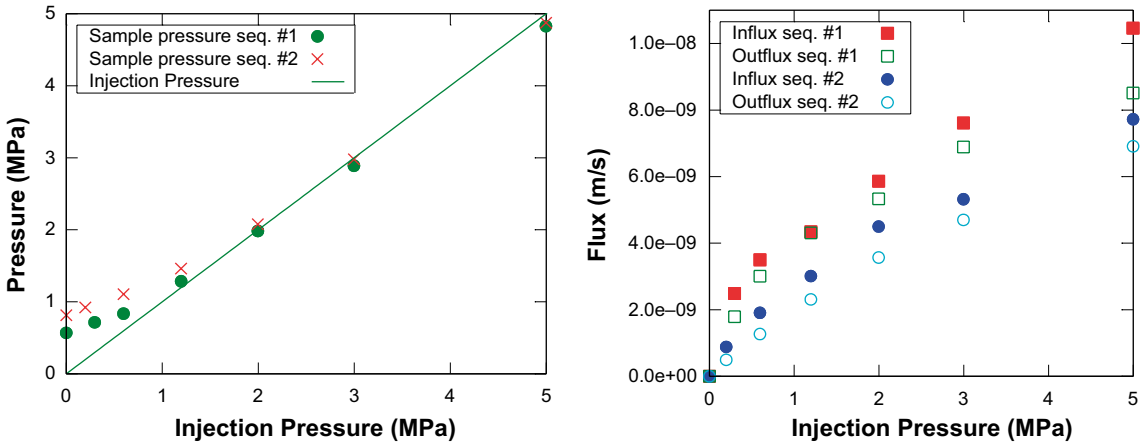

Figure 2-11. *Steady-state sample pressure (left) and in- and outflows (right) at different applied injection pressures in sample sample GenCh06.*

The sample pressure and flow response generally showed the same type of non-linear characteristics as in the pure montmorillonite samples (Section 2.1.1). The flow response, for instance, obeys Darcy's law up to approximately two times P_s^0, as also observed in the montmorillonite samples.

However, in contrast to the pure montmorillonite samples, the measured sample pressure for the largest applied gradients was (slightly) lower than the applied water pressure in this case. This indicates presence of friction forces between the clay and the inner wall of the sample holder as well as non-zero shear strength of the material, which could imply a difference in friction properties between pure montmorillonite and MX-80 bentonite. However, the length of the present sample was 4 times larger than any of the tested pure montmorillonite samples, and therefore the difference could rather be due to a larger clay/container interface area. Yet another difference is that the present sample has significantly higher density than the pure Na-montmorillonite samples (see discussion in Section 1.3).

The test was terminated at the end of the second step-up sequence, at injection pressure 5 MPa (corresponding to approximately 6.25 times P_s^0). The sample was quickly (within a few minutes) sectioned and the water-to-solid mass ratio was determined for each segment. Under the very reasonable assumption that the sample was water saturated, the induced steady-state density profile could be determined from the water-to-solid mass ratios (Equation 1-2). The profile is displayed in Figure 2-12, which clearly shows that bentonite have a huge response in density when exposed to large water pressure gradients. It is worth noting that the density of the injection side (850 kg/m^3) corresponds to a P_s^0 of approximately 0.2 MPa, while the density of the outlet side (1,350 kg/m^3) corresponds to a P_s^0 of around 3.0 MPa (comparing with data from Karnland et al. 2006). This pressure difference is similar to the external water pressure difference to which the sampled had adjusted.

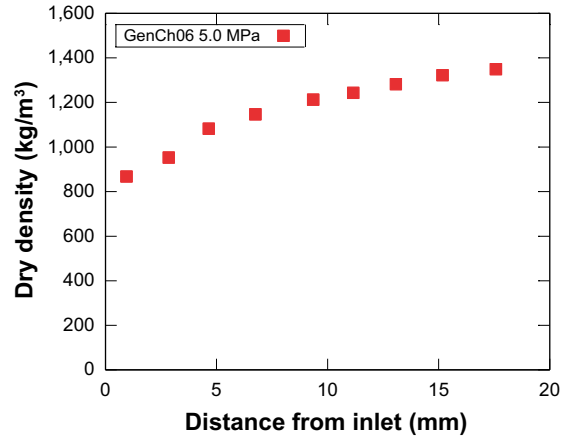

Figure 2-12. *Spatial density profile of sample GenCh06, sectioned directly after being exposed to a water pressure difference of 5 MPa after the second step-up sequence.*

2.1.2.2 GenCh21

Pressurization history of this sample is plotted in Figure 2-13. The sample was exposed to a sequence of external water pressure differences of increasing size in the range 0.5–5 MPa. In contrast to many of the other tests, the pressure was here put to zero in between each applied pressure difference. When the applied pressure was 5.0 MPa (992 h), a sequence of decreasing injection pressures was applied (without zero pressure in between). Finally a last pressure difference of 2.0 MPa was applied (1,393 h).

The steady-state sample pressures as a function of injection pressure are displayed in Figure 2-14. These pressure are quite different depending on whether a pressure increase or decrease has been applied (sequence 1 or sequence 2). This behavior indicates shear strength of the sample as well as friction between the sample and the wall of the sample holder. The presence of these mechanisms are also evident from the observation that sample pressure is lower than the corresponding injection pressure at high pressure. This effect was also observed in a similar MX-80 sample (GenCh06, Section 2.1.2.1).

Note that although there is a hysteresis in the result depending on whether pressure is increased or decreased, no significant hysteresis was observed in P_s^0 during this test (however, the sample showed large P_s^0-hysteresis during its early history, as described in Section 4.1.1.1).

Table 2-7. Properties of sample GenCh21.

Material	Nominal density	Post-analysis	Cell type	h
MX-80	ρ_{dry} = 1,166kg/m^3 ϕ = 0.576	Sliced and analyzed, see below	A	20 mm

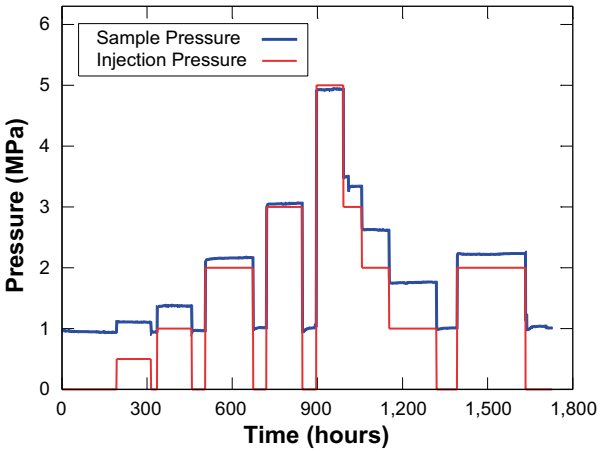

Figure 2-13. Water injection (red) and sample (blue) pressure history in sample GenCh21.

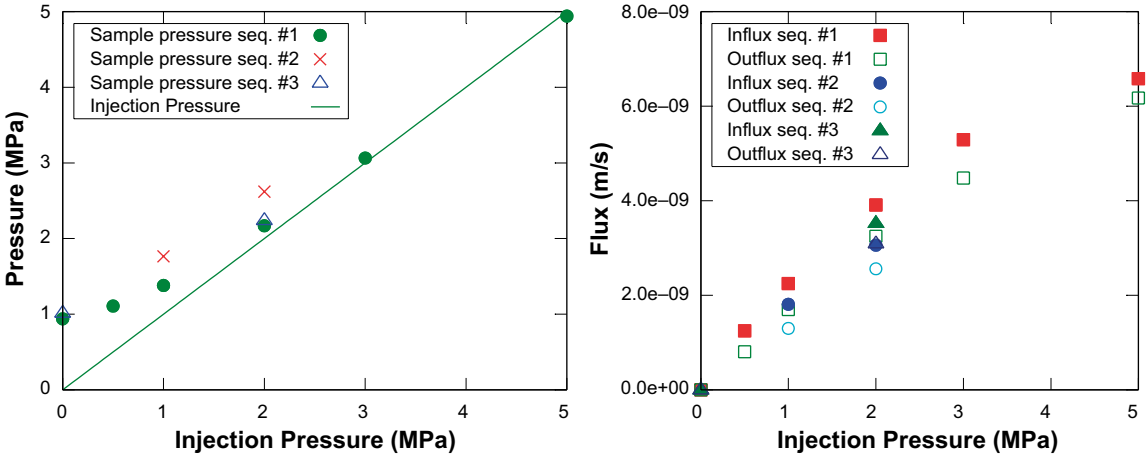

Figure 2-14. Steady-state sample pressure (left) and in- and outflows (right) at different applied injection pressures in sample sample GenCh21.

The corresponding steady-state flux, displayed in Figure 2-14, shows hysteresis similar to what was seen for the pressure. The flux is generally larger, at the same applied water pressure, when the injection pressure is being increased.

Response at elevated temperature (70°C)

The pressure and flow response of this sample was further tested at an elevated temperature of 70°C by placing it in an oven. The injection pressure and corresponding sample pressure evolution is shown in Figure 2-15, and the corresponding steady-state values are shown in Figure 2-16. The behavior is quite similar to the observations at room temperature: Again, influence of non-zero shear strength and friction was observed, while the P_s^0-value did not show significant hysteresis. At 70°C, however, it was more difficult to achieve a stable pressure in the sequence where pressure was successively lowered (see e.g. 600 h – 800 h in Figure 2-15). This may indicate that friction forces and/or shear strength weakens with temperature.

The same type of hysteresis in flow was observed as for the case of room temperature (Figure 2-16). In this case no outflux measurements could be done due to experimental constraints (significant evaporation of the top reservoir in the oven environment).

As a final test, this sample was exposed to an external water pressure difference of 4.9 MPa (at room temperature). After steady-state conditions were reached, the test was quickly (within minutes) terminated, and the sample was sectioned and analyzed. The corresponding density profile is shown in Figure 2-17.

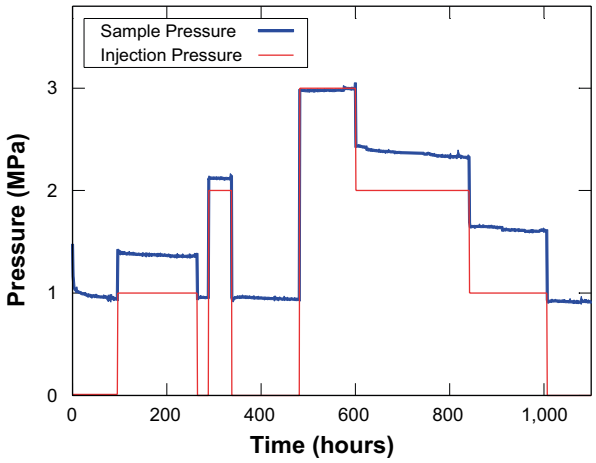

Figure 2-15. *Water injection (red) and sample (blue) pressure history in sample GenCh21 at 70°C.*

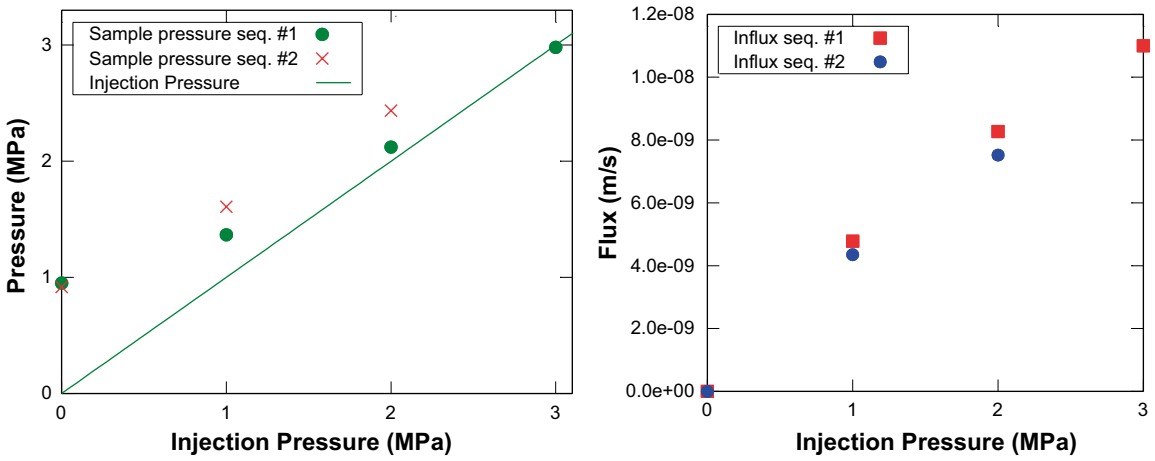

Figure 2-16. *Steady-state sample pressure (left) and in- and outflows (right) at different applied injection pressures in sample sample GenCh21 at 70°C.*

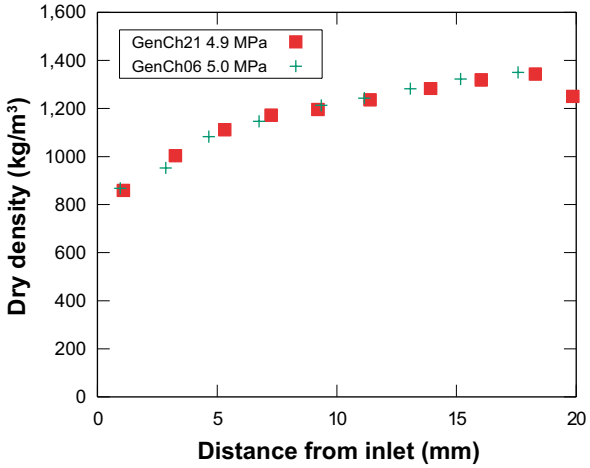

Figure 2-17. *Spatial density profile of sample GenCh21, sectioned directly after being exposed to a water pressure difference of 4.9 MPa. For comparison, the density profile of sample GenCh06 (see Section 2.1.2.1) is also shown.*

The density gradient is very pronounced and very similar to that seen in another sample under similar conditions (GenCh06, Section 2.1.2.1). Again, it can be noted that the expected swelling pressure difference corresponding to the density difference of the two ends of the sample basically corresponds to the entire externally applied pressure difference.

2.1.2.3 WP3Bench

This sample was exposed to increasing external water pressure gradients in two tests. The pressure response history is found in Figure 2-18 and corresponding plots of steady state sample pressures and flux as a function of injection pressure are displayed in Figure 2-19. The behavior of this sample is in complete accordance with previously tested samples of the same material and similar density: the flux as a function of applied water pressure increases slower than linear at higher pressure; the sample pressure increases approximately as half the applied water pressure at low pressures, but the response tends towards full water pressure increase at higher pressures.

Basically no hysteresis was observed in P_s^0 after each performed pressurization sequence. Similarly, only minor differences of flow response were observed in the different sequences.

Table 2-8. Properties of sample WP3Bench.

Material	Nominal density	Post-analysis	Cell type	h
MX-80	ρ_{dry} = 1,170 kg/m³ ϕ = 0.575	ρ_{dry} = 1,075 kg/m³ ϕ = 0.609	A	5 mm

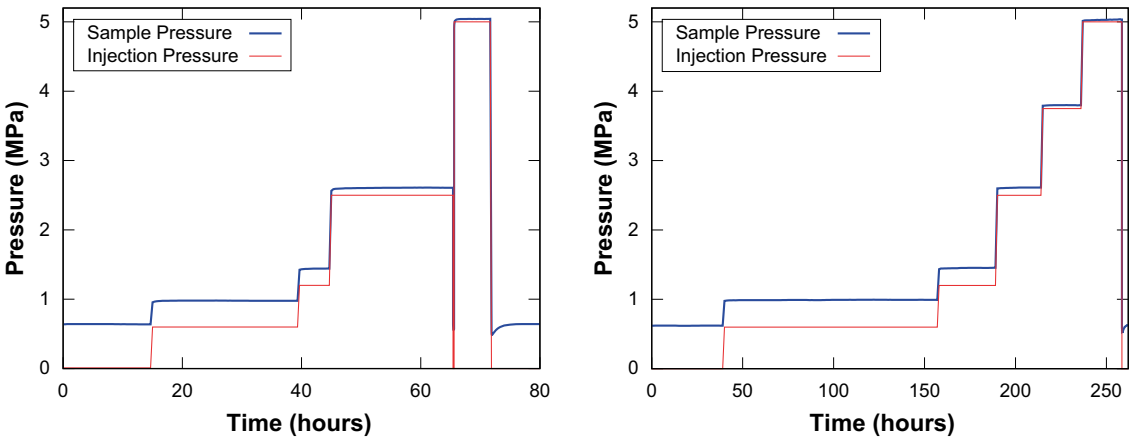

Figure 2-18. *Water injection (red) and sample (blue) pressure history of the two tests performed in sample WP3Bench.*

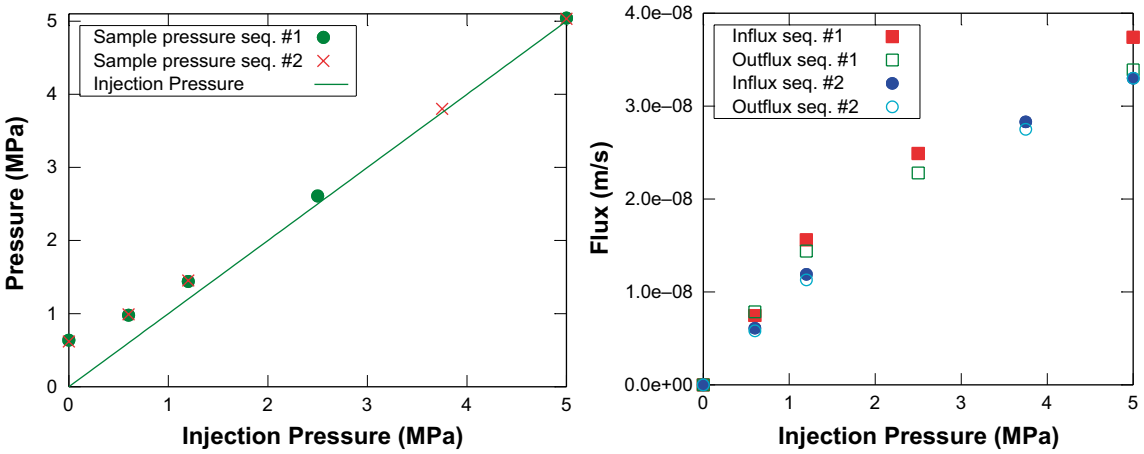

Figure 2-19. *Steady-state sample pressure (left) and in- and outflows (right) at different applied injection pressures in sample WP3Bench.*

2.1.3 Ca-montmorillonite

2.1.3.1 GenCh05

A swelling pressure and hydraulic conductivity test was made on a low density Ca-montmorillonite sample for comparison with the corresponding Na-montmorillonite samples. It was concluded that Ca-montmorillonite does not exert significant swelling pressure at these densities. Also, the permeability for water is many orders of magnitude larger than for a corresponding Na-montmorillonite. The hydraulic conductivity is so large that it was impossible to apply (large) gradients with the equipment used. In conclusion, low density Ca-montmorillonite behaves as a completely different substance as compared to Na-montmorillonite at similar densities. The former material resemble more a conventional soil materials (silt, sand).

Table 2-9. Properties of sample GenCh05.

Material	Nominal density	Post-analysis	Cell type	h
WyCa	ρ_{dry} = 440 kg/m^3 ϕ = 0.840	Not analyzed	A	5 mm

2.1.3.2 GenCh22

This sample was exposed to a single pressure increase sequence, shown in Figure 2-20. The corresponding steady-state pressures and fluxes are displayed in Figure 2-21. The response behavior is in agreement with observations in Na-montmorillonite and MX-80 samples, i.e. non-linearities of both flux and sample pressure at injection pressures considerably larger than P_s^0.

Table 2-10. Properties of sample GenCh22.

Material	Nominal density	Post-analysis	Cell type	h
WyCa	ρ_{dry} = 1,200 kg/m^3 ϕ = 0.564	ρ_{dry} = 1,137 kg/m^3 ϕ = 0.605	A	5 mm

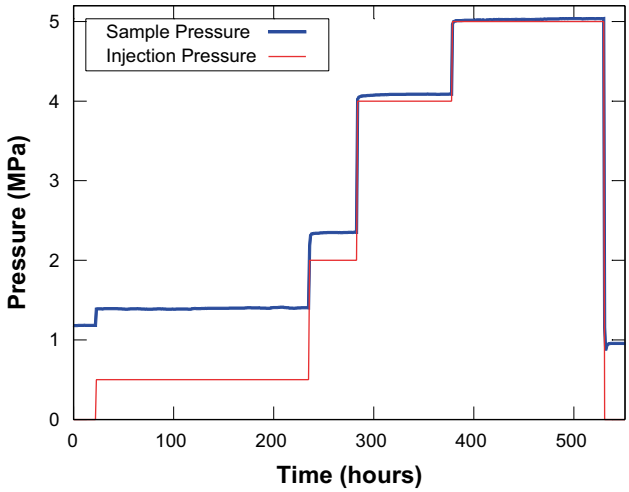

Figure 2-20. *Water injection (red) and sample (blue) pressure history in sample GenCh22.*

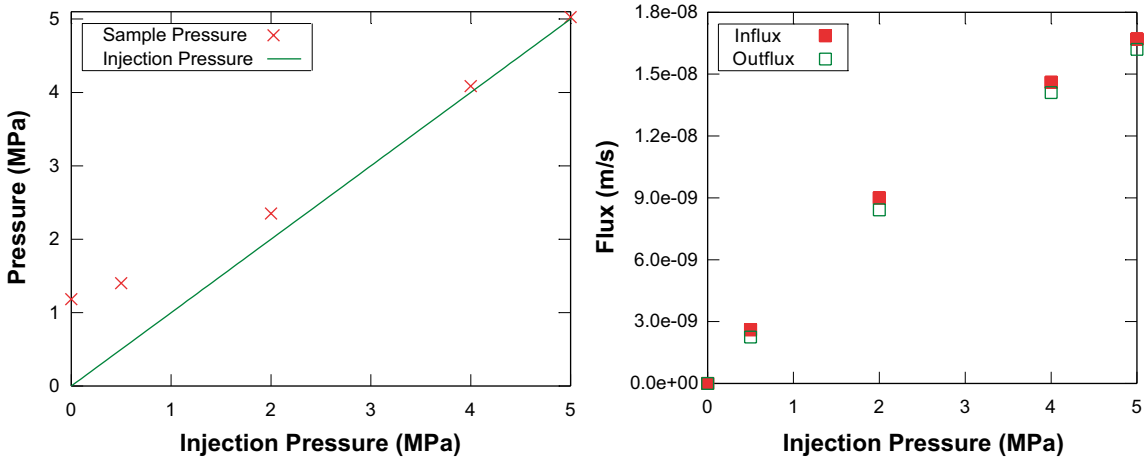

Figure 2-21. *Steady-state sample pressure (left) and in- and outflows (right) at different applied injection pressures in sample GenCh22.*

2.1.3.3 GenCh23

This sample was successively volume expanded in steps during the testing. At each density, it was tested for response to external water pressure differences, gas pressure differences, as well as to uniform water pressurization (see further Sections 3.1.2.2 and 4.1.2.2). Volume expansion was achieved by applying an external water pressure in the bottom of the test cell, while adjusting the screws on the top (see Figure 1). The volume increase could then be directly be read off – with great accuracy – from the pressure controlling unit.

Table 2-11. Properties of sample GenCh23.

Material	Nominal density	Post-analysis	Cell type	h
WyCa	ρ_{dry} = 1,250 kg/m^3 ρ_{dry} = 1,042 kg/m^3 ρ_{dry} = 893 kg/m^3 ρ_{dry} = 781 kg/m^3	Not made	A	5–8 mm (sample expanded)

Nominal density 1,250 kg/m^3

The pressure response due to applied water injection pressure, and corresponding steady-state sample pressures and fluxes for nominal density 1,250 kg/m^3 is shown in Figure 2-22 and Figure 2-23. The sample shows the same type of non-linear response that basically has been observed in all other samples with the same cell type. Note that the resulting sample pressure depends not only on the applied water pressure, but also to some extent on pressurization history (whether pressure was lowered or raised). The same type of hysteresis was also seen in sample GenCh21 (Section 2.1.2.2).

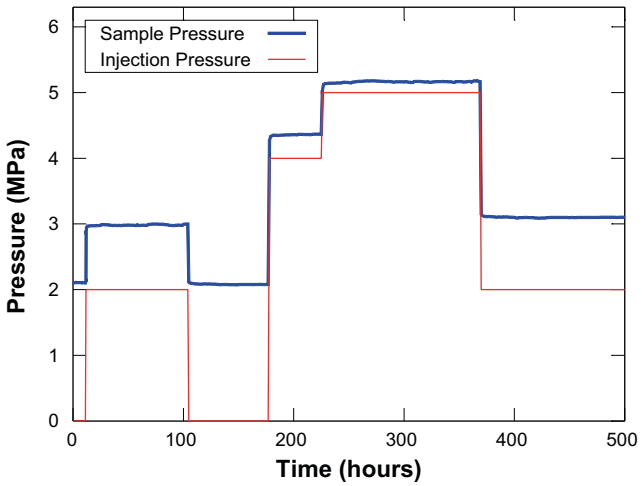

Figure 2-22. *External water injection (red) and sample (blue) pressure history in sample GenCh23 at nomial density 1,250 kg/m^3.*

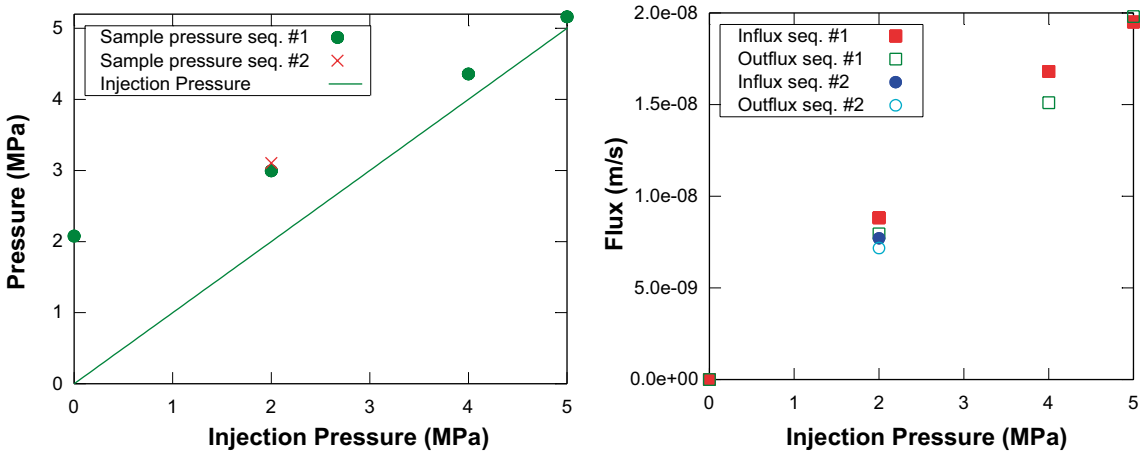

Figure 2-23. *Steady-state sample pressure (left) and in- and outflows (right) at different applied injection pressures in sample GenCh23 at nomial density 1,250 kg/m^3*

1,042 kg/m^3

Figure 2-24 and Figure 2-25 summarizes the response due to water injection pressure of the sample at nominal density 1,042 kg/m^3. The same type of nonlinear response is shown also at this density. Furthermore, the effect of friction is clearly seen at larger externally applied pressures (1.8 MPa, 3.0 MPa) where the sample pressure fall below the injection pressure.

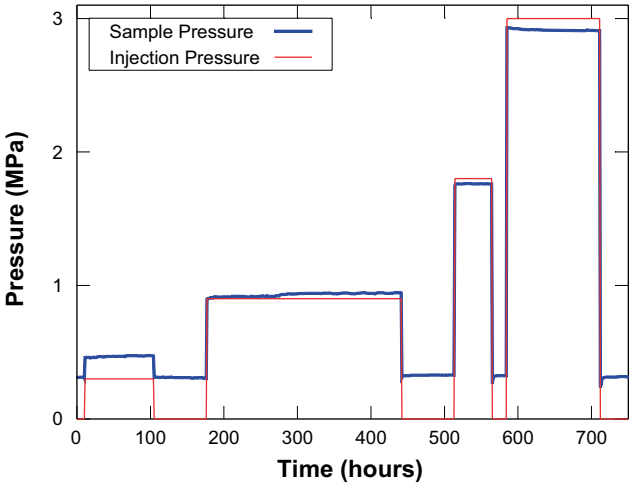

Figure 2-24. *External water injection (red) and sample (blue) pressure history in sample GenCh23 at nomial density 1,042 kg/m^3.*

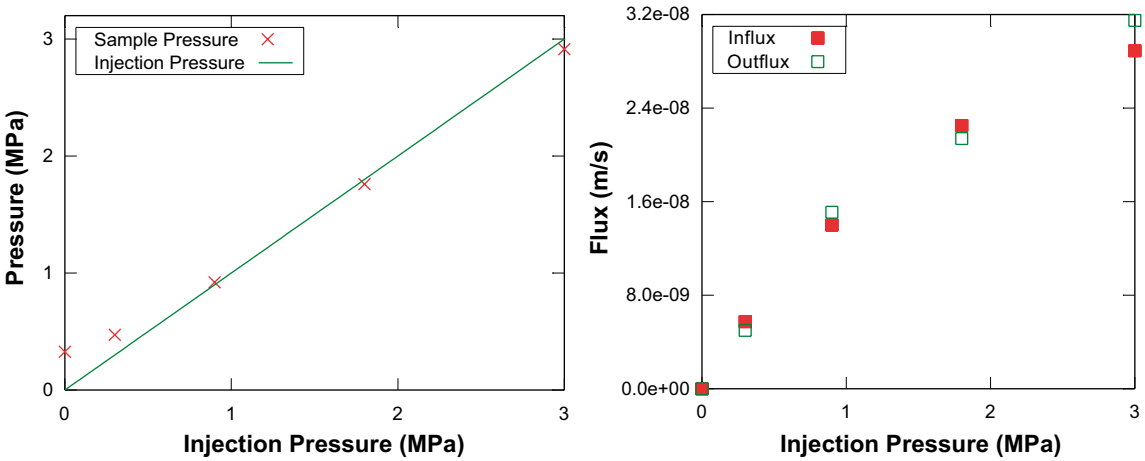

Figure 2-25. *Steady-state sample pressure (left) and in- and outflows (right) at different applied injection pressures in sample GenCh23 at nominal density 1,042 kg/m^3.*

893 kg/m^3

Figure 2-26 and Figure 2-27 summarizes the response of the sample due to water injection pressure at nominal density 893 kg/m^3. The response in sample pressure and flux show the same qualitative behavior as observed at the higher densities (and in basically any other sample tested using this cell type). The effect of friction is evident at the highest applied water pressure (3.0 MPa), where the sample pressure is lower than the applied pressure.

It is interesting to note that although P_s^0 is below 0.1 MPa at this density, the same type of flow and pressure response as seen in dense bentonite is observed also in this system. This observation suggests that Ca-montmorillonite is fairly homogeneous, also at densities where P_s^0 is approaching zero.

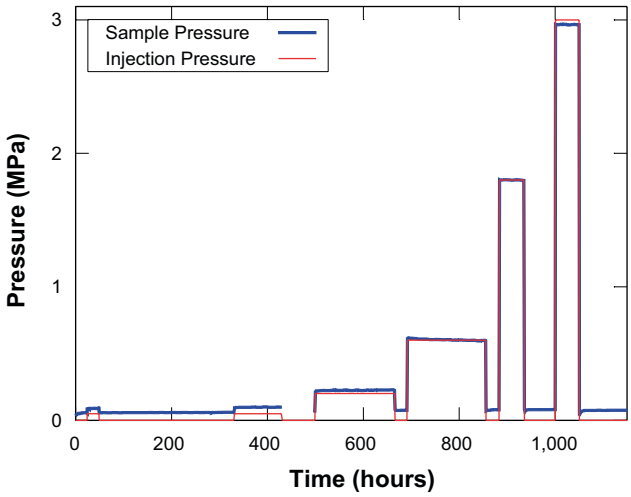

Figure 2-26. *External water injection (red) and sample (blue) pressure history in sample GenCh23 at nomial density 893 kg/m^3.*

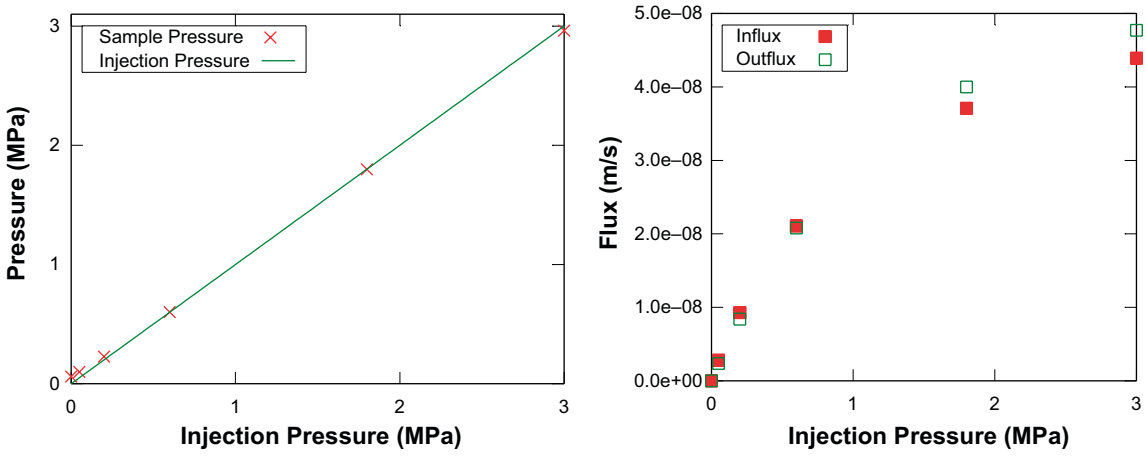

Figure 2-27. *Steady-state sample pressure (left) and in- and outflows (right) at different applied injection pressures in sample GenCh23 at nominal density 893 kg/m^3.*

781 kg/m^3

Figure 2-28 and Figure 2-29 summarizes the response of the sample due to water injection pressure at nominal density 781 kg/m^3.

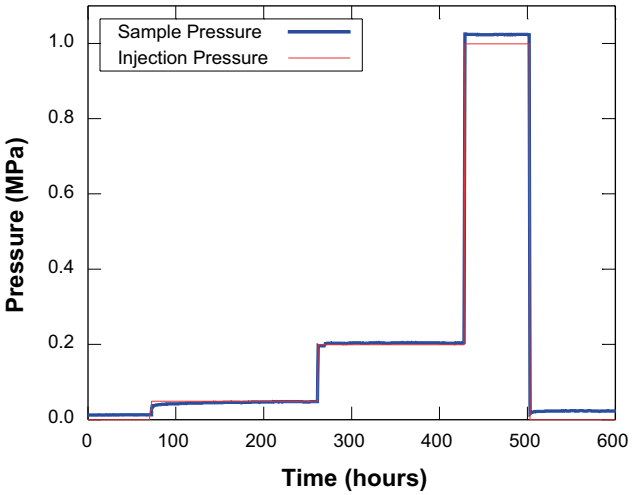

Figure 2-28. *External water injection (red) and sample (blue) pressure history in sample GenCh23 at nomial density 781 kg/m^3.*

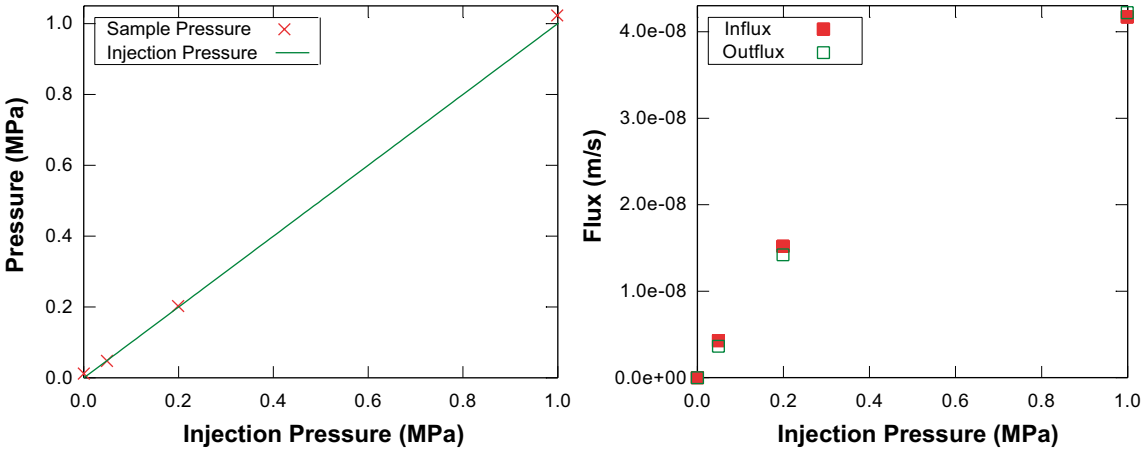

Figure 2-29. *Equilibrium sample pressure (left) and steady-state in- and outflows (right) at different applied injection pressures in sample GenCh23 at nominal density 781 kg/m^3.*

2.1.3.4 KuCa02

This sample actually belonged to a different set of experiments, and have had a slightly different history compared to the samples prepared specifically for tests within the FORGE project. Specifically, this sample had been water saturated for about eight months before the generalized hydraulic conductivity test was performed.

The pressurization history of this sample is found in Figure 2-30. The water pressure gradient test consisted of a step-up sequence of applied water pressure up to 1.2 MPa during a rather long time period (0–592 h). This pressurization sequence was followed by a huge drop in injection pressure and a subsequent increase back to 1.2 MPa (592–616 h). A quicker sequence was then performed, in two steps down to zero applied water pressure (616–682 h). The first period of testing was finished by applying a pressure of 0.3 MPa (759–785 h).

The set-up was thereafter left inactive (zero injection pressure) for 175 days before a last pressure step-up sequence was performed, now on a much faster time scale, up to a maximum pressure of 2.0 MPa (right diagram in Figure 2-30).

The steady-state sample pressure response, displayed in Figure 2-31, is similar to Na-montmorillonite samples of similar P_s^0 and dimensions. In this sample, however, sample pressure was slightly below the applied water pressure at higher pressures. Also, the corresponding steady-state flow showed less non-linearity as compared to Na-montmorillonite samples of similar P_s^0. It should be remembered that the density of the current sample is substantially larger than the Na-montmorillonite samples of comparable P_s^0.

As Ca-montmorillonite is a non-sol-forming material, erosion did not occur. The sample showed only minor hysteresis in pressure and flow response.

Table 2-12. Properties of sample KuCa02.

Material	Nominal density	Post-analysis	Cell type	h
KuCa	ρ_{dry} = 1,095 kg/m^3 ϕ = 0.590	ρ_{dry} = 1,068 kg/m^3 ϕ = 0.619	A	5 mm

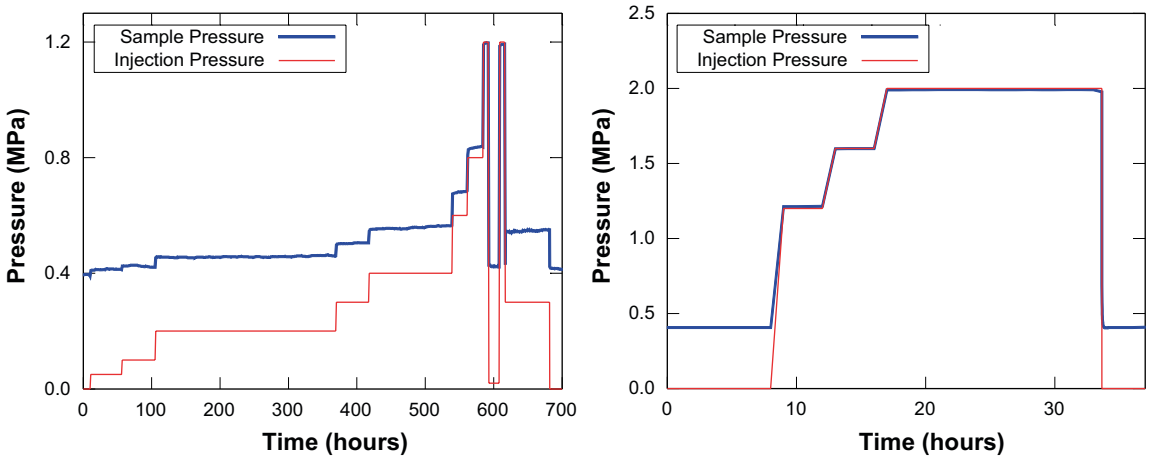

Figure 2-30. *External water injection (red) and sample (blue) pressure history in sample KuCa02. The pressurization sequence showed in the right diagram was performed approximately 175 days after the pressurization sequence showed in the left diagram.*

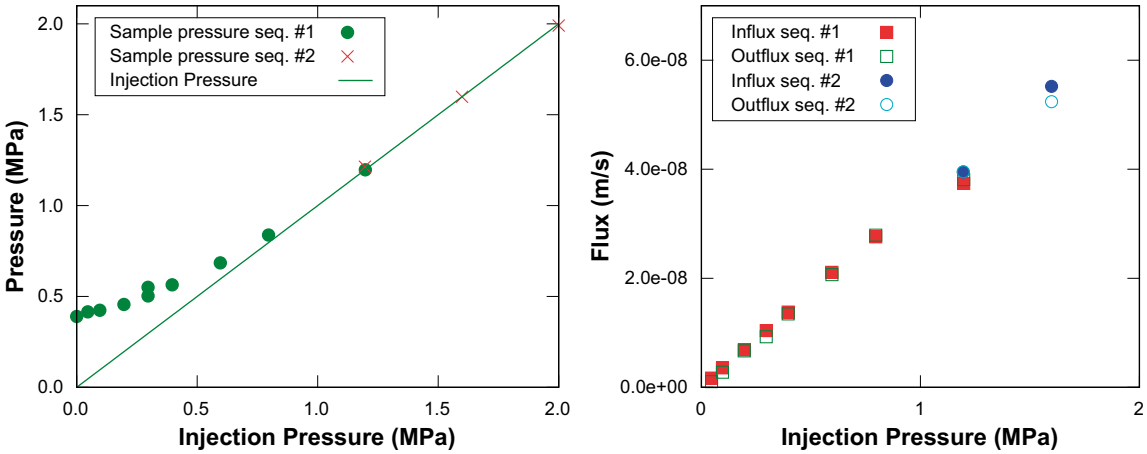

Figure 2-31. *Steady-state sample pressure (left) and in- and outflows (right) at different applied injection pressures in sample KuCa02.*

2.2 Injection filters B and C

2.2.1 Na-montmorillonite

2.2.1.1 GenCh04

The sample pressure response to various injection pressures is shown in Figure 2-33. It can be noted, particularly in the pressure sequences performed between 220 h and 425 h, that this response is very weak for any injection pressure lower than P_s^0, in sharp contrast to the response in samples with large injection filters (Section 2.1). This (lack of) response is expected as only approximately 2% of the bottom surface area is pressurized in samples with the present type of injection filters. For the same reason, the induced fluxes at injection pressures below P_s^0 were below detection limit and were not recorded.

Table 2-13. Properties of sample GenCh04.

Material	Nominal density	Post-analysis	Cell type	h
WyNa	ρ_{dry} = 440 kg/m^3 ϕ = 0.840	ρ_{dry} = 376 kg/m^3 ϕ = 0.863	B	5 mm

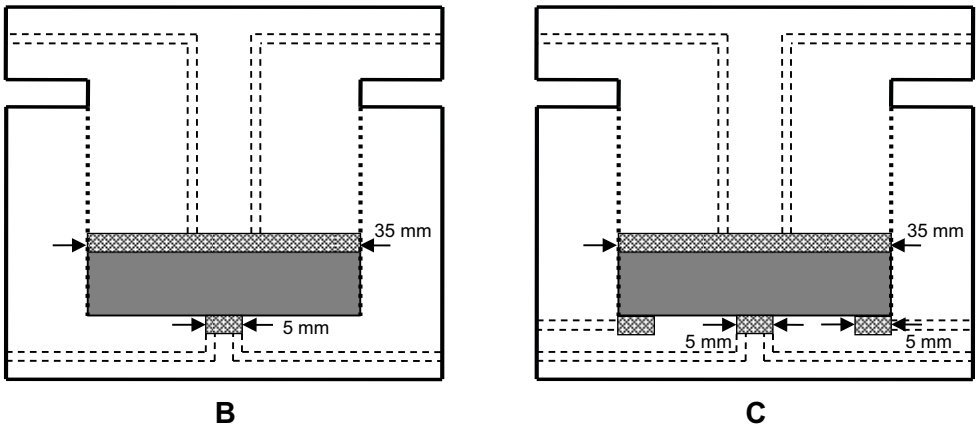

Figure 2-32. *Schematic illustation of injection filters type B and C.*

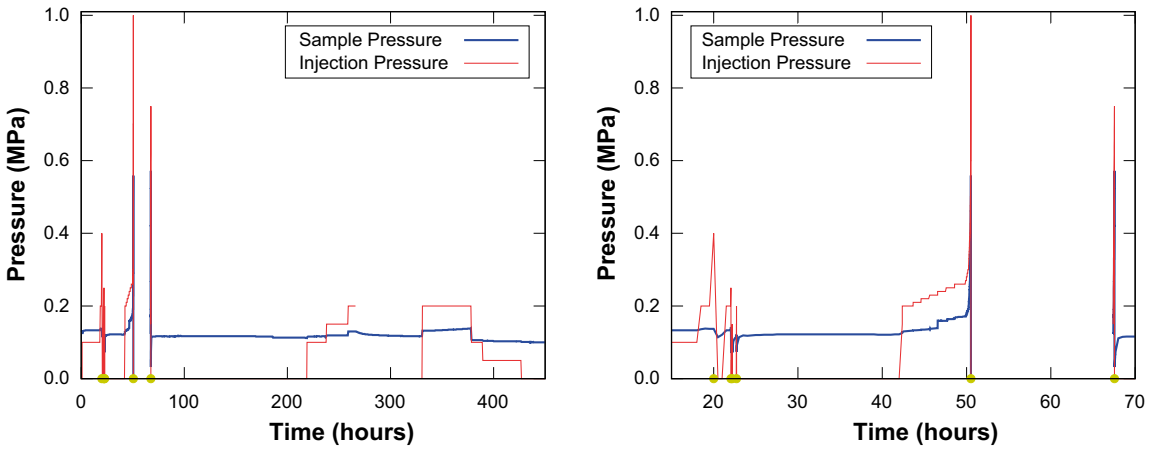

Figure 2-33. *Water injection (red) and sample (blue) pressure history in sample GenCh04. The right diagram shows a magnification of the period 10–70 h. The yellow dots on the time line indicates breakthrough events. The period between 51–67 h was not recorded (recording system was unintentionally turned off). During the time interval between 266–331 h, the injection was shut off which means that the (injection) pressure slowly decayed as water flowed through the sample. This pressure decay was not recorded.*

Figure 2-33 also shows that states could be maintained where the injection pressure quite substantially succeeded the sample pressure without inducing breakthrough events (238 h – 266 h, 331 h – 378 h). This behavior is somewhat in contrast to that observed in Na-montmorillonite of similar density, injected with a filter of type A (Section 2.1.1.2).

When an injection pressure of 0.2 was applied (331 h – 378 h), a detectable outflow was recorded. This outflow never reached steady state, but kept on increasing as shown in Figure 2-34. This behavior could be an effect due to continuous erosion of the sample, but would in such a case be correlated with a drop in sample pressure. On the contrary, a weak increase of the sample pressure is observed during the time of this pressurization. Therefore, the behavior rather suggests that mechanical processes (e.g. redistribution of mass) occur on quite long time scales in these samples, despite their small dimensions.

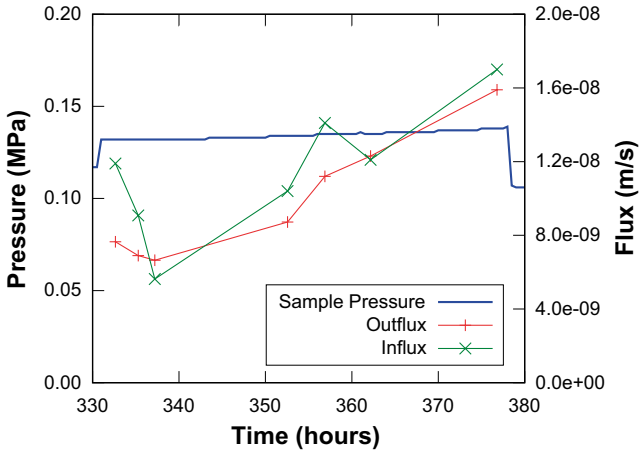

Figure 2-34. *In- and outflow of water during the pressurization of 0.2 MPa at 331–378 h. The sample pressure repsonse is also plotted.*

By applying increasingly larger injection pressure, breakthrough events could be induced in the present sample, as showed in detailed in the right diagram in Figure 2-33. For instance, at 20 h the injection pressure was increased in one step from 0.2 MPa to 0.4 MPa, resulting in an immediate breakthrough event. Breakthrough events could then be induced at even lower injection pressures directly after the first one, which indicates that the system has a finite relaxation (healing) time. By making a quick injection pressure increase in small steps, a much more pronounced sample pressure response could be induced and breakthrough did occur at as high pressures as 0.7 MPa (at 51 h and 68 h). These pressurization steps were kept constant for quite a short time and it was not evaluated how the system maintains pressures over long time periods above 0.2 MPa. All breakthrough events are listed in Table 2-14.

Table 2-14. Water breakthrough events in sample GenCh04.

Time (h)	Injection pressure step (MPa)	Sample pressure (MPa)
20	0.2 → 0.4	0.137
22.05	0.2 → 0.25	0.142
22.21	0.1 → 0.15	0.101
22.71	0.15 → 0.20	0.121
50.52	0.7 → 1.0	0.559
67.54	0.7 → 0.75	0.572

2.2.1.2 GenCh13

The pressurization history of the sample is plotted in Figure 2-35.

Pressurization started with a step-up of water injection pressure to 0.5 MPa. Although this pressure is similar to P_s^0, the sample pressure response was basically negligible, confirming the type of (non-) response also seen in sample GenCh04.

Table 2-15. Properties of sample GenCh13.

Material	Nominal density	Post-analysis	Cell type	h
WyNa	ρ_{dry} = 700 kg/m^3 ϕ = 0.745	ρ_{dry} = 620 kg/m^3 ϕ = 0.774	C	5 mm

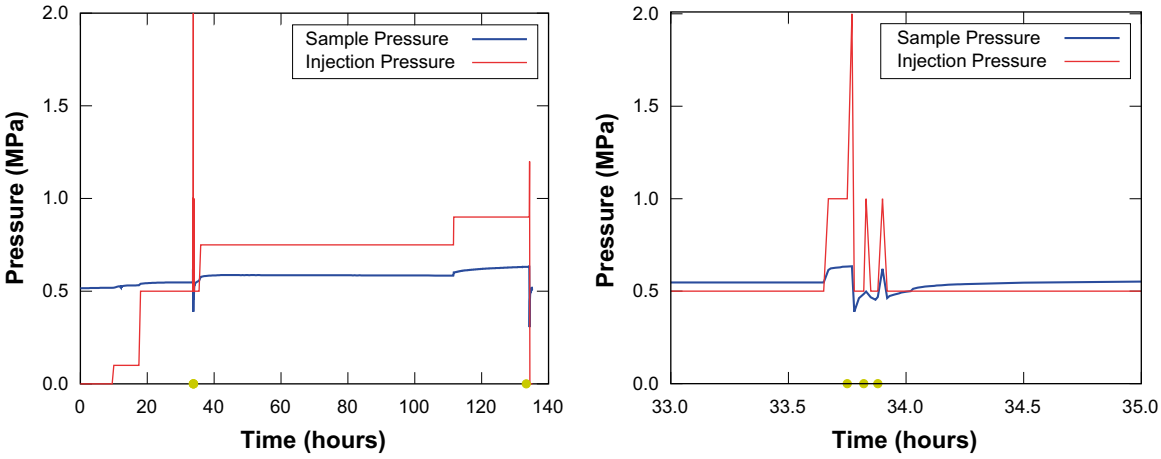

Figure 2-35. *Water injection (red) and sample (blue) pressure history in sample GenCh13. The right diagram shows a magnification of the period 33–35 h. The yellow dots on the time line indicates breakthrough events.*

The injection pressure was then increased to 1.0 MPa and maintained without breakthrough for approximately 5 minutes. In this state the sample pressure responded, increasing from ca 0.55 MPa to ca 0.63 MPa. The injection pressure was then further increased to 2.0 MPa with a resulting instantaneous water breakthrough (33.77 h). The water flowed out through the guard filter in the bottom of the cell. This indicates that water (as a separate phase) is entering the cell but not the clay.

The injection pressure was immediately lowered to 0.5 MPa which directly resulted in a termination of the breakthrough event. After about four minutes, the pressure was increased to 1.0 MPa, which immediately resulted in a second water breakthrough event through the guard filter. The pressure was again lowered to 0.5 MPa and the breakthrough event stopped. After about four more minutes, the injection pressure was raised again to 1.0 MPa. Also this time a breakthrough immediately followed. It seems very likely that these breakthrough events, occurring within very short periods of time, are not independent, i.e. that the clay did not have time to heal in between the events.

The system was once again stabilized at an injection pressure of 0.5 MPa which was increased to 0.75 MPa after approximately an hour (36 h). This state was then maintained for over 75 hours without any water breakthrough events occurring. Furthermore, after an initial small increase, the sample pressure stayed basically constant during this entire period. Thus, a steady-state was maintained where the injection pressure was higher than the sample pressure, which indicates a non-zero shear strength of the material. Similar states were maintained in sample GenCh04 (Section 2.2.1.1). In the present sample, however, also a steady-state flow was achieved. It is interesting to note that the steady-state flow occurred basically only through the top filter and not through the guard filters. Hence, the water is taking different paths in the breakthrough events (at the interface between clay and sample container) and in the steady state flow (through the clay). The recorded steady-state flow as a function of injection pressure is plotted in Figure 2-36.

At 112 h, the injection pressure was increased to 0.9 MPa and kept for about 22 hours without water breakthrough. The sample pressure responded weakly to this pressure increase, rising to 0.63 MPa. The steady-state flow continued to occur merely through the top filter and increased considerably as compared to the 0.75 MPa-state. Hence the steady-state flow response show non-linearities also in clays which are being injected in a small filter. In contrast to the typical response in samples with large injection filter, here the increase is stronger than linear (Figure 2-36).

As the injection pressure was further increased to 1.2 MPa, an instantaneous breakthrough event occurred (134 h). Once again the break through flow occurred at the interface between clay and sample holder, exiting through the guard filter.

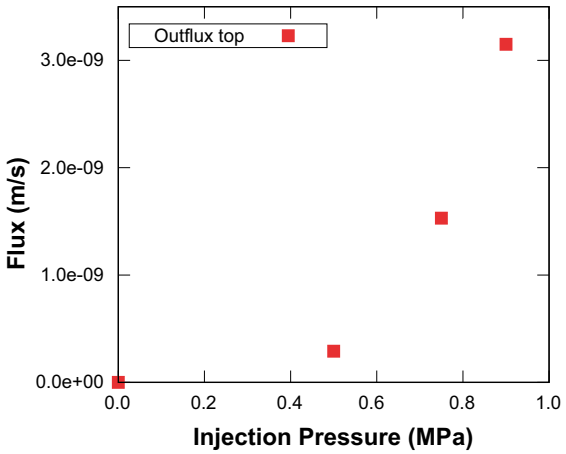

Figure 2-36. *Measured steady-state outflow in the top channel at different applied injection pressures in sample GenCh13. Note that the relative uncertainty is large for the low flow (near detection limit). The outflow through the guard filter was below detection limit for all of the displayed applied injection pressures.*

Table 2-16. Water breakthrough events in sample GenCh13.

Time (h)	Injection pressure step (MPa)	Sample pressure (MPa)	Path
33.77	1.0 → 2.0	0.635	Guard Filter
33.83	0.5 → 1.0	0.498	Guard Filter
33.90	0.5 → 1.0	0.621	Guard Filter
134.33	0.9 → 1.2	0.632	Guard Filter

2.2.1.3 PrefPath01

This sample was primarily tested for air response (see Section 3.2.1.2), but a small water pressure response test was performed before it was terminated. During the air pressure response tests, a substantial amount of erosion occurred under induced breakthrough events; the sample density at the time for water pressure response test was therefore very likely significantly below the nominal value. This notion was also confirmed by the relatively low value of P_s^0 (Figure 2-37). Because of low density and small sample height, it was not possible to extract this sample properly during dismantling. Therefore, no post-mortem density measurement was performed.

The water pressurization history of the sample is displayed in Figure 2-37. An injection pressure of 0.3 MPa, close to P_s^0, was applied (10 h) resulting in a very weak sample pressure response. This type of response is in accordance with the response in the previous samples with the same injection geometry. At 34 h the injection pressure was ramped up to 0.5 MPa at a rate of 0.05 MPa/h. A very weak sample pressure increase was observed during the ramping, while a larger increase was seen when the pressure was held constant at 0.5 MPa. After about one hour in this state a breakthrough event occurred (38 h). The flow path went through the sample, exiting in the top filter. This behavior is different from the breakthrough events occurring in sample GenCh13 (Section 2.2.1.2). It should be noticed that the height of the present sample is only 2 mm as compared to 5 mm for sample GenCh13.

Table 2-17. Properties of sample PrefPath01.

Material	Nominal density	Post-analysis	Cell type	h
WyNa	ρ_{dry} = 700 kg/m^3 ϕ = 0.745	not determined	C	2 mm

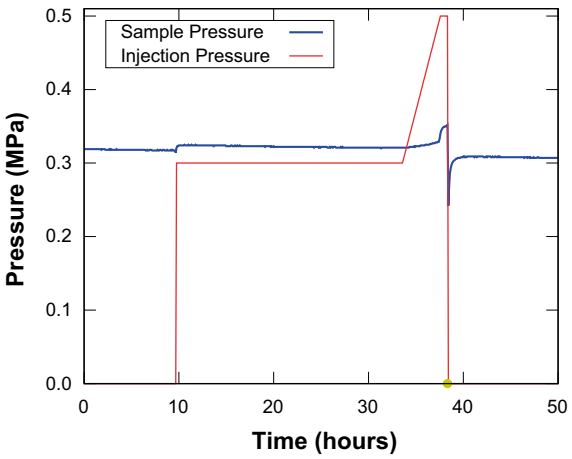

Figure 2-37. *Water injection (red) and sample (blue) pressure history in sample PrefPath01. The yellow dot on the time line indicates a breakthrough event.*

2.2.2 MX-80 Bentonite

2.2.2.1 GenCh11

The sample pressure history of this sample is found in Figure 2-38. The pressurization started with a quick step-up sequence to 1.6 MPa in injection pressure (0–42 h). When the injection pressure was below the sample pressure, the response in sample pressure was minor which is evident from the 18 hour period when the injection pressure was kept at 0.6 MPa (16–34 h). This response is in accordance with was observed in the pure Na-montmorillonite samples with the same injection geometry (Section 2.2.1). In contrast to these samples, however, a larger difference between injection pressure and sample pressure could be maintained without inducing breakthrough events when the injection pressure was above the sample pressure. This is clearly demonstrated during the over 200 hour period when the injection pressure was kept constant at 1.6 MPa (42–297 h). It is interesting to note that the sample pressure basically did not reach a steady value during this entire period. The transient times for sample pressure response can consequently be long although the sample size is quite small, which was also noted for sample GenCh04 (Section 2.2.1.1).

In a second sequence, the injection pressure was lowered in steps down to 0 MPa (297–441 h). The sample pressure response became less pronounced as the injection pressure lowered – in accordance with previous observations. A substantial hysteresis in P_s^0 was noted – as the injection pressure reached 0 MPa after the second pressure sequence the sample pressure was considerably higher, about 0.2 MPa (35%), than before the pressurization sequences. A similar type of hysteresis was noted in other MX-80 samples of similar density (see e.g. Section 2.1.2.1).

A third pressurization sequence was initiated at 852 h, when an injection pressure of 0.6 MPa was applied. The sample pressure response was weak as expected.

After performing gas pressurization tests on this sample (Section 3.2.2.1), two very long pressurization sequences was initiated, lasting for more than 6,000 hours (right diagram in Figure 2-38). In the first of these sequences, the pressure was increased in steps to a final injection pressure of 3.0 MPa. In each performed step stable sample pressures was achieved. The sample pressure response changed characteristics when the injection pressure increased: at low water pressure the sample pressure response was negligible, while at high water pressure the increase in sample pressure basically equaled the increase in water pressure. The latter behavior is similar to the sample pressure response at high water pressure in geometry a (Section 2.1). No water breakthrough events were induced although the injection pressure exceeded the sample pressure by approximately 0.75 MPa at the highest pressures. Furthermore, the highest applied injection pressure was more than 3 times larger than P_s^0. This type of stability was not seen in the less dense Na-montmorillonite samples (Section 2.2.1).

After the pressurization step-up sequence, the pressure was again lowered in steps down to zero. The corresponding sample pressure response was quite different as compared to the step-up sequence – the drop in pressure was significantly lower at the higher injection pressures, and significantly higher at the lower injection pressures. In fact, the drop in sample pressure was quite constant for the entire sequence.

Figure 2-39 displays the corresponding sample pressures at different injection pressures and the corresponding steady-state fluxes. For pressurization sequences 1–3, the steady-state flux shows the same type of non-linearity as was observed in other samples with point injection (Section 2.2.1), with an accelerated increase in flow as the injection pressure is increased. In the fifth sequence, however, the flux does not at all behave in this way: the flux drops from a large value back to zero in an approximately linear way, a behavior which more resemble the flux response in tests with the injection filter covering the whole bottom area of the test cell (Section 2.1). Note that the flux was only measured at the highest injection pressure in the fourth pressurization sequence (which is the same point as for the highest injection pressure of sequence 5).

Table 2-18. Properties of sample GenCh11.

Material	Nominal density	Post-analysis	Cell type	h
MX-80	ρ_{dry} = 1,179 kg/m^3 ϕ = 0.571	ρ_{dry} = 1,097 kg/m^3 ϕ = 0.601	B	5 mm

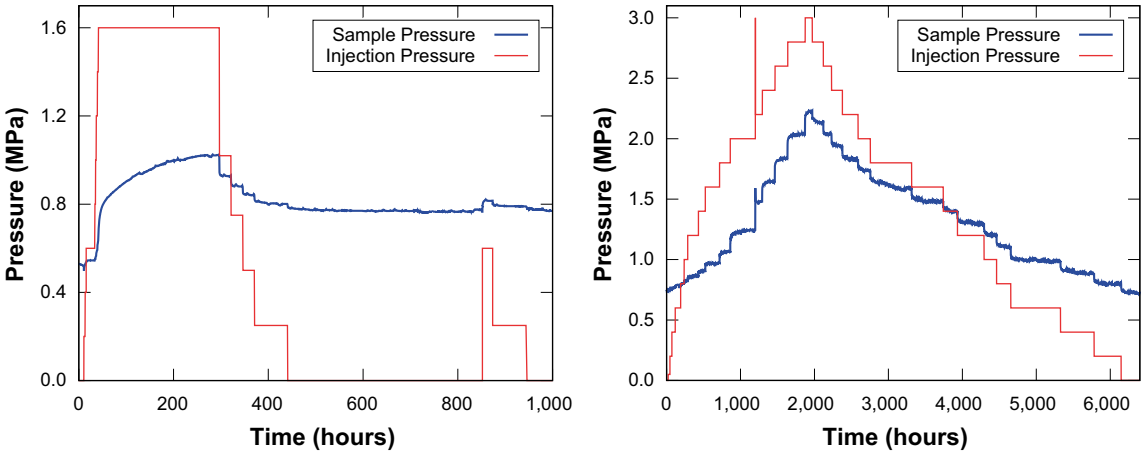

Figure 2-38. *Water injection (red) and sample (blue) pressure history (left: sequences 1–3, right: sequences 4 and 5) in sample GenCh11.*

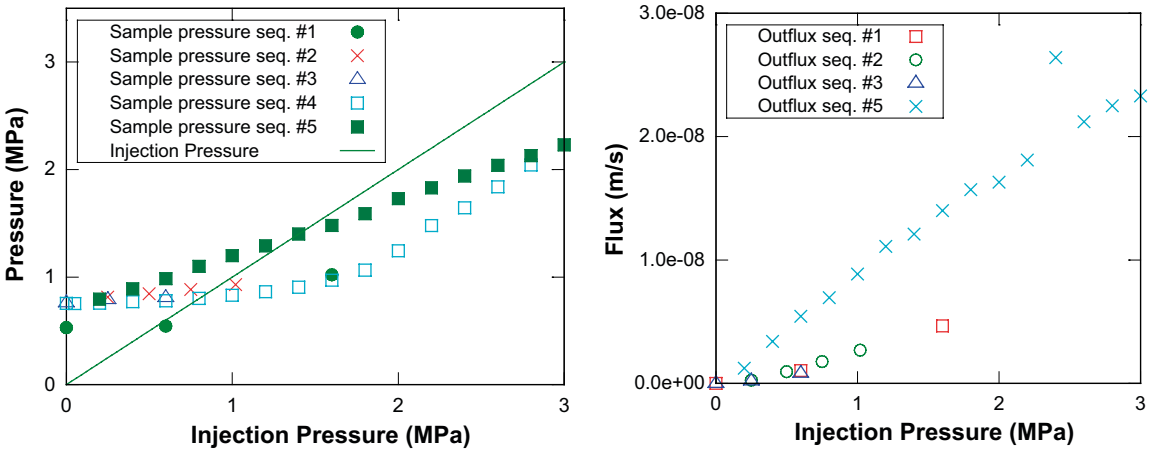

Figure 2-39. *Steady-state sample pressure (left) and in- and outflows (right) at different applied injection pressures in sample GenCh11. Note that the relative uncertainty is large for the low flow (near detection limit).*

2.2.2.2 PrefPath02

The pressurization history of this sample is shown in Figure 2-40. Initially a water injection pressure of 5.0 MPa was applied (11 h), a pressure corresponding to more than 3 times P_s^0. Initially, this pressurization gave a rather weak sample pressure response (the order of 0.1 MPa). However, the sample pressure never reached a steady value, and after about 15 hours started to display an accelerated pressure increase, ending in a water breakthrough event (31 h). Hence, the time scale for processes can be rather long also in a sample as small as this (height ~ 2 mm). The breakthrough event occurred *through* the sample, i.e. water was detected through the top filter. The details of the sample pressure response during this pressurization are shown in the right diagram of Figure 2-40.

Table 2-19. Properties of sample PrefPath02.

Material	Nominal density	Post-analysis	Cell type	h
MX-80 Bentonite	ρ_{dry} = 1,179 kg/m^3 ϕ = 0.571	ρ_{dry} = 1,189 kg/m^3 ϕ = 0.568	C	2 mm

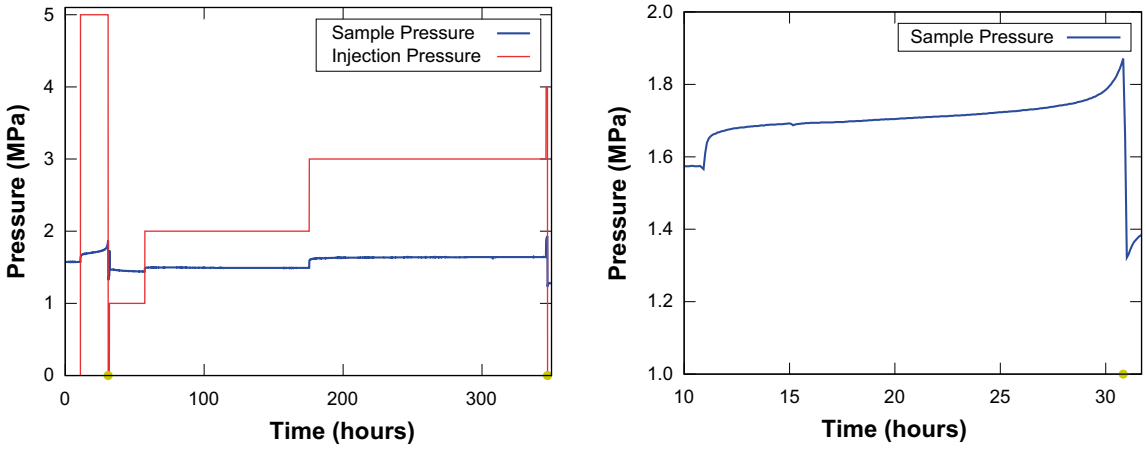

Figure 2-40. *Water injection (red) and sample (blue) pressure history in sample PrefPath02. The right diagram shows a magnification of the period 10–32 h. The yellow dots on the time line indicate breakthrough events.*

After the initial breakthrough event, injection pressure was increased in steps of 1.0 MPa. Stable states were achieved (at least on the time scale of 100 hours) both with applied injection pressure of 2.0 MPa and 3.0 MPa. For both of these pressures, the corresponding sample pressure response was small. This is somewhat in contrast with observations made in sample GenCh11, which showed larger response at similar injection pressures (Section 2.2.2.1). It should be kept in mind, though, that P_s^0 is considerably larger in the present sample. Similar to sample GenCh11, a rather large difference between injection pressure and (stable) sample pressure could be maintained (with the injection pressure exceeding the sample pressure) – in the present case the largest difference measured was ca 1.36 MPa.

When the pressure was increased from 3.0 MPa to 4.0 MPa a second water breakthrough event occurred approximately one hour after the pressure increase (347 h). Also this time the breakthrough occurred through the sample, flowing out at the top of the cell. The much smaller amount of time before breakthrough in the second event might suggest a memory of the path formed in the first event. It could, however, also be so that unnoticed mechanical processes where active during the 2.0 MPa and 3.0 MPa pressurizations.

Table 2-20. Water breakthrough events in sample PrefPath02.

Time (h)	Injection pressure (step) (MPa)	Sample pressure (MPa)	Path
31	5.0	1.871	Top Filter
347	4.0 → 5.0	1.931	Top Filter

2.2.3 Ca-montmorillonite

2.2.3.1 GenCh01

This test constituted a prototype test for geometry B (see Figure 3-1). A small injection hole was accomplished in a cell of type A (see Figure 3-1) by placing a thin copper plate with a 5 mm diameter hole drilled in it, between the bottom filter and the clay sample (see Figure 2-41). The pressure response of the sample was probably influenced by this design, and comparisons with other samples with this injection geometry should be made with caution. For completeness, however, also the results of this test are presented here.

Table 2-21. Properties of sample GenCh01.

Material	Nominal density	Post-analysis	Cell type	h
KuCa	ρ_{dry} = 1,200 kg/m^3 ϕ = 0.586	ρ_{dry} = 1,130 kg/m^3 ϕ = 0.598	B (prototype)	5 mm

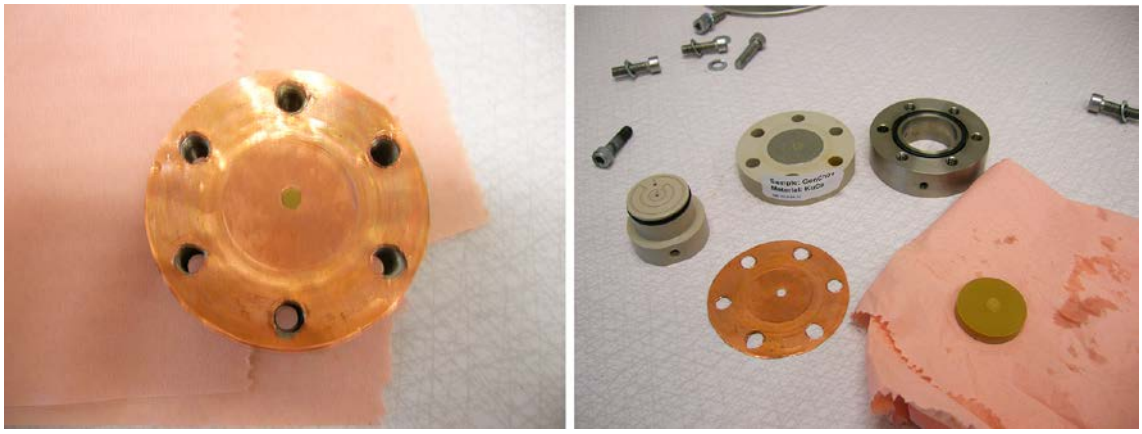

Figure 2-41. *Sample GenCh01 after termination. The left picture shows the copper plate (with the central injection hole) covering the sample. The right picture show the dimantled test cell and the actual clay sample (lower left).*

A first injection pressure step-up sequence was performed up to a maximum injection pressure of 1.6 MPa (0–332 h). The sample pressure response was weak for low pressures but increased with increasing injection pressure. For the two highest injection pressures (0.8 MPa and 1.6 MPa), the sample pressure was below injection pressure. At 332 h the inflow was turned off giving a gradual lowering of the injection pressure as the water flowed through. As the pressure dropped it was noticed that P_s^0 was significantly lower than before the performed pressure step-up sequence.

At 404 h the injection pressure was increased to 1.6 MPa giving basically identical sample pressure response as before. Again the inflow was turned off (414 h), leaving the sample to slowly lose its pressure.

In a second pressure step-up sequence (573–741 h), injection pressure was increased to a maximum of 0.8 MPa. It can be noted that no breakthrough events was induced in neither of the two pressure step-up sequences.

Figure 2-43 shows measured steady-state sample pressures and fluxes. Fluxes were only measured in the first pressure step-up sequence.

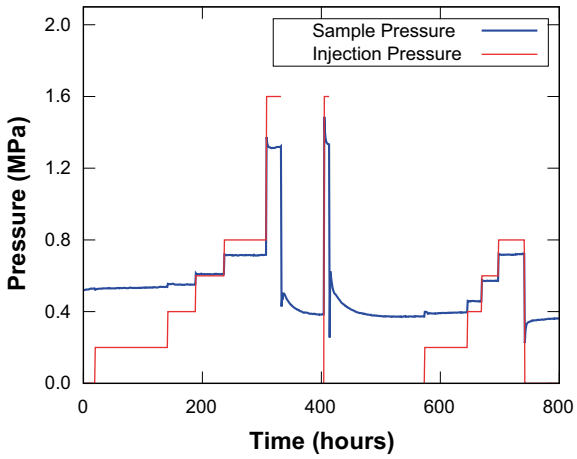

Figure 2-42. *Injection (red) and sample (blue) pressure history in sample GenCh01.*

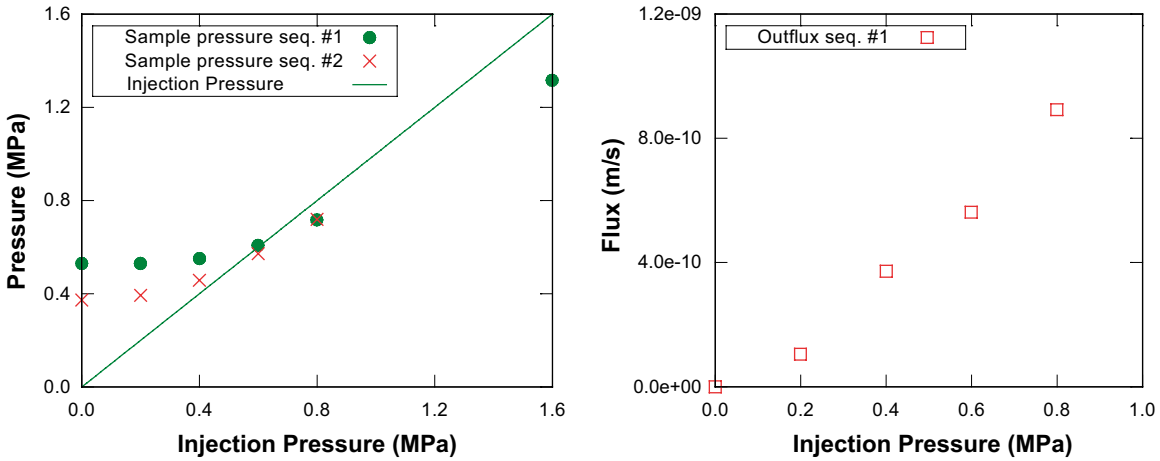

Figure 2-43. *Steady-state sample pressure (left) and in- and outflows (right) at different applied injection pressures in sample GenCh01.*

2.3 Summary: water pressure gradient tests

The following list summarizes the observed behavior of bentonite/montmorillonite samples exposed to external water pressure differences.

- Non-linear response in sample pressure.
  - Using injection filter of type A gives a typical sample pressure increase of half the applied injection pressure, when the applied injection pressure is low compared to P_s^0. Using injection filter of type B, the sample pressure response is negligible in the same pressure regime.
  - At injection pressures substantially larger than P_s^0, the sample pressure increase typically equals the increase in injection pressure in both types of injection geometries.
  - In some cases where injection filter type B were used, states could be maintained where the injection pressure was substantially higher than the sample pressure. This was not the case for injection using filter type A.
- Non-linear response in water flow.
  - For filter type A, Darcy's law hold up to applied water pressure of approximately two times P_s^0 (i.e. a linear dependence between steady-state flow and applied water pressure). At higher pressures the flow increase is weaker than linear.
  - In geometry B, the flow response is negligible at low injection pressures (in comparison with P_s^0). At higher pressures (in the samples which can maintain them), the flow increase with increasing injection pressure is stronger than linear.
  - In the samples with guard filters (type C), it can be concluded that this type of flow mainly occurs through top filter.
- Water breakthrough events.
  - Events were induced in several samples, where the system seems to "break". During these events, the flow completely changes characteristics as compared to "normal" flow; in particular the flow rates increase tremendously (a factor 10^4 or more).
  - The events only occur when injection pressure exceeds sample pressure. States have also been maintained, however, with injection pressures significantly larger than sample pressure without induced breakthrough events.
  - In many cases the flow during these events follows the interface between sample holder and clay, in contrast to the "normal" flow which goes through the clay.
  - In the two MX-80 samples tested with point injection (geometry B and C), states with water injection pressures considerably higher than sample pressure could be maintained. In the thinnest sample (2 mm) breakthrough occurred *through* the clay.

- The process of inducing a breakthrough event has a complex time dependence – by quickly ramping up injection pressure, higher (sample) pressure states could be maintained before breakthrough. Also, in the 2 mm MX-80 sample tested in geometry C, it took 19 hours before the breakthrough occurred after increasing the injection pressure to three times P_s^0.

- Strong density response, i.e. the clay redistributes in an external water pressure gradient, as observed in samples with injection filters of type A.
- Hysteresis in P_s^0
  - When "coming back" to zero gradient, some of the samples show substantial increase of P_s^0 (up to 60% increase).
- Friction between the clay and the wall of the container was observed in the longer MX-80 samples, which showed lower sample pressure than applied water pressure in geometry A.
- Although the tested samples are small in size, the transient times for the sample pressure response are sometimes long, up to several hundred hours.

3 External air pressure difference

This chapter describes the performed tests of pressure and flow response due to applied external air pressure differences. The experimental set-up is in principal the same as for the water pressure difference tests (Chapter 2), although the boundaries need some extra concern in this case. A well-defined swelling pressure requires the bentonite to have access to external water. When pressurizing the system with air, the boundary condition thereby becomes rather complicated as schematically illustrated in Figure 3-1. In the present set-up, the top side of the sample is always contacted with water. This water is kept at atmospheric (absolute) pressure, or slightly above (dm:s of water column). The inlet tube was filled with air before connecting it to the pressure controlling unit. As the water in this unit pushes on the confined air, the pressurized gas/clay interface at the bottom of the sample is thereby created.

Note that the described set-up implies, in principle, that when the inlet is not pressurized there is a water pressure gradient applied over the sample, transporting water to the inlet. In these tests this water pressure gradient is very small, but it cannot be guaranteed that the fluid/clay interface at the inlet (the bottom filter) initially is not water/clay rather than air/clay. Furthermore, it is likely that the bottom filter initially contains some water, although the bottom part of the test cell usually was treated with (partial) vacuum before the tests, in order to get rid of residual water.

Consequently, initial effects due to water pressurization might be expected in these tests, and the knowledge of sample pressure response due to water pressure gradients, reported in the previous chapter, is of great value when interpreting the present tests.

As in the case of the water pressure gradient test, these tests consist of certain sequences of applied injection pressures. Table 3-1 summarizes the samples on which air pressure gradient tests have been performed. Below follows a description of the tests on each specific sample.

Table 3-1. Samples on which air pressure gradient tests was performed.

	Sample-Id	Material	Nominal dry density (kg/m^3)	Injection filter	Max. injection pressure (MPa)	Height (mm)
1.	GenCh11	MX-80	1,179	B (small)	1.0	5
2.	GenCh12	WyNa	700	A (large)	0.9	5
3.	GenCh13	WyNa	700	C (small+guard)	0.75	5
4.	PrefPath01	WyNa	700	C (small+guard)	1.2	2
5.	PrefPath02	MX-80	1,179	C (small+guard)	5.0	2
6.	GenCh21	MX-80	1,166	A (large)	5.0	20
7.	GenCh22	WyCa	1,200	A (large)	5.0	5
8.	GenCh23	WyCa	1,250*)	A (large)	5.0	5–8*)
9.	WP3Bench	MX-80	1,179	A (large)	5.0	5

*) Successively volume expanded, see Section 2.1.3.3.

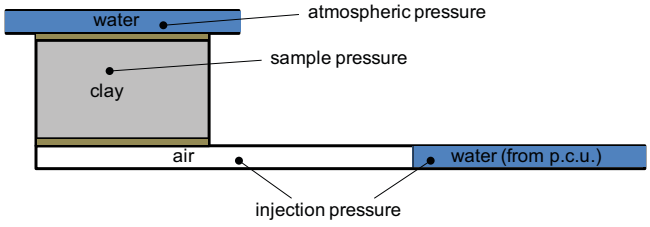

Figure 3-1. *Set-up schematics for air pressure gradient tests.*

3.1 Injection filter A

3.1.1 Na-montmorillonite

3.1.1.1 GenCh12

In order to evaluate the effect of having (unwanted) water at the clay interface when pressurizing with air, the tests in this sample started by investigating the sample pressure response as a water phase is replaced by air at the inlet at a fixed injection pressure. This was accomplished by preparing the system as described above, but with the difference that a minor amount of water was intentionally left at the inlet, thereby creating a pressurized water/air/water system as illustrated in Figure 3-3.

The sample pressure response as the water in the front of the inlet tube entered and flowed through the clay sample is shown in Figure 3-4. The initial sample pressure increase (19 h) is in complete accordance with what is expected from water pressure gradient test is this geometry (see Section 2.1.1.3). It is further seen that the sample pressure drops back to the initial pressure (P_s^0) as air replaces water at the inlet. Hence it is demonstrated that the chosen experimental set-up do function in a satisfying way, i.e. that a pressurized air/clay interface is established in these systems.

Also, the observation that the sample pressure equals P_s^0 when an air pressure gradient is imposed implies that a sample pressure response to air pressure is absent. The fact that air and water gives very different sample pressure response in the present geometry makes it easy to verify when the system is pressurized by air, and was used frequently during the course of the tests.

Table 3-2. Properties of sample GenCh12.

Material	Nominal density	Post-analysis	Cell type	h
WyNa	ρ_{dry} = 700 kg/m^3 ϕ = 0.745	ρ_{dry} = 616 kg/m^3 ϕ = 0.776	A	5 mm

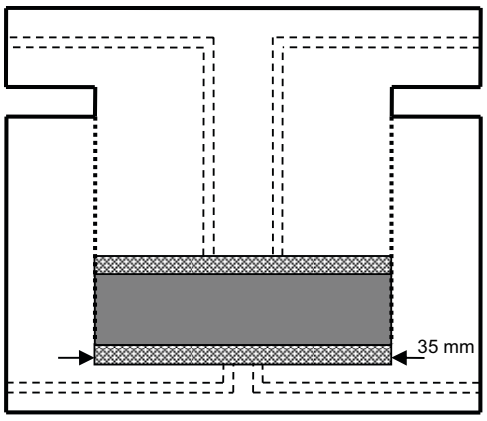

Figure 3-2. *Schematic illustration of injection filter geometry type A.*

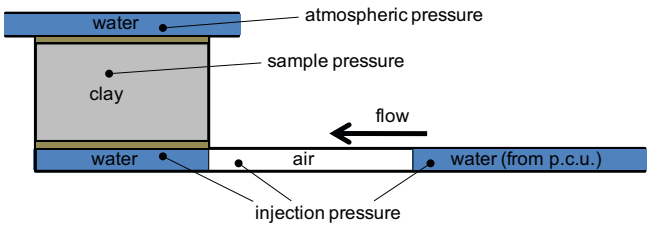

Figure 3-3. *Schematics of the water/air injection test in GenCh12.*

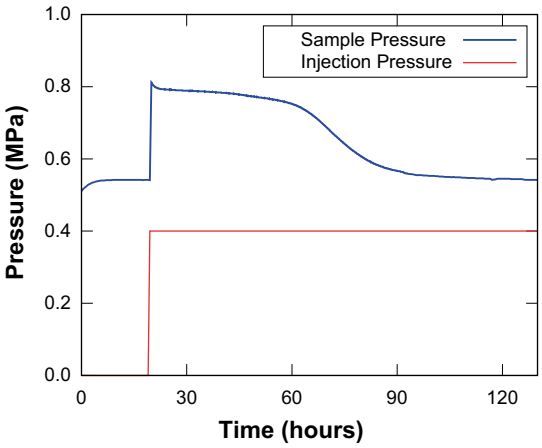

Figure 3-4. *Sample pressure repsonse in the water/air injection test in GenCh12. The initial response when the injection pressure is increased to 0.4 MPa is in full accordance with the response to a water pressure gradient in this type of sample. As water flows through and is replaced by air, the sample pressure drops back to* P_s^0. *Note that the injection pressure is constant (0.4 MPa) throughout the process.*

The complete pressurization/response history of the sample is found in Figure 3-5. At about 142 h the injection air pressure was lowered to 0.1 MPa. A quite large transient response is seen in the corresponding sample pressure evolution, but it is also seen that the equilibrium pressure again approaches P_s^0. The same type of transient behavior, but less pronounced, is seen when the air pressure is further lowered to zero (at 158 h). These observations further confirm that equilibrium sample pressure is insensitive to applied air pressures below P_s^0.

At 261 h, the injection pressure was increased to 0.1 MPa, with a resulting transient pressure peak. The air pressure was then quickly ramped up from 0.1 to 0.5 MPa and then kept constant at 0.5 MPa. Once again a transient peak of the sample pressure was observed as well as an equilibration towards P_s^0.

During this stage of an imposed air pressure difference of 0.5 MPa over the sample, a steady flow through the sample was measured. This flow was detected by measuring displacement of water on the outflow side of the sample. By flushing the outflow side, air bubbles was revealed, indicating that the detected flow was an air flow. The outflow rate was determined to $2.6 \cdot 10^{-9}$ m/s which is considerably lower than the corresponding flow under water pressurized conditions (see Section 2.1.1.3). A main candidate for this flow is for it to be a diffusive flow of dissolved air. The reasonability of this assumption can be estimated as follows.

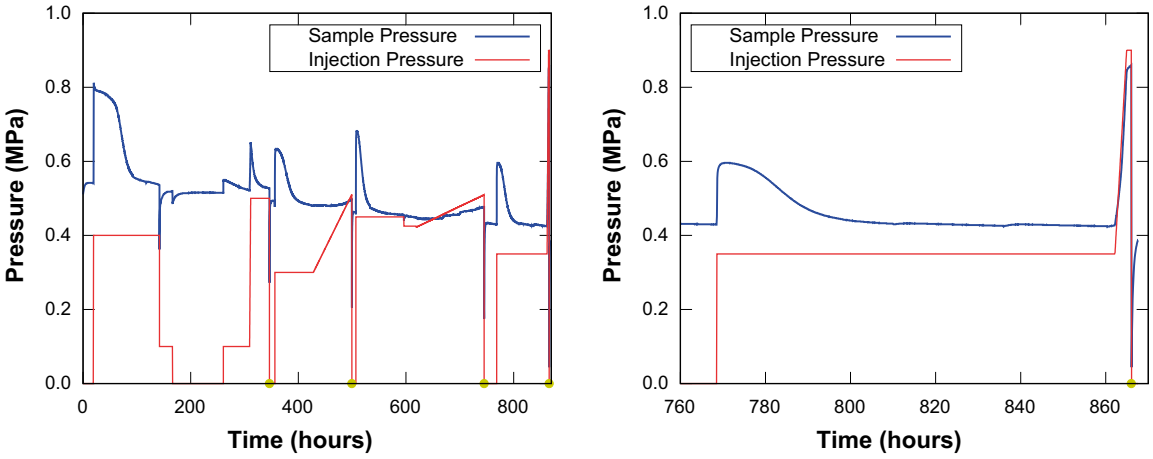

Figure 3-5. *Air injection (red) and sample (blue) pressure history in sample GenCh12. The right diagram shows a magnification of the period 760–870 h.The yellow dots on the time line indicates breakthrough events. The initial pressurization is actually by water (see Figure 3-4). Also, the sample pressure repsonse directly after the breakthrough events suggests that there is residual water left in the injection filter which is being pressurized initially.*

The volumetric flow on the outlet side, q, is related to the diffusive flux, $j = -D_e \nabla c_{air}$ by the molar volume of the gas on the outlet side, v_{outlet}. This molar volume, in turn, can be evaluated using the ideal gas law $v_{outlet} = RT/P_{outlet}$, where T is absolute temperature, R the universal gas constant and P_{outlet} (absolute) pressure on the outlet side

$$q = j \cdot v = -D_e \nabla c_{air} \frac{RT}{P_{outlet}} \tag{3-1}$$

The steady-state concentration gradient of dissolved air can be converted to the external pressure difference by assuming Henry's law ($c_{air} = P/K_H$)

$$\nabla c_{air} = \frac{P_{outlet} - P_{inlet}}{K_H \cdot h} \tag{3-2}$$

where K_H is Henry's constant for air and h is the height of the clay sample (Figure 1-1). Combining Equations 3-1 and 3-2 gives an expression for the diffusion coefficient

$$D_e = q \cdot \frac{K_H \cdot h}{RT} \frac{P_{outlet}}{P_{inlet} - P_{outlet}} \tag{3-3}$$

By plugging in the known/measured quantities in this expression and assuming the value for Henry's constant to equal that for nitrogen in bulk water, 0.16 MPa/mM (Sander 1999), gives an estimate for the diffusion coefficient

$$D_e \approx 1.3 \cdot 10^{-10} \text{ m}^2/\text{s} \tag{3-4}$$

This is a reasonable value for gas diffusion in compacted clay (Jacops et al. 2015) and this estimation is a strong indication that the identified gas flow, when the injection pressure is below P_s^0, is air diffusion.

At ca 346 h a breakthrough event occurred, and the reservoir of pressurized air quickly emptied. Also, the tailing water from the pressure controlling unit (see Figure 3-3) continued to quickly flow through the sample after the air reservoir was emptied. Apparently, the pathway opened by the gas was also accessible for water. As a consequence the pressure controlling device was emptied of water and quite a lot of erosion of the sample occurred during the breakthrough event. Hence, the lower equilibrium pressure after the event should be ascribed to mass loss of the sample. It is worth noting that this particular air breakthrough occurred when the injection pressure (0.50 MPa) was slightly lower than the sample pressure (0.53 MPa).

After this gas breakthrough event, an air pressure difference of 0.3 MPa was imposed over the sample (357 h). Judging from the sample pressure response, and given the knowledge gathered about the different types of responses to different fluids, it is seems very likely that there was some water being expelled from the injection filter at the beginning of this pressurization. After a stable sample pressure was established (P_s^0), the injection air pressure was ramped up at a speed of 0.00294 MPa/h. The sample pressure response to this ramping was very small, again showing that equilibrium sample pressure is independent of air pressures below P_s^0. When the inlet pressure had reached 0.51 MPa (499 h), a second gas breakthrough event occurred at a sample pressure of 0.50 MPa, i.e. just when the gas pressure exceeded the sample pressure. Also this breakthrough event flushed the sample with quite a lot of tailing water, resulting in further erosion and a drop in P_s^0.

At around 507 h an injection pressure of 0.45 MPa was applied. The same type of transient behavior as previously was seen, indicating initial pressure response due to residual water at the sample interface. The sample pressure then dropped almost below the injection pressure, and to avoid a breakthrough at this stage, the injection pressure was lowered to 0.425 MPa (at 596 h).

At 618 h, a slow ramping of the injection pressure was started, at the speed of $6.94 \cdot 10^{-4}$ MPa/h. A weak sample pressure response was observed, and a state where the injection pressure was larger than the sample pressure was maintained during approximately 94 hours before a breakthrough event occurred (745 h). The difference between injection pressure and sample pressure was however never larger than 0.033 MPa. At the breakthrough, the sample pressure was 0.48 MPa and the injection pressure 0.51 MPa.

Next, in order to investigate the influence of time on the process, a fast ramping procedure was conducted at the speed of 0.2 MPa/h up to an injection pressure of 0.9 MPa (after an equilibration

phase with injection pressure 0.35 MPa in order to expel residual water). In this case, as seen in detail in the right diagram of Figure 3-5, the sample demonstrated a quite substantial sample pressure response. Also, injection pressure exceeded sample pressure for about 3 hours, with a maximum difference of 0.08 MPa. After the injection pressure had reached 0.9 MPa, it took about an hour before a break-through occurred (866 h).

All breakthrough events of sample GenCh12 are summarized in Table 3-3.

Table 3-3. Air breakthrough events in sample GenCh12.

Time (h)	Injection pressure (MPa)	Sample pressure (MPa)	Tailing water
346	0.50	0.527	Yes
499	0.51	0.498	Yes
745	0.51	0.477	Yes
866	0.9	0.86	Yes

The overall conclusion from the gas response tests performed on this sample is that the equilibrium sample pressure is not affected by gas pressure as long as the gas pressure is below P_s^0 (which is in deep contrast to the response to water – compare Figure 2-6 and Figure 3-5). In these states gas is transported through the clay only due to dissolution and diffusion. When gas injection pressure exceeds sample pressure, the system appears rather unstable, and gas breakthrough events are easily induced.

These observations indicate that the criterion for air to enter the system (as a separate phase) is that air pressure exceeds sample pressure. By increasing injection pressure quickly (above P_s^0), rather large transient sample pressure responses can be achieved.

3.1.2 Ca-montmorillonite

3.1.2.1 GenCh22

The applied air pressurization protocol and corresponding sample pressure response of this sample is shown in Figure 3-6. A P_s^0 of 0.96 MPa was noted before pressurization. The first 100 hours of pressurization (injection pressure 0.7 MPa) shows the typical response due to water pressurization. At about 100 hours the sample pressure dropped quickly back to P_s^0 as air replaced water at the inlet interface. It is thus verified that also pure Ca-montmorillonite shows the characteristic difference in response of the sample pressure depending on whether water or gas is the pressurizing fluid; the pressure response due to gas pressurization is absent at injection pressures below P_s^0, as was also demonstrated in Na-montmorillonite (Section 3.1.1).

At 208 h the injection pressure was increased first to 1.0 MPa, for approximately an hour, and then to 1.1 MPa. A gas breakthrough event occurred after keeping the pressure at 1.1 MPa for about an hour. In contrast to the sample of Na-montmorillonite using the same cell type (Section 3.1.1.1), this breakthrough event ceased when water from the pressure controlling unit reached the clay. At this point water was again the pressurizing fluid at the inlet interface, which is also evident from the sample pressure response, which is in accordance with results from water pressurization tests (Section 2.1.3.2). At 226 h the system was refilled with gas and an injection pressure of 0.7 MPa was applied. Again, an initial water response of the sample pressure was followed by a drop to P_s^0. This state was kept stable for a long time (> 200 hours) after which a quick ramping of the injection pressure was initiated, at a rate of 0.36 MPa/h. A gas breakthrough event was induced as soon as the injection pressure became comparable in size to P_s^0 (490 h).

Table 3-4. Properties of sample GenCh22.

Material	Nominal density	Post-analysis	Cell type	h
WyCa	ρ_{dry} = 1,200 kg/m^3 ϕ = 0.564	ρ_{dry} = 1,137 kg/m^3 ϕ = 0.605	A	5 mm

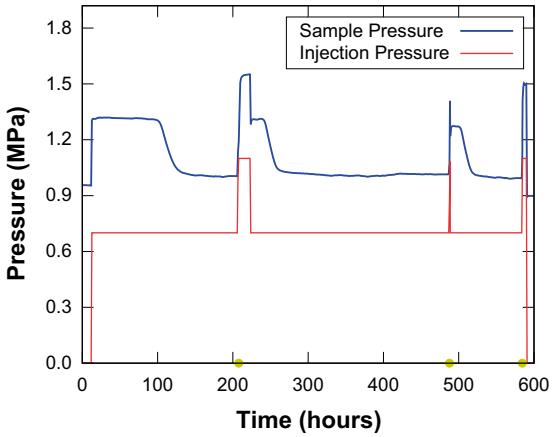

Figure 3-6. *Air injection (red) and sample (blue) pressure history of sample GenCh22. The yellow dots on the time line indicates breakthrough events. The initial pressurization is actually by water. Also, the sample pressure repsonse directly after the breakthrough events suggests that there is residual water left in the injection filter which is being pressurized initially.*

A third pressurization at 0.7 MPa was initiated after refilling the system with gas (491h – 586 h). At 586 h a new pressure ramping at 0.36 MPa/h was started, and a gas breakthrough event occurred when the injection pressure was in the range 0.96 MPa and 1.0 MPa, i.e. at P_s^0 (587 h).

Note that as the pressure was released (593 h), a P_s^0 (0.9 MPa) lower than what was measured before the performed air pressurization sequence was observed. A significant drop in P_s^0 was also observed after performing a water pressure gradient test on this sample (Section 2.1.3.2), while only minor hysteresis in this variable was detected when the sample was uniformly pressurized with water (Section 4.1.2.1).

It is also worth noting that this sample was purposefully prepared to initially be more inhomogeneous than the other samples tested – the test cell was filled with coarse grains of dry Ca-montmorillonite rather than finely milled powder, as shown in Figure 3-7. Despite this way of preparing the sample, the gas migration behavior is comparable with that observed in all other samples, which demonstrates that the Ca-montmorillonite homogenizes to a high degree also in rather low density systems (no sustained preferential paths within the clay).

All breakthrough events of sample GenCh22 are summarized in Table 3-5.

Figure 3-7. *The dry Ca-montmorillonite grains used in the preparation of sample GenCh22. These were placed directly in the test cell, as shown in the picture, during preparation of the sample.*

Table 3-5. Air breakthrough events in sample GenCh22.

Time (h)	Injection pressure (MPa)	Sample pressure (MPa)	Tailing water
210	1.1	~ 1.19	No
490	0.88–1.03	~ 1.08	No
587	0.96–1.0	1.1	No

3.1.2.2 GenCh23

This sample was tested for response due to gas pressurization at three different densities (see Section 2.1.3.3).

1,250 kg/m^3

The pressurization protocol and corresponding sample pressure response for (nominal) density 1,250 kg/m^3 is shown in Figure 3-8. This sample had a recorded value of P_s^0 at this density of about 2.1 MPa (see Section 4.1.2.2) and was initially exposed to an injection pressure of 1.5 MPa. The sample pressure response is a bit different as compared to other observations, as well as compared to responses in the same sample at lower density (see below). The sample pressure is initially strongly elevated above P_s^0 which indicates water pressurization (the typical behavior) but the drop in sample pressure, due to air replacing water in the injection filter, occurred more slowly as compared to many other samples. At 72 h the pressure was released for a short moment while the system was replenished with air. After this event a "normal" response in sample pressure was observed – first a significant increase due to water pressurization and then a (quick) drop back to P_s^0 (72–100 h). The reason for the slow response during the initial pressurization has not fully been identified, but may be attributed to strong(er) fiction forces in this sample (this sample has the highest average density of the tested samples).

Table 3-6. Properties of sample GenCh23.

Material	Nominal density	Post-analysis	Cell type	h
WyCa	ρ_{dry} = 1,250 kg/m^3 ρ_{dry} = 1,042 kg/m^3 ρ_{dry} = 893 kg/m^3 ρ_{dry} = 781 kg/m^3	Not made	A	5–8 mm (sample expanded)

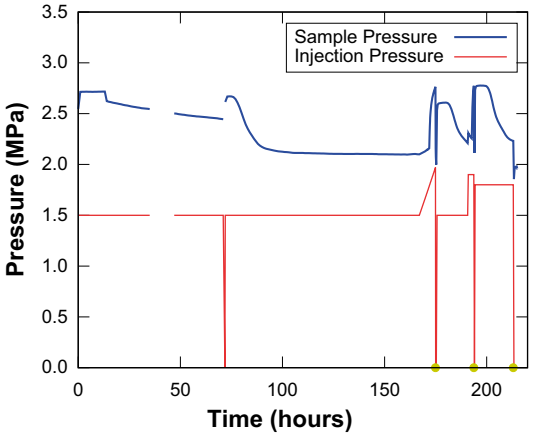

Figure 3-8. *Air injection (red) and sample (blue) pressure history of sample GenCh23 at nominal dry density 1,250 kg/m^3. The yellow dots on the time line indicates breakthrough events.The initial pressurization is actually by water. Also, the sample pressure repsonse directly after the breakthrough events suggests that there is residual water left in the injection filter which is being pressurized initially.*

An injection pressure ramping at 0.06 MPa/h was initiated at 167 h and a gas breakthrough event occurred at 172 h, when the injection pressure was ~ 1.8 MPa, ca 0.35 MPa below sample pressure. In the major part of the recorded breakthrough events recorded in this study, breakthrough occurred when injection pressure equaled or exceeded sample pressure. The deviation from this behavior in this sample may signify qualitative differences in breakthrough behavior as compared to the other tested samples. It should be kept in mind, however, that the sample pressure is measured at the top side of the sample, while the gas pressure is applied at the bottom. If friction forces are present, the pressure which actually prevail at the bottom of the sample may be different from that measured at the top.

After the breakthrough event, the set-up was refilled with gas and again pressurized at 1.5 MPa. The sample pressure responded in the expected way as air replaced water at the injection filter. At 191 h, injection pressure was increased to 1.9 MPa, and after less than two hours a new breakthrough event occurred. The system was immediately refilled with gas and pressurized at 1.8 MPa. During the characteristic decline of the sample pressure following this pressurization a third breakthrough event occurred (213 h).

All recorded breakthrough events for this sample at nominal density 1,250 kg/m^3 are summarized in Table 3-7.

Table 3-7. Air breakthrough events in sample GenCh23 at nomial density 1,250 kg/m^3.

Time (h)	Injection pressure (MPa)	Sample pressure (MPa)	Tailing water
172	1.785	2.158	No
193	1.9	2.256	No
213	1.8	2.232	No

1,042 kg/m^3

Prior to this gas test, P_s^0 was ~ 0.32 MPa of this sample at (nominal) density 1,042 kg/m^3. Figure 3-9 shows the applied gas pressurization protocol and corresponding sample pressure response. Initially, an injection pressure of 0.25 MPa was applied, and the sample pressure showed water pressurization response (8–60 h). As air replaced the water at the inlet interface, the sample pressure dropped back to P_s^0 (60–100 h). This state, with the sample being pressurized by air at 0.25 MPa, was then maintained for approximately 300 hours. At 420 h, the injection pressure was released for a short period as the system was replenished with gas. The sample pressure before and after this event is seen to differ slightly, which may indicate friction in the system.

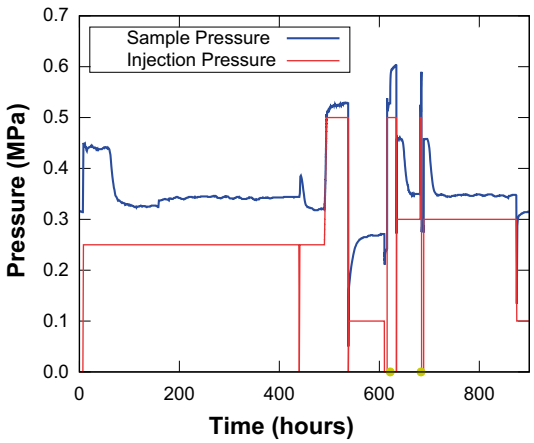

Figure 3-9. *Air injection (red) and sample (blue) pressure history of sample GenCh23 at nominal dry density 1,042 kg/m^3. The yellow dots on the time line indicates breakthrough events.The initial pressurization is actually by water. Also, the sample pressure repsonse directly after the breakthrough events suggests that there is residual water left in the injection filter which is being pressurized initially.*

At 520 h ramping of the injection pressure up to 0.5 MPa was initiated, at a rate of 0.06 MPa/h. The state with injection pressure of 0.5 MPa was maintained for 43 hours, without inducing any gas breakthrough event. Note that the injection pressure in this state is below the sample pressure, although it is significantly above P_s^0.

The injection pressure was subsequently completely released for a short while, as the system was refilled with gas, before it was repressurized at 0.1 MPa. The corresponding sample pressure dropped to almost zero (571 h). This behavior strongly indicates that the sample was consolidated by the gas in the previously pressurized state (0.5 MPa) – as pressurization was released, the clay body basically did not fill out the cell volume. This interpretation is further supported by the continued sample pressure response, which increases in a manner typical for a sample taking up external water. Yet another argument for this interpretation is to compare this pressure response with that of a corresponding pressure drop as water is the pressurizing fluid; as seen in e.g. Figure 2-24, a drop in external water pressure of several MPa barely induces any drop at all below P_s^0 in sample pressure.

Note that the sample at this stage equilibrated at a pressure quite a bit lower than the previously recorded value of P_s^0 (0.27 MPa). The interpretation of this behavior is not straightforward, as many processes are at play simultaneously (swelling of a previously consolidated clay body, gas pressurization).

At 610 h, injection pressure was released and the system replenished with gas. At 616 h, an injection pressure of 0.5 MPa was applied, and about 5 hours later a gas breakthrough event occurred. The sample pressure was again larger than injection pressure, also before the breakthrough event, but its significant increase in connection with the event clearly demonstrates that water replaced air at the inlet interface.

Yet a strong indication that water is pressurizing at this time, in contrast to the previous 0.5 MPa pressure pulse, is given by the sample pressure response as the injection pressure was released (621 h) – this time the sample pressure only displayed a minor drop below P_s^0.

After the pressure release, the system was again filled with gas and an injection pressure of 0.3 MPa was applied. After the sample pressure response confirmed that residual water had flowed through (i.e. confirming that gas is the pressurizing fluid), injection pressure was instantly increased to 0.5 MPa. The behavior was similar to the previous 0.5 MPa pressurization: a gas breakthrough event was induced after some hours, and the sample pressure was larger than injection pressure at all times (also before breakthrough).

Lastly, an injection pressure of 0.3 MPa was applied and kept for a long time. The sample pressure response was very similar to before.

All recorded breakthrough events for this sample at nominal density 1,042 kg/m^3 are summarized in Table 3-8.

Table 3-8. Air breakthrough events in sample GenCh23 at nomial density 1,042 kg/m^3.

Time (h)	Injection pressure (MPa)	Sample pressure (MPa)	Tailing water
622	0.5	0.528	No
683	0.5	0.525	No

893 kg/m^3

The pressure evolution during testing of the sample at (nominal) density 893 kg/m^3 is displayed in Figure 3-10. The gas response testing of this sample started immediately after it had been exposed to an external water pressure difference of 0.2 MPa. The injection fluid was then changed to air (as always with some residual water left in the injection filter) and an injection pressure of 0.05 MPa was applied. The sample pressure response was initially due to pressurization from residual water and later dropped down to P_s^0 (~ 0.075 MPa) as air was entering the interface to the clay (72 h – 100 h). In this state, when it was assured that air was the pressurizing fluid, a ramping of the injection pressure up to 0.1 MPa was conducted, at a rate of 0.0208 MPa/h. The sample pressure followed quite closely the injection pressure, as this exceeded P_s^0 (120 h – 145 h), in accordance with observations in other systems with stable states above P_s^0.

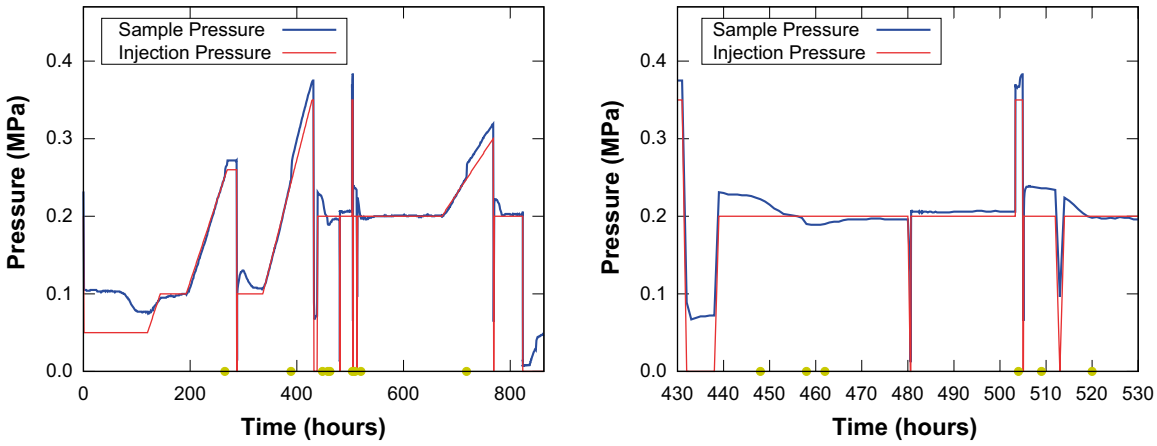

Figure 3-10. *Air injection (red) and sample (blue) pressure history of sample GenCh23 at nominal dry density 893 kg/m^3. The right diagram shows a magnification of the period 430–530 h. The yellow dots on the time line indicates breakthrough events.The initial pressurization is actually by water. Also, the sample pressure repsonse directly after the breakthrough events suggests that there is residual water left in the injection filter which is being pressurized initially.*

The injection pressure of 0.1 MPa was maintained for 24 hours without inducing any gas breakthrough event. At this point a new injection pressure ramping was initiated, at the same rate as previously. This ramping was conducted until a gas breakthrough event occurred (265 h), at an injection pressure of approximately 0.25 MPa. The breakthrough event ended as the inlet air reservoir was emptied and water (from the pressure controlling unit) reached the clay interface. At this point a change in sample pressure response is clearly seen – from having closely followed the injection pressure, the sample pressure now increased in accordance with what is expected from water pressurization.

The system was then pressure released, refilled with gas, and an injection pressure of 0.1 MPa was applied, without inducing any gas breakthrough event (288 h – 336 h). After the residual water had flowed through, an injection pressure ramping was initiated, this time at the rate 0.0271 MPa/h. A gas breakthrough event again occurred at approximate injection pressure of 0.25 MPa, which is also clearly seen from the sample pressure response (389 h).

After again preparing the system, an injection pressure of 0.2 MPa was directly applied to the sample (439 h). In this state "partial" gas breakthrough events occurred – some of the gas went through quickly, but the system shut close before the inlet reservoir was emptied. This behavior, which was not seen in the other tests, demonstrates that the gas flow which is induced during a breakthrough event is irregular, rather than a "two-phase"-flow phenomena.

The gas reservoir was refilled at 481 h, after which the injection pressure of 0.2 MPa was maintained for 24 hours without inducing gas breakthrough events. A gas breakthrough event occurred, however, rather quickly after the injection pressure was raised to 0.35 MPa (503 h).

The system was then replenished with gas and again pressurized at 0.2 MPa. Again, several "partial" gas breakthrough events was initially observed, but the system stabilized with time and the state were kept stable (no breakthrough events) for 120 hours (550 h – 670 h). Then yet another ramping process was initiated, at the rate of 0.0104 MPa/h. A gas breakthrough event occurred at the approximate injection pressure value of 0.25 MPa (718 h).

Finally a pressurized state at injection pressure 0.2 MPa was obtained (around 800 h), after which the pressure was released (823 h). At that moment it was possible to push the piston of the test cell downward, thus opening a slit between the force sensor and the cell, shown in Figure 3-11. This is a direct visual proof that the gas phase had consolidated the bentonite sample, something which also has been implicitly shown in many of the other tested samples.

Note that the sample pressure measured just after 823 h corresponds to an unloaded force sensor and should consequently be zero. The deviation from zero (0.007 MPa) thus shows the accuracy of the present pressure measurements.

Table 3-9. Air breakthrough events in sample GenCh23 at nomial density 893 kg/m^3.

Time (h)	Injection pressure (MPa)	Sample pressure (MPa)	Tailing water
265	0.251	0.251	No
389	0.243	0.245	No
440–455	0.200	0.230–0.200	No, “partial BT”
457–459	0.200	0.190	No, “partial BT”
459–465	0.200	0.190	No, “partial BT”
504	0.350	0.367	No
506–513	0.200	0.238–0.234	Water response?
513–528	0.200	~ 0.198	No, “partial BT”
718	0.248	0.251	No

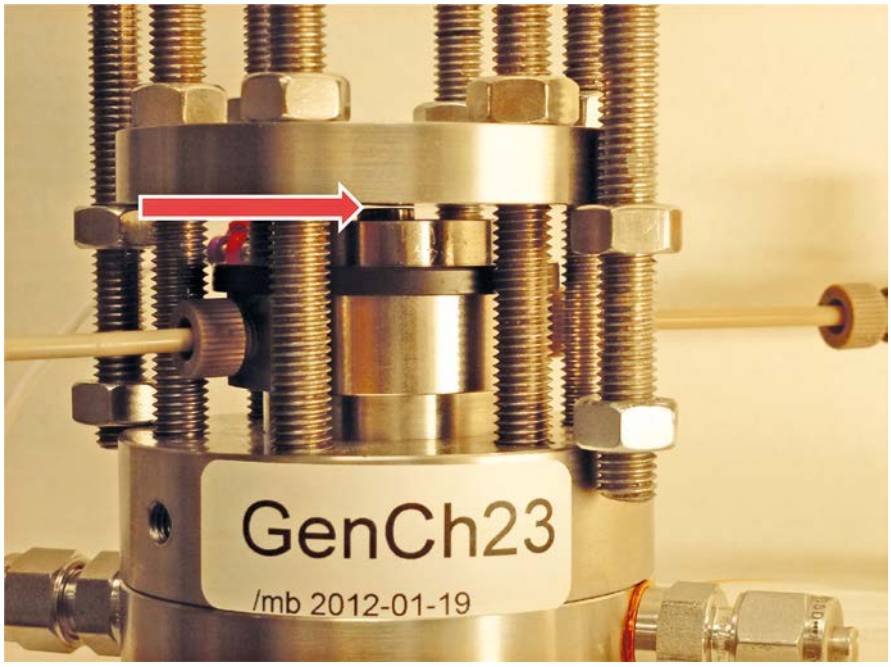

Figure 3-11. *After being pressurized with air at 0.2 MPa on the injection side, the piston of the test cell could be pushed down, opening a slit between the force sensor and the top of the cell in sample GenCh23. This is a visual demonstration that air has the ability to (macroscopically) consolidate bentonite clay.*

781 kg/m^3

Evolution of injection pressure and sample pressure during air pressurization of sample GenCh23 at nominal dry density 781 kg/m^3 is displayed in Figure 3-12. At this density there is barely any detectable pressure of the sample – a P_s^0 of 0.022 MPa was recorded initially. A constant injection pressure of 0.025 MPa was applied at 11 h. At 178h a ramping of the injection pressure up to 0.050 MPa was initiated, at a rate of $3.6 \cdot 10^{-4}$ MPa/h. A few hours after completion of this ramping, a new ramping was conducted at a rate of $7.2 \cdot 10^{-4}$ MPa/h. During these rampings, the sample pressure basically followed the injection pressure. At 413 h an air breakthrough event occurred, when the injection (and sample) pressure had reached a value of 0.167 MPa. Obviously, consolidation of the sample could also be accomplished at this density.

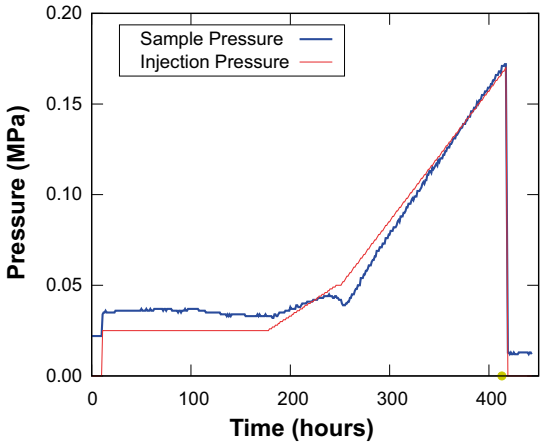

Figure 3-12. *Air injection (red) and sample (blue) pressure history of sample GenCh23 at nominal dry density 781 kg/m³. The yellow dot on the time line indicates a breakthrough event.*

3.1.3 MX-80 Bentonite

3.1.3.1 WP3Bench

The pressurization history is displayed in Figure 3-13 and Figure 3-15. Initially an injection pressure of 0.65 MPa was applied. The response in sample pressure was initially from pressurized residual water in the injection filter (0–40 h). After that period the sample pressure dropped down to P_s^0, as water at the interface was replaced by air. This is the typical (non-)response due to gas pressure below P_s^0, as has been observed in all samples where it has been tested. Air pressurization of 0.65 MPa was maintained for a long time (50 h – 150 h) before it was raised instantaneously to 0.9 MPa, i.e. slightly above P_s^0. The increased pressure resulted in a weak response of the sample pressure, in accordance with observations in other samples – above P_s^0, sample pressure and applied gas pressure are typically very similar, if a stable state can be achieved. The minor discrepancy seen between applied pressure and sample pressure should be ascribed to friction between clay body and the wall of the test cell.

After about 100 more hours (245 h) a ramping of the injection pressure was initiated, from 0.9 MPa to 1.2 MPa during the course of 60 hours (i.e. at the rate 0.005 MPa/h). The response in sample pressure confirms the previous interpretation: it basically follows the injection pressure.

At 297 h, the inlet gas reservoir was emptied (not because of any gas breakthrough, but due to diffusive flow-through and most probably also some leakage on the injection side of the experimental set-up). At this point water from the pressure controlling unit reached the interface to the clay (see e.g. Figure 3-3), and the sample pressure consequently showed water pressurization response (Section 2.1.2.3).

The corresponding volumetric outflow during 0 h – 320 h, plotted in Figure 3-13, further demonstrate the difference in response as the system is pressurized by water or by air. In the initial stage, when water is the pressurizing fluid, the flow is relatively large, but drops as air is reaching the clay/filter interface; when water again reaches the interface, a distinct increase in flow is observed.

Table 3-10. Properties of sample WP3Bench.

Material	Nominal density	Post-analysis	Cell type	h
MX-80	ρ_{dry} = 1,170 kg/m³ ϕ = 0.575	ρ_{dry} = 1,075 kg/m³ ϕ = 0.609	A	5 mm

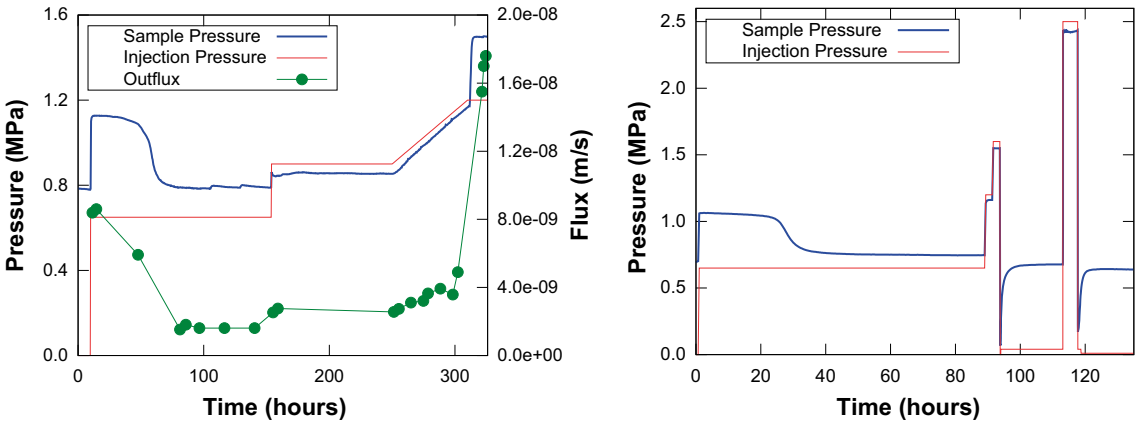

Figure 3-13. *Air injection (red) and sample (blue) pressure history of the first and second air pressurization sequences in sample WP3Bench. The initial pressurization is actually by water.*

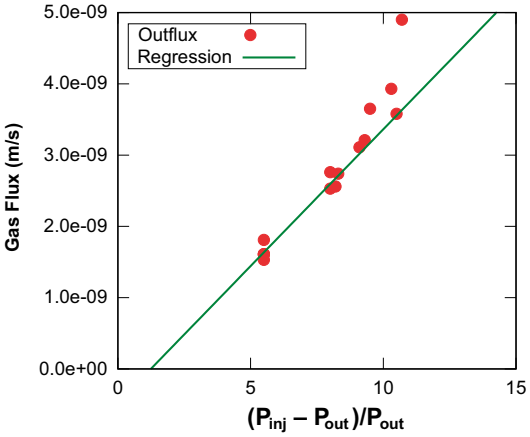

Figure 3-14. *Corresponding values of flow of dissolved gas and normalized injection pressure. The diagram also show the result of a linear regression analysis made on the experimental data.*

Figure 3-14 shows corresponding "steady-state" gasflow and ratio of the pressure difference across the sample to the absolute pressure on the outlet side (some of these data points are quasi-steady-state because when the pressure is slowly ramped, the state is not strictly time independent). From the relationship between these quantities, the diffusion coefficient of dissolved air can be achieved (Equation 3-3). Figure 3-14 also show the linear relation resulting from performing regression analysis on the data (data points up to 8.2 in relative pressure difference was used). From this analysis a diffusion coefficient of $1.25 \cdot 10^{-10}$ m^2/s was evaluated. This value is very close to the diffusion coefficient evaluated for sample GenCh12. Note, however that the present sample is significantly denser than that sample.

The system was replenished with gas and again pressurized at 0.65 (right diagram in Figure 3-13). After the typical transient response where gas replaced water at the inlet clay interface (0 h – 89 h), the injection pressure was raised quickly in two steps to 1.6 MPa, and rather quickly again released to 0.05 MPa. The response in sample pressure at this stage is quite interesting, as it basically drops to zero. This behavior has also been observed in other samples (see e.g. Section 3.1.2.2) and is a strong indication that the clay body at this point is smaller than available sample volume, i.e. that the gas has consolidated the sample. Subsequently, sample pressure is regained (to P_s^0) by water uptake (94 h – 113 h).

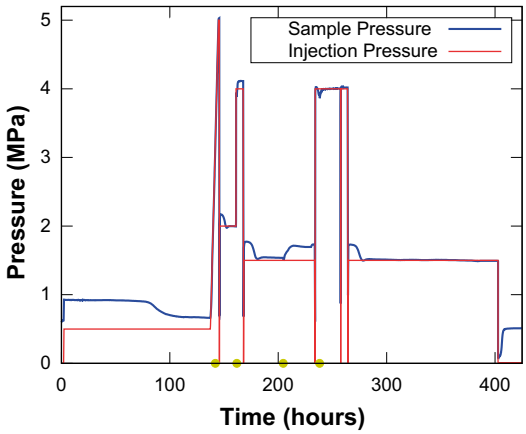

Figure 3-15. *Air injection (red) and sample (blue) pressure history of the third air pressurization sequence in sample WP3Bench. The yellow dots on the time line indicates breakthrough events.The initial pressurization is actually by water.*

Injection pressure was then instantaneously increased to 2.5 MPa (113 h). This pressure was kept for a few hours without inducing gas breakthrough, before it was released (to 0 MPa). Again, a pressure drop to (almost) zero was observed (118 h).

In a third pressurization sequence (Figure 3-15), an injection pressure of 0.5 MPa was initially applied. The characteristic response in sample pressure, when air replaces water, was observed (0 h – 136 h). Then the injection pressure was quickly ramped up at a rate of 0.6 MPa/h which induced a gas breakthrough event (141 h) at a pressure of approximately 3.25 MPa.

The system was replenished with air directly after this breakthrough event and exposed to an injection pressure of 2.0 MPa. The characteristic pressure response when air replaces water occurred also here. Note, however, that the sample pressure in this case fell down to the value of the injection pressure (2.0 MPa) rather than to P_s^0, because injection pressure is larger than P_s^0. This type of behavior demonstrates that it is possible to achieve a consolidated clay (rather than inducing gas breakthrough) by directly applying an injection pressure larger than P_s^0. After some time the pressure was increased to 4.0 MPa, which resulted in a new gas breakthrough event (161 h).

At 167 h, the gas reservoir was replenished and the procedure of directly applying an injection pressure above P_s^0 was repeated, this time at 1.5 MPa. Again, a consolidation of the clay body by the gas phase was achieved, as revealed by the characteristic sample pressure response (167–180 h). This time, however, a gas breakthrough "spontaneously" occurred at 204 h (i.e. without changes in injection pressure).

The gas reservoir was refilled at 233 h and the system was directly exposed to an injection pressure of 4.0 MPa. This time a gas breakthrough event occurred just a few hours later (237 h).

Finally an injection pressure of 1.5 MPa was applied (after refilling the gas reservoir), and a consolidated state was maintained for over 100 hours (263 h – 402 h). After this period the injection pressure was released and sample pressure dropped to zero, confirming that the clay body was in a consolidated state.

Table 3-11. Air breakthrough events in sample WP3Bench.

Time (h)	Injection pressure (MPa)	Sample pressure (MPa)	Tailing water
141	3.25	3.173	No
161	4.0	3.932	No
204	1.5	1.536	No
237	4.0	3.915	No

3.1.3.2 GenCh21

The entire gas pressurization history of this sample is displayed in Figure 3-16. Starting at a P_s^0 of 0.94 MPa, the sample was exposed to an injection pressure of 0.9 MPa. Immediately after pressurization, the sample pressure response indicates that water is the pressurizing fluid at the interface to the clay. During the next 400 hours, this water flowed through and was replaced by air, with a corresponding drop in sample pressure, down to P_s^0. This process took considerable longer time as compared to e.g. sample WP3Bench, which is of the same material (MX-80 bentonite) and comparable density (see e.g. Figure 3-13). The reason is most probably that the present sample is considerably higher which means that the induced flow is smaller at any given injection pressure (the gradient is smaller).

It can also be noted that the processes of lowering the pressure was more irregular in this sample, which indicates that the influence of friction against the test cell wall is more pronounced as compared to samples of smaller height.

Between 851 h – 855 h, the injection pressure was quickly ramped to 1.1 MPa. The corresponding response in sample pressure was in accordance with previous gas pressurizations above P_s^0, i.e. sample pressure was similar to injection pressure. It can, however, be noted that the discrepancy between measured sample pressure and applied gas pressure is larger than in corresponding states in sample WP3Bench (Section 3.1.3.1), which is another indication that friction effects are more pronounced in the present sample. At 898 h the gas pressure was instantaneously increased to 1.5 MPa. The sample pressure responded more slowly to this change in injection pressure in comparison to observations in other samples. Again, this difference in behavior may be attributed to stronger friction effects in the present sample.

At 970 h, the gas pressure was dropped to zero, and the sample pressure responded by falling to a fairly low value (0.34 MPa) which indicates a consolidated clay body (see also Sections 3.1.3.1 and 3.1.2.2). After about six hours the gas pressure was again raised to 1.5 MPa, and then to 2.5 MPa at 995 h. After about 20 hours in this state, a gas breakthrough event was induced (1,015 h).

Table 3-12. Properties of sample GenCh21.

Material	Nominal density	Post-analysis	Cell type	h
MX-80	ρ_{dry} = 1,166kg/m^3 ϕ = 0.576	Sliced and analyzed, see Section 2.1.2.2.	A	20 mm

Table 3-13. Air breakthrough events in sample GenCh21.

Time (h)	Injection pressure (MPa)	Sample pressure (MPa)	Tailing water
1,015	2.5	2.449	No
1,268	1.95	1.89	No

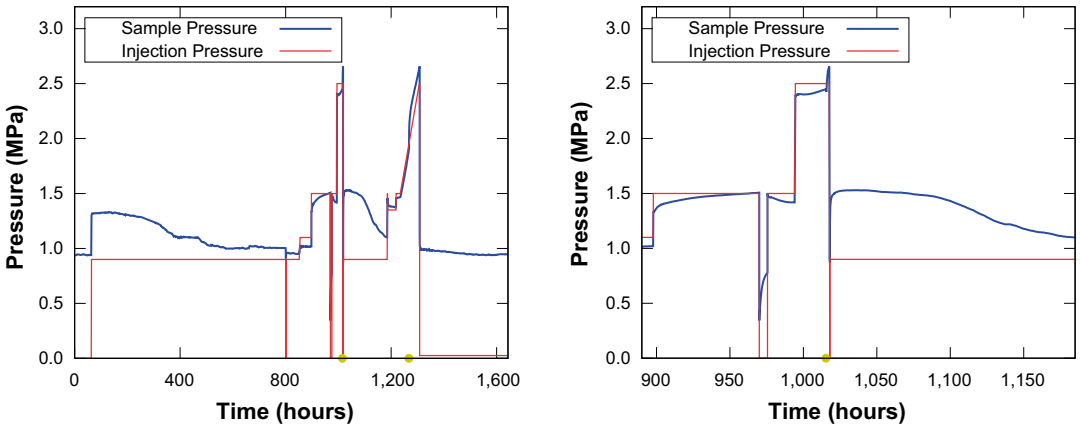

Figure 3-16. *Air injection (red) and sample (blue) pressure history of sample GenCh21. The right diagram shows a magnification of the period 890–1,180 h. The yellow dots on the time line indicates breakthrough events.The initial pressurization is actually by water.*

The system was refilled with gas and an injection pressure of 0.9 MPa was applied (1,018 h). After the characteristic response where air replaced water at the inlet (1,018 h – 1,186 h) the gas pressure was raised in steps to 1.35 MPa and 1.5 MPa with typical gas response behavior of the sample pressure response (sample pressure close to air pressure). Then an injection pressure ramping was initiated at the rate of approximately 0.14 MPa/h. A new gas breakthrough event occurred at the injection pressure of approximately 1.95 MPa (1,268 h) which is also clearly seen in Figure 3-16 as a change in sample pressure response when water from the pressure controlling unit reached the clay interface after the breakthrough event.

3.2 Injection filters B and C

3.2.1 Na-Montmorillonite

3.2.1.1 GenCh13

The complete air pressurization history of sample GenCh13 is found in Figure 3-19. Figure 3-18 shows the details of the early pressurization history. Gas pressurization started by applying an air injection pressure of 0.5 MPa for about 15 hours, to which the sample showed a negligible response. Although the sample pressure response is negligible, it should be recognized that this may not be used as a criteria for that air is the pressurizing fluid in this case; in the present injection geometry, also water pressurization gives a weak response (Section 2.2.1.2). The injection pressure was then quickly raised in steps up to 0.75 MPa where a breakthrough event occurred. As in the case of water breakthrough in this sample, the flow path went through the guard filter in the bottom of the cell. Two more breakthrough events were induced in a similar manner by ramping injection pressure (at 27 h and at 45 h), both occurring through the guard filter. However, as the system was not left pressurized below P_s^0 for a very long time prior to these events, it was not resolved whether they were caused by air or by residual water.

In order to ensure that air was the pressurizing fluid at the breakthrough event, a very long period of pressurization below sample pressure was conducted (46 h – 375 h). Apart from smaller transients, when the injection pressure occasionally was changed, the system stayed basically indifferent to this pressurization, once again confirming that swelling clay in unaffected by gas pressures below P_s^0. It is also worth noticing that no breakthrough event occurred during this long period of time although injection pressure was very close to sample pressure.

Table 3-14. Properties of sample GenCh13.

Material	Nominal density	Post-analysis	Cell type	h
WyNa	ρ_{dry} = 700 kg/m^3 ϕ = 0.745	ρ_{dry} = 620 kg/m^3 ϕ = 0.774	C	5 mm

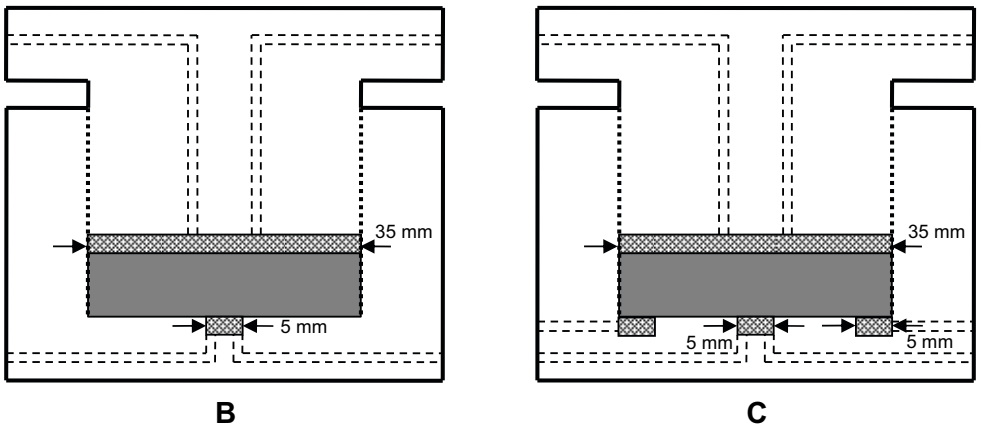

Figure 3-17. *Schematic illustration of filter injection geometries type B and C.*

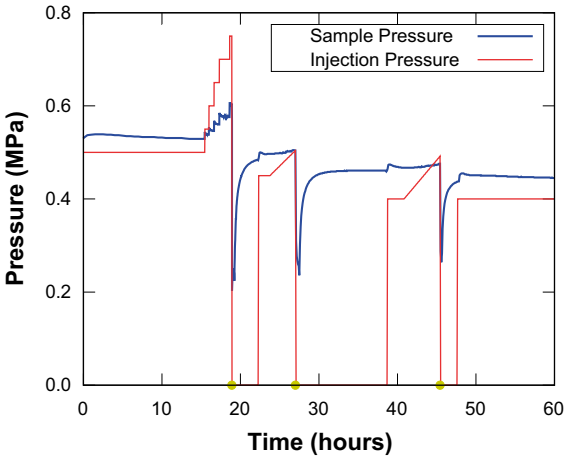

Figure 3-18. *Initial air injection (red) and sample (blue) pressure history in sample GenCh13. The yellow dots on the time line indicate breakthrough events.*

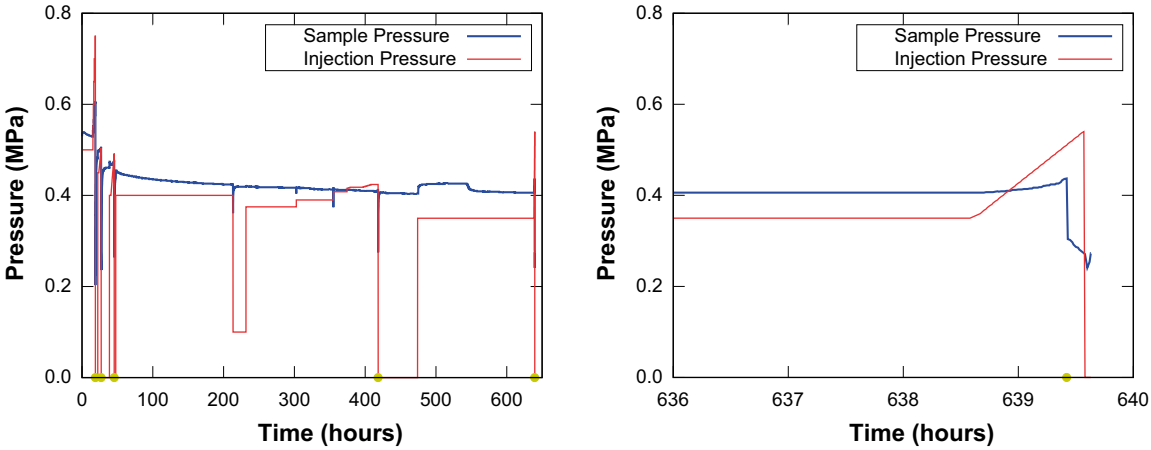

Figure 3-19. *Full air injection (red) and sample (blue) pressure history in sample GenCh13. The right diagram shows a magnification of the period 636–640 h.The yellow dots on the time line indicate breakthrough events.*

The weak trend of a drop in sample pressure during the course of the test is probably a homogenization/swelling effect – it should be noticed that the samples are rather small, a minor swelling into filters etc. might thereby change density, with a corresponding change in P_s^0.

At 375 h, injection pressure was increased to 0.416 MPa, exceeding sample pressure (0.413 MPa). Injection pressure was subsequently slightly increased even further, and after approximately 33 hours a gas breakthrough event occurred. At this point the injection pressure was 0.424 MPa and the sample pressure 0.412 MPa. As in sample GenCh12 (Section 3.1.1.1), it is thereby demonstrated that air is able to enter the system when its pressure exceeds the sample pressure, and that the system may be unstable in such states which leads to breakthrough events. Also this breakthrough event occurred through the guard filter, indicating that the air was entering the sample volume (by consolidating the clay) but not the clay. The air was furthermore tailed by the water of the pressure controlling unit. Thus, at the breakthrough event the pressure controlling unit emptied and injection pressure fell to zero.

At 474 h, the inlet was pressurized to 0.35 MPa with a small amount of water in direct contact with the clay at the injection side (the air reservoir was furthermore refilled). A small, but typical, water pressure gradient response was seen in the sample pressure (compare Section 2.2.1.2). Furthermore, at around 550 h a small drop in sample pressure was noted as the injection filter was emptied of water. Thus it was demonstrated that it is actually possible, also in the present injection geometry, to judge from the sample pressure response whether it is water or air which is pressurizing the system (something which was much easier to do in geometry A, sample GenCh12, see Section 3.1.1.1).

At 638 h, the injection pressure was quickly ramped up at the speed of 0.2 MPa/h. As seen in the right diagram of Figure 3-19, a weak but accelerating sample pressure response occurred before a breakthrough event took place. Also this time the breakthrough occurred through the guard filter. The pressure controlling unit emptied during the event, resulting in a drop of the injection pressure to zero. The right diagram of Figure 3-19 shows that this happened about 10 minutes after the breakthrough, i.e. this was the time scale for flushing a water volume of the order of 100 ml through the system.

Table 3-15. Air breakthrough events in sample GenCh13.

Time (h)	Injection pressure (MPa)	Sample pressure (MPa)	Path	Tailing water
19	0.75	0.685	Guard filter	Yes
27	0.5	0.626	Guard filter	Yes
45	0.49	0.468	Guard filter	Yes
412	0.424	0.414	Guard filter	Yes
639	0.5	0.43	Guard filter	Yes

3.2.1.2 PrefPath01

The air pressurization tests of this sample consisted of two separate pressurization sequences, plotted in Figure 3-20.

The sample was pressurized to 0.6 MPa with air in the injection filter after about 24 hours of water saturation. After 7 hours the injection pressure was quickly raised to 1.2 MPa, giving rise to a breakthrough event. The flow path during the breakthrough event went through the guard filter. The sample was then left undisturbed for about a week before a slow ramping of injection pressure was performed beginning at 0.55 MPa, at the speed of 0.0025 MPa/h. This lead to a new breakthrough event at 325 h. During 72 hours injection pressure exceeded sample pressure and at the breakthrough event the difference between these pressures was 0.192 MPa. Also for this breakthrough event, the flow path went through the guard filter.

Table 3-16. Properties of sample PrefPath01.

Material	Nominal density	Post-analysis	Cell type	h
WyNa	ρ_{dry} = 700 kg/m^3 ϕ = 0.745	not determined	C	2 mm

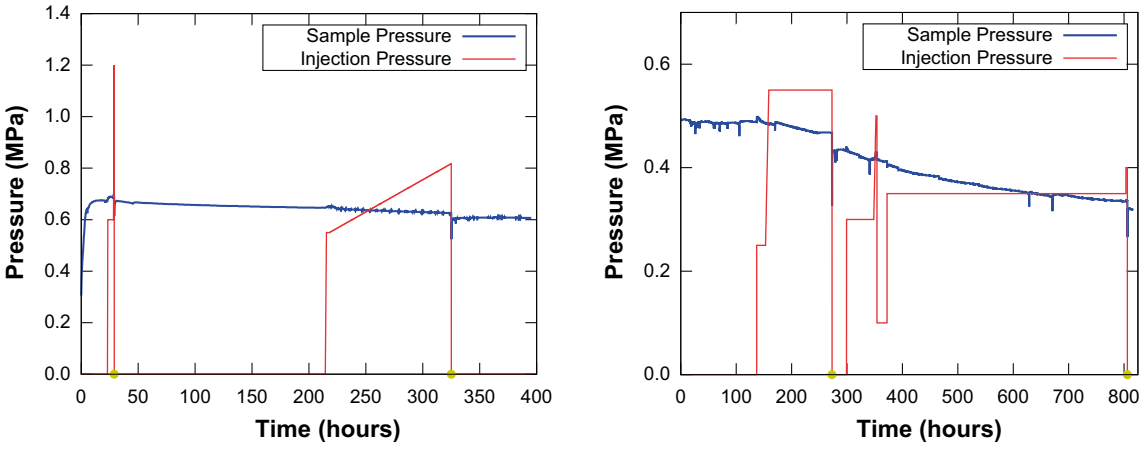

Figure 3-20. *Initial air injection (red) and sample (blue) pressure history of the two test sequences in sample PrefPath01. The yellow dots on the time line indicate breakthrough events.*

The second phase of gas injection tests was performed on this sample about one and a half month later (right diagram in Figure 3-20). An initial injection pressure of 0.25 MPa was applied for about 16 hours and then raised via a quick ramping to 0.55 MPa. This pressure was maintained for 114 hours before a breakthrough occurred (273 h). Injection pressure exceeded sample pressure during this entire period. In contrast to the earlier breakthrough events in this sample, the flow path in this case went *through* the sample and out through the top filter.

At 300 h the injection filter was pressurized to 0.3 MPa. A quick step-up in injection pressure to 0.5 MPa was performed between 349 h and 353 h. At 354 h it was discovered that the air reservoir at the injection side had diminished strongly which indicates that a breakthrough event had occurred in the time interval between 349 h and 354 h. As no water tailed the gas in this event, however, the flow path was not determined in this case (with tailing water, it is easy to determine the flow path, even if the actual event was not observed, because water accumulate at the reservoir of the involved outlet). Neither does the sample pressure response give any hint of the exact timing of the event.

Between 373 h and 804 h the injection pressure was kept constant at 0.35 MPa. In the same time interval the sample pressure fell from ca 0.4 MPa to 0.335 MPa (with these very small samples it is difficult to keep a fully constant P_s^0). At 804 h the injection pressure was increased to 0.4 MPa, leading to a breakthrough event at 806 h. Also this breakthrough went through the sample and out through the top filter.

Table 3-17. Air breakthrough events in sample PrefPath01.

Time (h)	Injection pressure (MPa)	Sample pressure (MPa)	Path	Tailing water
29 (seq. 1)	1.2	0.685	Guard filter	Yes
325 (seq. 1)	0.82	0.626	Guard filter	Yes
273 (seq. 2)	0.55	0.468	Top filter	Yes
349–354 (seq. 2)	0.3–0.5	0.415–0.430	Undetermined	No
806 (seq.2)	0.4	0.338	Top filter	Yes

3.2.2 MX-80 Bentonite

3.2.2.1 GenCh11

The air pressurization history of sample GenCh11 is found in Figure 3-21. The system was first pressurized with air at 0.7 MPa (112 h). The injection pressure was kept constant for 114 hours. As seen from the sample pressure response, which first increased slightly and then fell back towards P_s^0, it is evident that some residual water was initially pushed through the system (compare GenCh13, Section 3.2.1.1). At 226 h a ramping of the injection pressure at the speed of 0.0025 MPa/h was initiated. At 346 h it was discovered that the air reservoir on the inlet side was emptied and that water was actually pressurizing the clay. Consequently an air breakthrough event had occurred somewhere in the time interval of the ramping, but without any tailing water, meaning that the system shut close when the water entered the inlet. This behavior is different from what was typically observed in the tested Na-montmorillonite samples, in which air breakthrough typically is followed by tailing water, making it easy to detect the flow path and exact time of the event (as the pressure controlling unit then usually empties and loses its pressure). It is also worth noting that in the present sample, no water breakthrough events has been induced even at injection pressures as high as 3.0 MPa (Section 2.2.2.1). The reason for this difference in behavior between bentonite and pure Na-montmorillonite could be the presence of accessory minerals, or the fact that the MX-80 bentonite is considerably denser at similar swelling pressures (in this pressure range).

Table 3-18. Properties of sample GenCh11.

Material	Nominal density	Post-analysis	Cell type	h
MX-80	ρ_{dry} = 1,179 kg/m^3 ϕ = 0.571	ρ_{dry} = 1,097 kg/m^3 ϕ = 0.601	B	5 mm

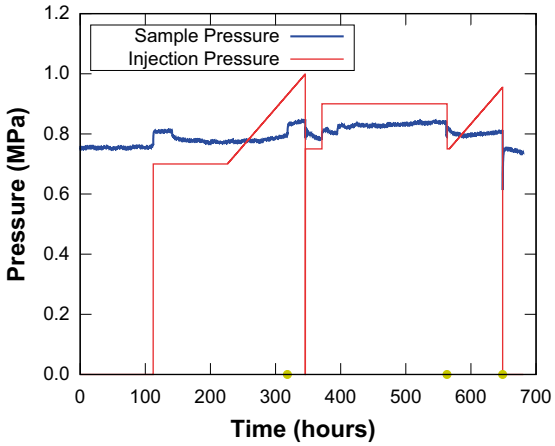

Figure 3-21. *Air injection (red) and sample (blue) pressure evolution in sample GenCh11. The yellow dot on the time line indicates a breakthrough event.*

Judging from the sample pressure response it seems very likely that the breakthrough event occurred around 318 h where a sudden jump in the sample pressure indicates that the system becomes pressurized by water (compare with the step in pressure at 112 h).

The inlet reservoir was refilled with air and the injection filter was re-pressurized at 0.75 MPa. At 371 h, the injection pressure was increased to 0.9 MPa, slightly above sample pressure. This state was maintained for about 109 hours before a breakthrough event occurred (563 h). Obviously, the time scale of certain processes in small samples can be quite long. As in the previous breakthrough event, no water tailed the air.

Air was again replenished and the injection filter re-pressurized to 0.75 MPa. At 567 h an injection pressure ramping was initiated at the speed of 0.0025 MPa/h. At 649 h a breakthrough event occurred, this time with tailing water, resulting in emptying of the pressure controlling unit and zero injection pressure. At the initiation of the event the injection pressure exceeded the sample pressure by 0.145 MPa.

Table 3-19. Air breakthrough events in sample GenCh11.

Time (h)	Injection pressure (MPa)	Sample pressure (MPa)	Tailing water
318	0.925	0.795	No
560	0.9	0.84	No
649	0.955	0.81	Yes

The gas tests on sample GenCh11 so far reported, were performed before the sample was exposed to a very long sequence of water pressurization (Section 2.2.2.1). Additional gas testing was done after this treatment, giving an opportunity to compare the gas migration behavior before and after such rather extreme water pressure exposure.

The applied injection pressure protocol and the corresponding sample pressure for the second stage of gas tests is shown in Figure 3-22. P_s^0 was initially ~ 0.72 MPa, and the testing started by applying an injection pressure of 0.6 MPa (42 h). After a few hours a gas breakthrough event was induced. Note that this occurred at an injection pressure below P_s^0. The system was refilled with gas and an injection pressure of 0.5 MPa was applied (58 h). This injection pressure was kept for about 144 hours without inducing any gas breakthrough event. The injection pressure was then increased to 0.7 MPa, leading to an immediate gas breakthrough event (202 h).

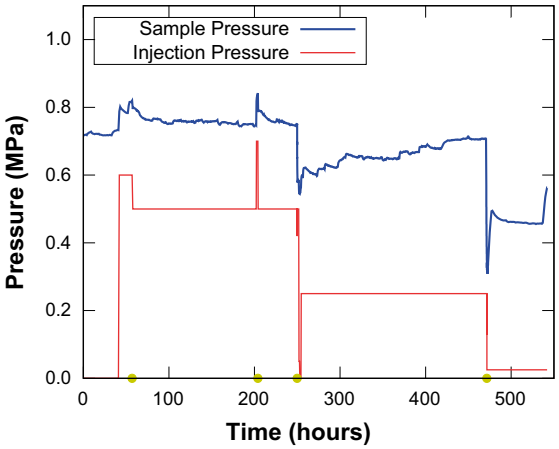

Figure 3-22. *Air injection (red) and sample (blue) pressure history of sample GenCh11 in testing performed after extensive water pressurization (see Section 2.2.2.1). The yellow dots on the time line indicates breakthrough events.*

In the gas injection test performed before the water pressure gradient tests, and in basically all other tested samples, gas breakthrough events was only induced when injection pressure was comparable with, or larger than P_s^0. Here, in contrast, gas breakthrough events were induced at injection pressure slightly below P_s^0. This may indicate that the clay density was differently distributed in the sample during the two tests, caused by the intermediate water gradient pressurization test.

Air breakthrough induced by flushing salt solution

After the second gas breakthrough event, the system was refilled with gas and an injection pressure of 0.5 MPa applied. This state was maintained for ca 46 hours, without any induced gas breakthrough events. Then the deionized water at the top side was replaced by a NaCl solution of concentration 3 mol/kgw. This change of boundary condition caused the sample pressure to begin to decline, and after just a few minutes a gas breakthrough event was induced. It was thus demonstrated that a gas breakthrough event can be induced by lowering sample pressure, rather than increasing injection pressure. Note that this gas breakthrough event was not caused by salt entering the clay, as it would take the salt several hours to diffuse through the sample and reach the air interface on the injection side. The details of the sample pressure response in this breakthrough event are displayed in Figure 3-23.

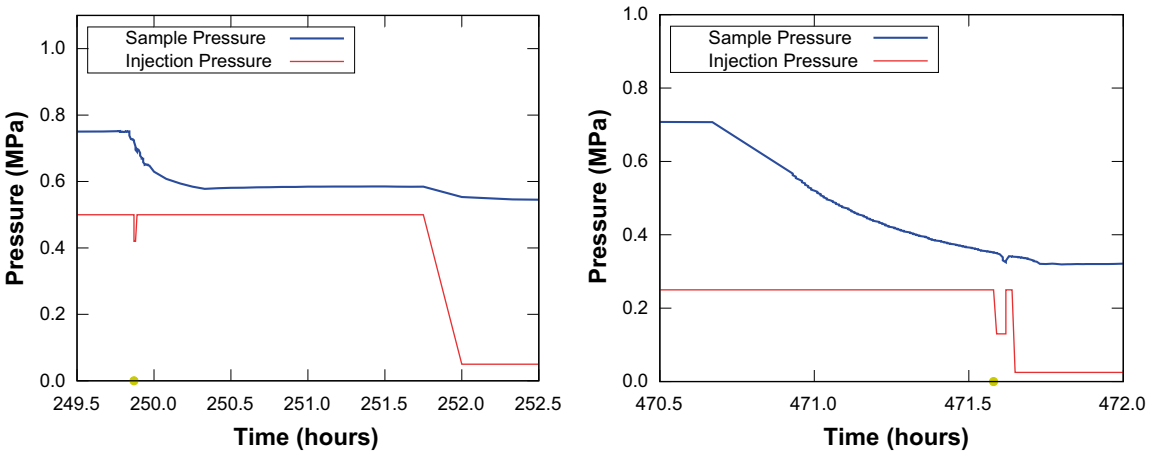

Figure 3-23. *Breakthrough events in sample GenCh11 induced by lowering sample pressure by flushing salt solution on the top side.*

Directly after the breakthrough event, the salt solution on the outlet side was replaced by deionized water and sample pressure started to increase (251 h). The system was again refilled with gas and pressurized, now at injection pressure 0.25 MPa. This state was kept for a long time (over 200 hours), during which flushing of the top side with deionized water was done from time to time in order to regain the full sample pressure (P_s^0). Eventually a P_s^0 of just above 0.7 MPa was achieved (425 h – 459 h). At this stage, the top side was again flushed with a NaCl solution of the same concentration as before (3 mol/kgw). As a result, the sample pressure started to decline (Figure 3-23) and a gas breakthrough event was again induced as the sample pressure became comparable in size with the injection pressure; at the breakthrough event, which occurred ca 46 minutes after flushing with the salt solution, sample pressure was 0.35 MPa.

Table 3-20. Air breakthrough events in sample GenCh11 induced by flushing 3 mol/kgw NaCl solution on the outlet side.

Time (h)	Injection pressure (MPa)	Sample pressure (MPa)	Tailing water
250	0.7	0.5	No
272	0.25	0.35	No

This second breakthrough event, induced by flushing of a saline solution, does not only confirm that gas breakthrough can be induced by lowering the sample pressure rather than increasing injection pressure, it also shows that the sample pressure at which breakthrough occurs is correlated with the applied injection pressure. Thus it can be concluded that it is the sample pressure which primarily set the criteria for when gas will interact mechanically with the clay. Note that, again, no salt would have had time to diffuse through the clay sample – these breakthrough events are consequently not caused by any changes occurring at the interface between gas and clay on the injection side. If the breakthrough mechanism depended on e.g. capillarity, breakthrough should occur at the same injection pressure – something which is contradicted by the present observations.

3.2.2.2 PrefPath02

Three separate phases of air pressurization was performed in this sample at different times. The pressurization history is displayed in Figure 3-24 and Figure 3-25.

In the first pressurization phase, the injection filter was initially pressurized with air at 1.5 MPa, slightly below the sample pressure. After about 4 hours, the injection pressure was raised to 1.8 MPa. The sample pressure response seen in the left diagram in Figure 3-24 at this time (4 h) was caused by mechanical adjustment of the couplings between injection tube and test cell, and is not a sign of a gas breakthrough event. The injection pressure was then kept constant until 144 h when it was increased to 2.0 MPa (after a quick drop to 0 MPa, as the gas reservoir was refilled). The 2.0 MPa state was kept until 199 h and the corresponding sample pressure response was basically absent. No significant sample pressure response was noticed when injection pressure was further increased to 2.25 MPa (199 h) and 2.5 MPa (215 h). This (lack of) response at pressures above P_s^0 is quite different from the earlier discussed systems. Also, maintaining this large difference (> 0.9 MPa) between injection and sample pressure was not possible in other tested systems. It should be kept in mind that the present sample is the densest, but also the thinnest, tested. Similar maintenance of difference between injection and sample pressure is seen in sample GenCh11 in the case of water injection (Section 2.2.2.1), which also was one of the densest samples tested.

Table 3-21. Properties of sample PrefPath02.

Material	Nominal density	Post-analysis	Cell type	h
MX-80 Bentonite	ρ_{dry} = 1,179 kg/m^3 ϕ = 0.571	ρ_{dry} = 1,189 kg/m^3 ϕ = 0.568	C	2 mm

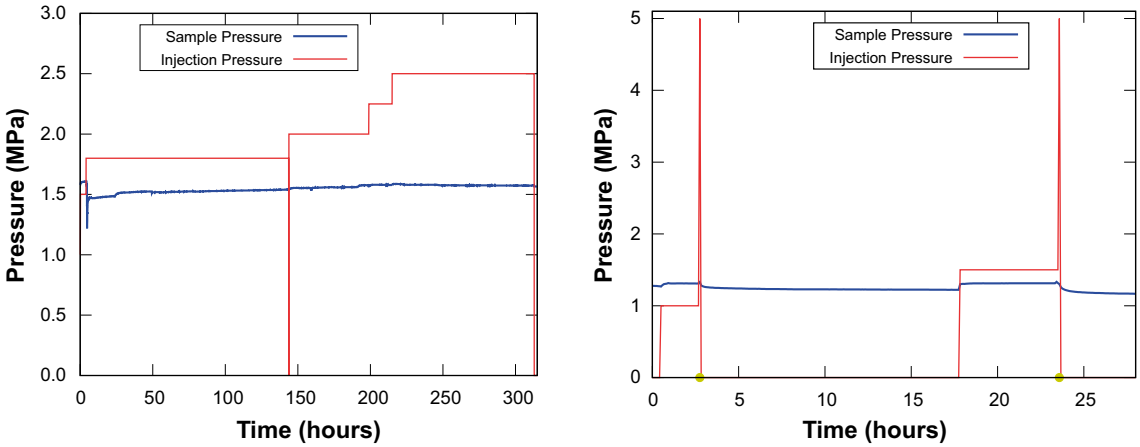

Figure 3-24. *Air injection (red) and sample (blue) pressure evolution during the first (left) and second (right) pressurization sequence in sample PrefPath02. The yellow dots on the time line indicate breakthrough events. The yellow dots on the time line indicate breakthrough events.*

After performing water injection tests on this sample (Section 2.2.2.2), a second air pressurization sequence was performed, starting at injection pressure 1.0 MPa (right diagram in Figure 3-24). At 3 h the pressure was increased to 5 MPa which immediately led to a breakthrough event with the path going through the guard filter.

At 17 h, the system was re-pressurized to 1.5 MPa and the pressure was once again raised to 5 MPa at 24 h, leading directly to a second breakthrough event. This time, however, the flow path was through the clay (top filter). It could be noted that this time the sample pressure showed a more distinct, albeit small, response to the pressurization (17 h), in comparison to the response in the earlier pressurization phase. This difference could indicate that the set-up was malfunctioning at the initial phase. However, it could also be that the response seen in the present phase is due to residual water in the injection filter. Hence it cannot be excluded that the breakthrough events induced in this phase were actually caused by water pressurization.

The third air pressurization phase (Figure 3-25) was initiated by applying an injection pressure of 1.0 MPa. This state was only maintained for less than two hours before a breakthrough event took place, going through the top filter. Note that the breakthrough event occurred when injection pressure was below sample pressure. The injection pressure was re-adjusted to 0.5 MPa and maintained for about 15 hours. Then the pressure was raised to 0.75 MPa, giving rise to a new breakthrough event through the top filter. Once again this breakthrough event occurred when injection pressure was (quite significantly) below the sample pressure. This breakthrough event did not give rise to emptying of the pressure controlling unit and it is not known exactly when in the time range 24 h – 28 h it occurred (the sample pressure response does not give any hint). The same pressurization procedure was repeated one more time with a maintained injection pressure of 0.5 MPa for 15 hours (33 h – 48 h) and a breakthrough event through the top filter when the pressure was increased to 0.75 MPa (48 h). During this breakthrough event it was observed that the system shut close when water replaced air at the inlet. After the breakthrough event, the injection pressure of 0.75 MPa was maintained with water as pressurizing fluid.

A final air pressurization at 0.75 MPa was performed at 121 h. Once again a breakthrough occurred through the top filter. Also for this event, the pressure controlling unit was not emptied, and the exact time for the event was not determined. However, it occurred somewhere in the interval 123 h – 125 h.

It is interesting to note the big difference in behavior of this sample in the first pressurization sequence as compared to the last ones. In the initial phase, air was not able to break through at pressures as high as 2.5 MPa – more 0.9 MPa above sample pressure – while in the later tests several breakthrough events was induced at 0.75 MPa (0.35 MPa below sample pressure). A speculation is that irreparable preferential paths were induced when the system was pressurized to 5.0 MPa in the second pressurization sequence. These should then be viewed as “artifacts” due to the small size of the sample – the height is comparable to the largest grain size in MX-80 bentonite.

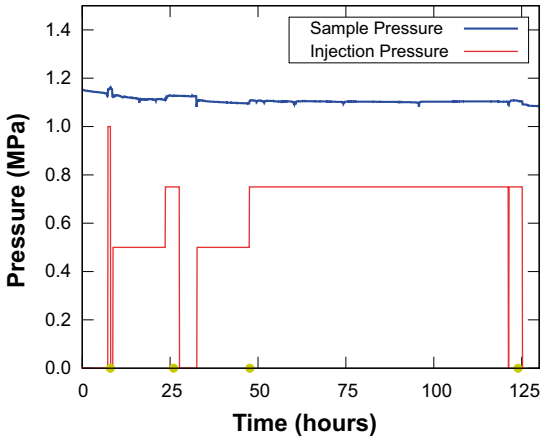

Figure 3-25. *Air injection (red) and sample (blue) pressure evolution during the third pressurization sequence in sample PrefPath02. The yellow dots on the time line indicate breakthrough events.*

Table 3-22. Breakthrough events in sample PrefPath02.

Time (h)	Injection pressure (MPa)	Sample pressure (MPa)	Tailing water	Path
3 (seq. 2)	5.0	1.33	No	Guard filter
24 (seq. 2)	5.0	1.30	No	Top filter
8 (seq. 3)	1.0	1.16	Yes	Top filter
24–28 (seq. 3)	0.75	~ 1.12	No	Top filter
123–125 (seq. 3)	0.75	~ 1.11	No	Top filter

3.3 Summary: air pressure gradient tests

The following list summarizes the observed behavior of bentonite/montmorillonite samples exposed to external air pressure differences

For air pressure below sample pressure:

- There is no response in equilibrium sample pressure when applied gas pressure is below sample pressure.
- In contrast to water pressurization, the (lack of) response due to gas pressure does not depend on injection geometry.
- For applied air pressures below sample pressure, the only transport mechanism is diffusion of dissolved gas.

For air pressure above sample pressure:

- Gas breakthrough events.
  - The flow during a breakthrough event is distinctly different than the diffusive flow. The mechanisms are completely different. At the breakthrough event the flow increases tremendously (a factor 10^4 or more).
  - In many cases the flow path is at the interface between sample holder and clay.
  - In the thinnest samples (2mm) some events occurred *through* the clay.

- In the looser Na-montmorillonite samples breakthrough occurred when air pressure exceeded sample pressure. States with air injection pressures higher than sample pressure could be maintained in samples with higher density (MX-80 and Ca-montmorillonite).
- Breakthrough events can be induced either by increasing injection pressure or by lowering sample pressure (e.g. by contacting the sample with a saline solution). The criteria for breakthrough is thus not coupled to a particular pressure (e.g. P_s^0), but is purely mechanical – gas pressure should exceed sample pressure at the point of injection. This behavior directly demonstrates that gas migration in bentonite is not a two-phase flow phenomena, i.e. it is not associated with capillarity.
- Tailing water from the pressurization unit always followed the air in the less dense Na-montmorillonite samples. In the MX-80 and Ca-montmorillonite samples this was not always the case – sometimes the system shut close when the water reached the clay interface. There are, however, strong similarities between gas and water breakthrough events.
- The process(es) has a complex time dependence. With fast ramping rather high sample pressures can be achieved. Also transient times on the order of hundred hours were observed.
- In a few cases, breakthrough events was induced at injection pressures significantly below sample pressure. These events should, however, be viewed as special cases: either the sample height was comparable to the size of the largest accessory mineral grains in the bentonite (sample PrefPath02), or the sample had been preconditioned by extreme water pressurization prior to gas testing (sample GenCh11). It should also be kept in mind that what is here referred to as sample pressure is the average axial stress measured on the top of each sample, while gas is always injected in the bottom.

• Consolidation by gas phase.
- In some samples states could be maintained where injection pressure exceed the initial sample pressure without inducing gas breakthrough. In these states, sample pressure do respond to the applied air pressure: in some cases sample pressure basically equaled injection pressure, while in others injection pressure could exceed sample pressure quite extensively. This type of behavior is interpreted as consolidation of the clay body (i.e. volume reduction by release of water). In one specific case, consolidation was also confirmed visually.

4 Uniform water pressurization

The series of tests reported in this chapter investigated the sample pressure response due to uniform external water pressurization, i.e. *without* imposed gradients over the samples. Consequently no flow response was induced. The evaluation was made by assuming a generalized linear response of the sample pressure (P) due to applied external water pressure (P_l)

$$P = P_s^0 + \beta + \alpha \cdot P_l \tag{4-1}$$

Here P_s^0 denotes, as before, the sample pressure measured without applied water pressure. β is generally a negative quantity, accounting for possible friction influences on the response. Thus, Equation 4-1 should only be applied to pressurized states (where $P \neq P_s^0$). The main parameters determined in the tests are α and β, but also possible hysteresis in P_s^0 was observed.

Table 4-1 shows the samples on which these tests were performed. Below follows a more detailed discussion on each of them.

The test descriptions are organized firstly according to injection geometry (i.e. bottom filter type) and then according to type of material.

Table 4-1. Samples on which uniform water pressurization tests was performed.

	Sample-Id	Material	Nominal dry density (kg/m^3)	Injection filter*)	Max. pressure (MPa)	Height (mm)
1.	GenCh11	MX-80	1,179	B (small)	1.0	5
2.	GenCh21	MX-80	1,166	A (large)	1.5	20
3.	GenCh22	WyCa	1,200	A (large)	1.5	5
4.	GenCh23	WyCa	1,250*)	A (large)	1.0	5–8*)
5.	PrefPath01	WyNa	700	C (small+guard)	2.0	2
6.	WP3Bench	MX-80	1,179	A (large)	1.0	5

*) Successively volume expanded, see Section 2.1.3.3.

4.1 Injection filter A

4.1.1 MX-80 Bentonite

4.1.1.1 GenCh21

The pressurization history is shown in Figure 4-2. This sample was exposed to 19 pressurization events of various size and durations. After the saturation stage (0 h – 384 h) 13 pressurization pulses of 0.2 MPa was performed (384 h – 5,300 h), then 3 pulses of 1.0 MPa (5,300 h – 6,500 h), and finally 3 pulses of 1.5 MPa (6,500 h – 8,100 h). The duration of each pulse was determined by when a (relatively) stable sample pressure was achieved.

The sample pressure achieved when water pressure was released after each pulse, i.e P_s^0, is plotted in Figure 4-3. This figure reveals a huge hysteresis in this quantity: the initial value of P_s^0 is 0.56 MPa, rising to 0.98 MPa after 10 pressurization pulses. After this rise, P_s^0 stays stable, only decreasing slightly to ca 0.95 MPa after increasing the pulse amplitudes.

Table 4-2. Properties of sample GenCh21.

Material	Nominal density	Post-analysis	Cell type	h
MX-80	ρ_{dry} = 1,166kg/m^3 ϕ = 0.576	Sliced and analyzed, see below	A	20 mm

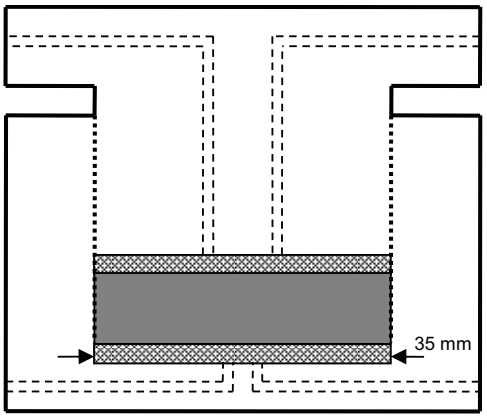

Figure 4-1. *Schematic illustration of injection filter geometry type A.*

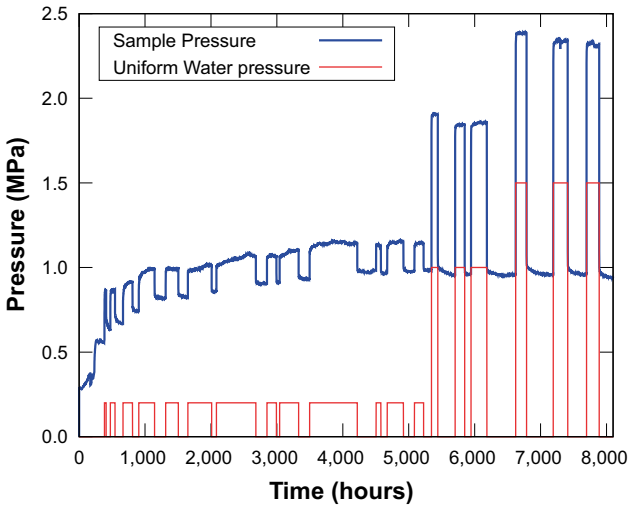

Figure 4-2. *External water (red) and sample (blue) pressure history in sample GenCh21.*

From the time series (Figure 4-2) it is seen that the path towards the high pressure value of P_s^0 is quite unsmooth. After about 1,000 h, for example, P_s^0 seems to have been stabilized at ca 0.82 MPa for a couple of pulses before starting to increase again. Also, after the pressurization initiated at 2,083 h, a slow sample pressure response is induced lasting for approximately 500 hours. On the other hand, after the high value of P_s^0 has been established, the system behaves quite robust (the continued pressure history of this sample is documented in Sections 2.1.2.2 and 3.1.3.2). Note that the time to reach this robust value was more than 4,000 hours, i.e. almost half a year.

The hysteresis in P_s^0 obviously complicates the evaluation of the α-factor. Here this factor is evaluated only from the pressure pulses conducted after the P_s^0-values had leveled out (at around 4,300 h). The evaluation is performed by correlating the sample pressure difference $P_{after} - P_{before}$ with the corresponding change in applied external water pressure. Thus P_{before} is the sample pressure just before the water pressure is changed (day average) and P_{after} is the value of the leveled out sample pressure after the water pressure change. Figure 4-4 shows the result of regression analyses performed on such sample pressure differences and corresponding changes in applied water pressure, using Equation 4-1.

The α-factor is quite consistently evaluated to 0.94–0.95 for the two cases of increasing or decreasing the water pressure. Furthermore the β-parameter (see Equation 4-1) is consistently evaluated to 0.027 MPa in both cases.

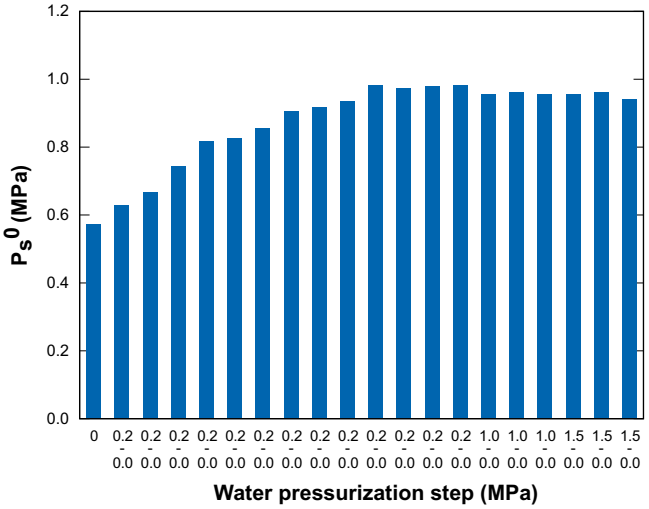

Figure 4-3. *Sample pressure after returning to zero water pressure (P_s^0) after each pressurization pulse in sample GenCh21.*

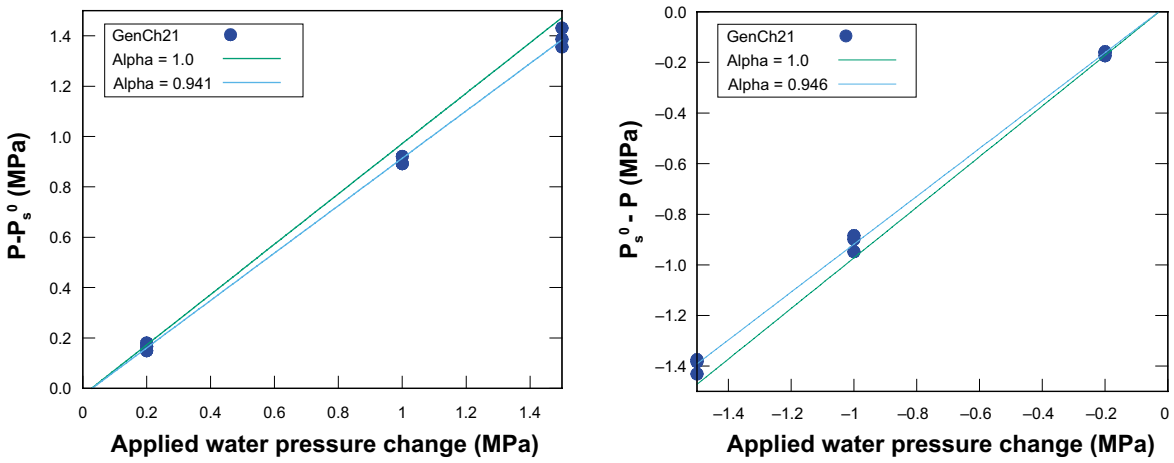

Figure 4-4. *Regression analysis performed on sample pressure response data of sample GenCh21.*

4.1.1.2 WP3Bench

The pressurization history is shown in Figure 4-5. This sample was exposed to seven pressure pulses: four of size 0.2 MPa, two of size 0.5 MPa, and one of size 1.0 MPa. The resulting P_s^0 after each pressurization pulse is also displayed in Figure 4-5. As with the case of sample GenCh21 (Section 4.1.1.1), a large hysteresis effect is observed in the P_s^0-parameter: from an initial value of 0.57 MPa, P_s^0 increases to a final value of 0.78 MPa. As this sample is of the same material (MX-80 bentonite) and of similar density as sample GenCh21, it may be speculated that the shorter time needed to stabilize the P_s^0-value in this case is due to the shorter height (5 mm vs. 20 mm).

Figure 4-6 shows the same type of regression analysis performed on the pressure data of this sample as was made for sample GenCh21 (Section 4.1.1.1). Again, quite consistent parameters are evaluated from considering either water pressure increases or decreases. In this sample the α-factor is 0.90 for both evaluations, while the β-parameter is 0.047 MPa and 0.052 MPa respectively for the two evaluated cases. However, both the α-factor and the β-parameters are significantly different as compared to sample GenCh21.

Table 4-3. Properties of sample WP3Bench.

Material	Nominal density	Post-analysis	Cell type	h
MX-80	ρ_{dry} = 1,170 kg/m^3 ϕ = 0.575	ρ_{dry} = 1,075 kg/m^3 ϕ = 0.609	A	5 mm

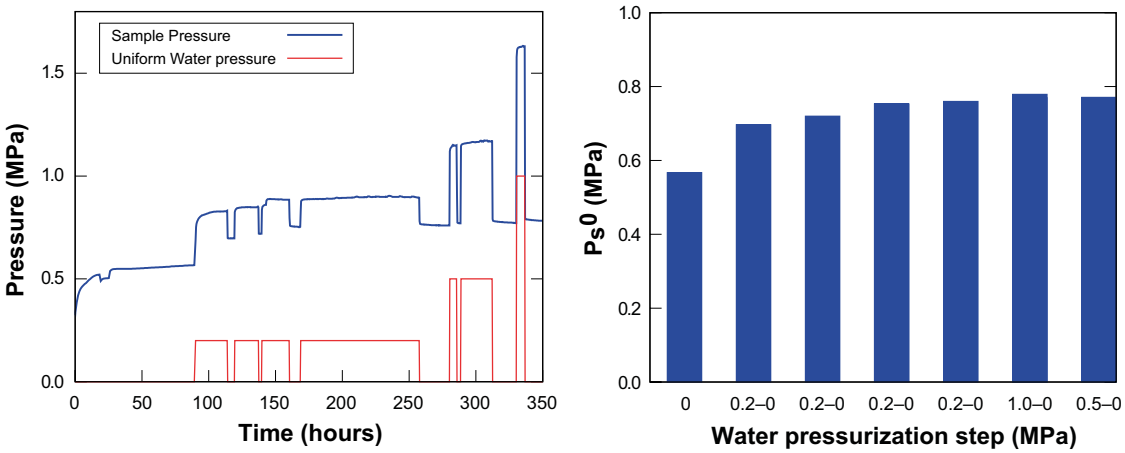

Figure 4-5. *Left External water (red) and sample (blue) pressure history in sample WP3Bench Right: Sample pressure after returning to zero water pressure (P_s^0) after each pressurization pulse.*

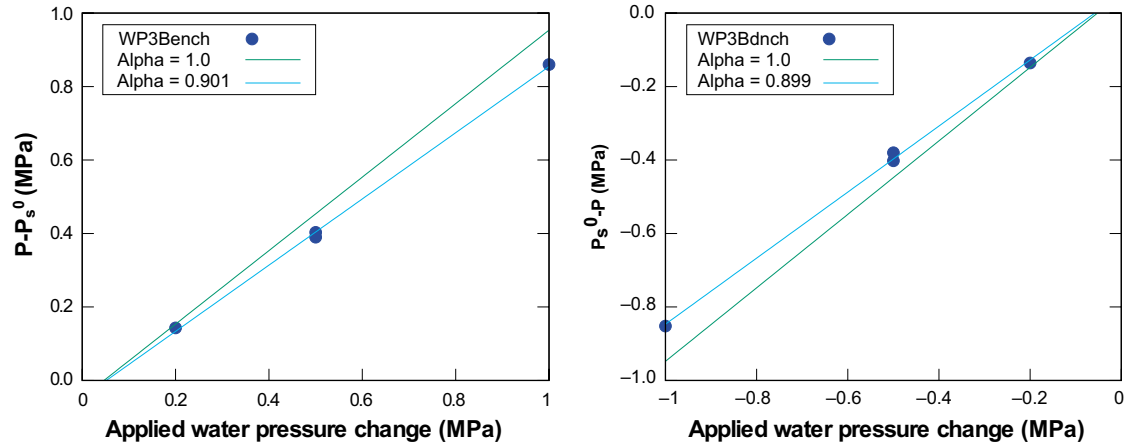

Figure 4-6. *Regression analysis performed on sample pressure response data of sample WP3Bench.*

4.1.2 Ca-montmorillonite

4.1.2.1 GenCh22

This sample was exposed to four different pressure pulses: one of 0.2 MPa, two of 1.0 MPa, and one of 1.5 MPa. The pressurization history is displayed in Figure 4-7. In contrast to samples GenCh21 and WP3Bench (Sections 4.1.1.1 and 4.1.1.2), this sample only shows negligible hysteresis in P_s^0 (Figure 4-7). In general, it has been observed that hysteresis effects in sample pressure are, if not absent, substantially less pronounced in pure, homoionic montmorillonite as compared to MX-80 bentonite (looking also at hysteresis effects in water pressure gradient tests, Chapter 2). It may thus be speculated that the hysteresis behavior is associated with the presence of accessory minerals and/or dissolved chemicals in the latter samples.

Figure 4-8 displays the regression analysis made to evaluate the α-factor. A consistent value of 0.88–0.89 is achieved. However, the analysis gives a larger deviation for the β-factor: 0.021 MPa and 0.034 MPa, for the case of increasing or decreasing the applied pressure, respectively. Notice that the number of performed pressurization cycles were quite few in this sample, leading to less accurate statistics.

Table 4-4. Properties of sample GenCh22.

Material	Nominal density	Post-analysis	Cell type	h
WyCa	ρ_{dry} = 1,200 kg/m^3 ϕ = 0.564	ρ_{dry} = 1,137 kg/m^3 ϕ = 0.605	A	5 mm

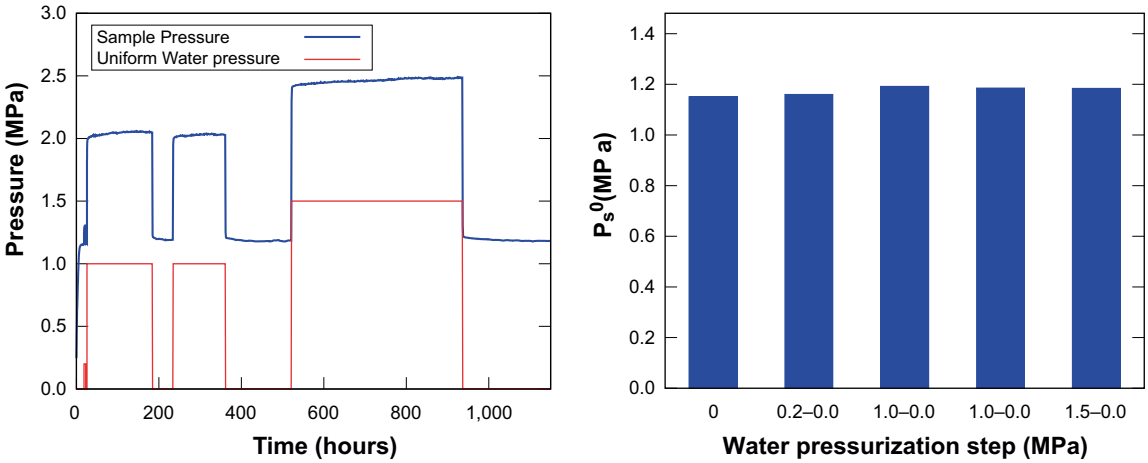

Figure 4-7. *Left External water (red) and sample (blue) pressure history in sample GenCh22 Right: Sample pressure after returning to zero water pressure (P_s^0) after each pressurization pulse.*

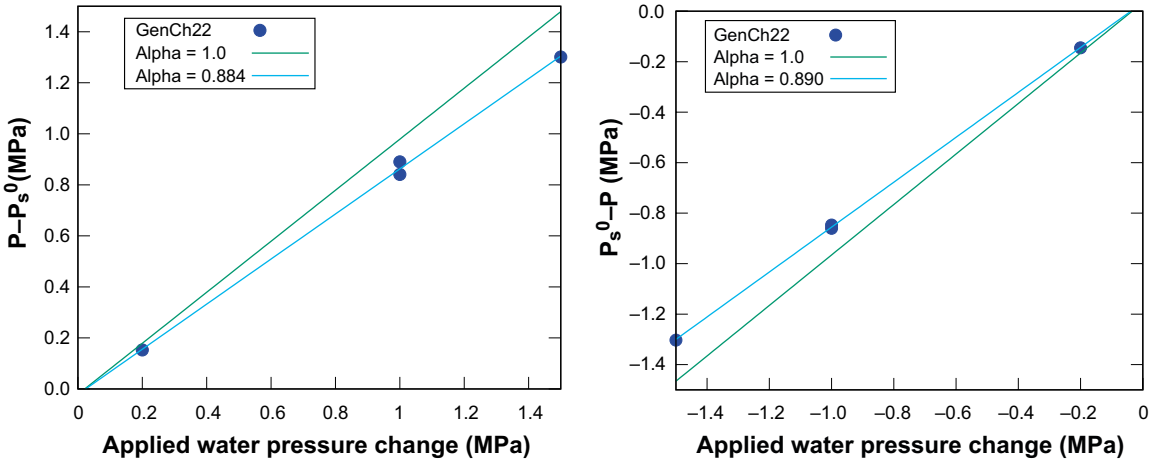

Figure 4-8. *Regression analysis performed on sample pressure response data of sample GenCh22.*

4.1.2.2 GenCh23

This sample was tested for response due uniform water pressurization at three different densities (see Section 2.1.3.3).

1,250 kg/m^3

At the initial density (nominal value 1,250 kg/m^3, $P_s^0 \sim 2.1$ MPa) three pressurization cycles were conducted, as shown in Figure 4-9. one at 0.5 MPa and two at 1.0 MPa. The hysteresis effect observed in P_s^0 was rather small, an observation similar to what was seen in the Ca-montmorillonite sample GenCh22 at similar density (Section 4.1.2.1).

The alpha factor in this sample was as low as 0.808 (Figure 4-10), but the amount of data was limited, giving large uncertainties in the evaluation (the amount of data was so small, that no adequate regression analysis could be performed for the case of increasing water pressures).

Table 4-5. Properties of sample GenCh23.

Material	Nominal density	Post-analysis	Cell type	h
WyCa	ρ_{dry} = 1,250kg/m^3 ρ_{dry} = 1,042kg/m^3 ρ_{dry} = 893kg/m^3	Not made	A	5–8 mm (sample expanded)

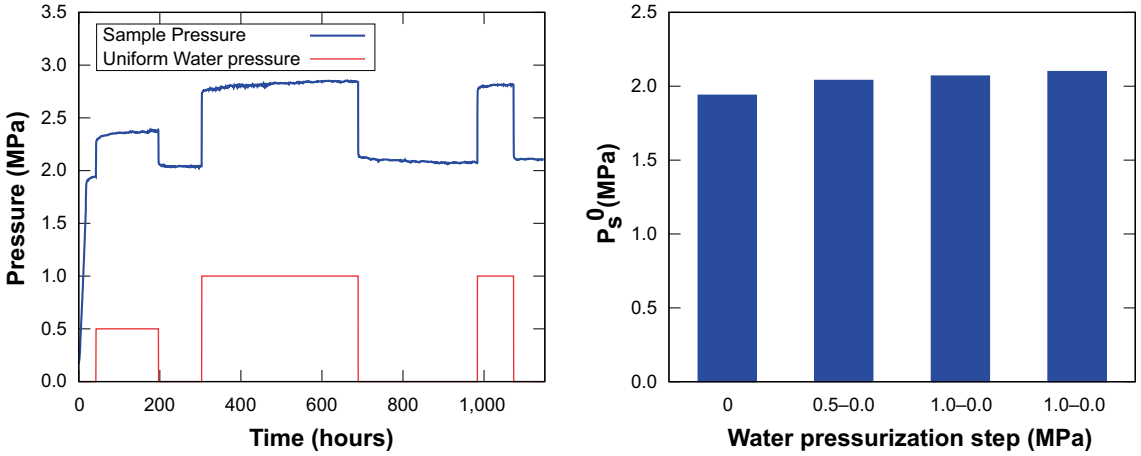

Figure 4-9. *Left External water (red) and sample (blue) pressure history in sample GenCh23 at nominal density 1,250 kg/m³. Right: Sample pressure after returning to zero water pressure (P_s^0) after each pressurization pulse.*

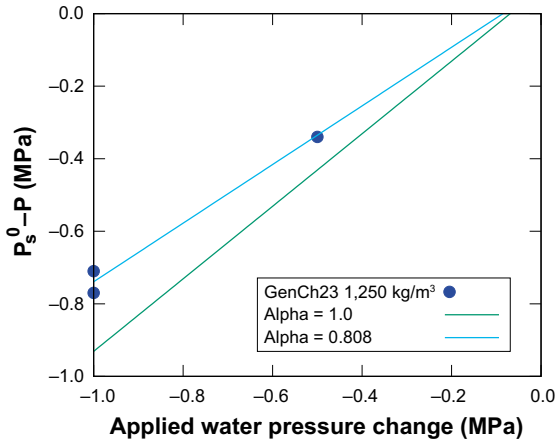

Figure 4-10. *Regression analysis performed on sample pressure response data of sample GenCh23 at nomial density 1,250 kg/m³.*

1,042 kg/m³

At the density achieved after the first volume expansion (nominal value 1,042 kg/m³, P_s^0 0.31 MPa), two pressure cycles were performed, both of magnitude 1.0 MPa. Pressure evolution and P_s^0-values are plotted in Figure 4-11. It may be noted that there is a significant difference between the P_s^0-value recorded before and after the first pressurization event. This hysteresis effect should be attributed to the fact that the sample was volume expanded just before these tests were made. Note that no significant change in P_s^0 is observed before and after the second pressurization event. No alpha factor evaluation was done for this test due to lack of data – regression analysis cannot be performed because only a single value of water pressure was used in the test.

893 kg/m³

A uniform pressurization test was again performed on this sample when it had been further volume expanded (nominal density 893, P_s^0 0.06–0.09 MPa). In this test, the sample was exposed to six pressure pulses (2 of size 0.1 MPa, 2 of size 0.25 MPa, and 2 of size 0.5 MPa) but also a sequence of increasing pressurization (0.1 MPa, 0.25 MPa, and 0.5 MPa). The pressurization history and P_s^0-values is shown in Figure 4-12.

In this test a (relatively) large hysteresis effect is observed: P_s^0 increases from 0.06 MPa to almost 0.09 MPa during the pressurization phase. It should be kept in mind, though, that the absolute values of the pressures are rather small (resolution is typically 0.01 MPa).

The evaluation of the alpha-factor is shown in Figure 4-13. Its value, 0.96–0.97, is closer to unity than in any of the previously tested densities.

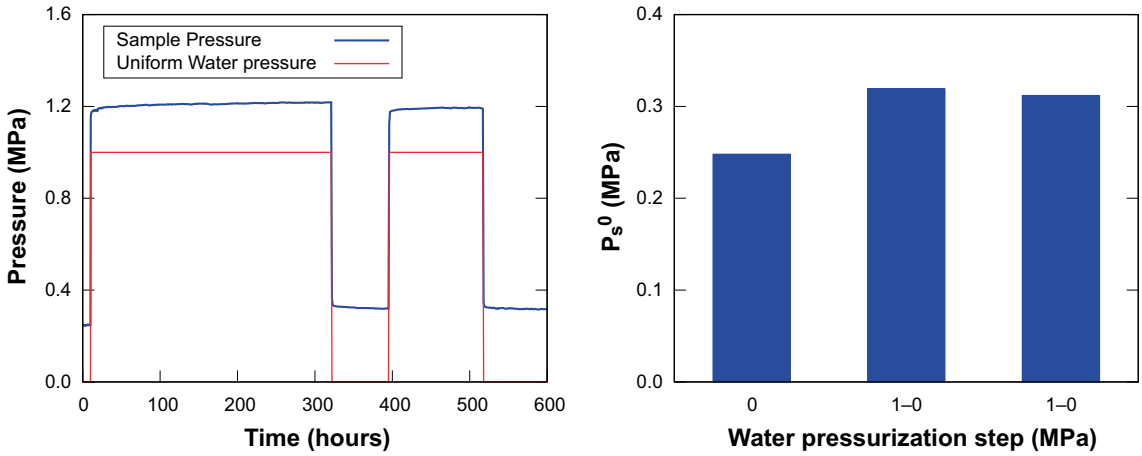

Figure 4-11. *Left External water (red) and sample (blue) pressure history in sample GenCh23 at nominal density 1,042 kg/m³. Right:Sample pressure after returning to zero water pressure (P_s^0) after each pressurization pulse.*

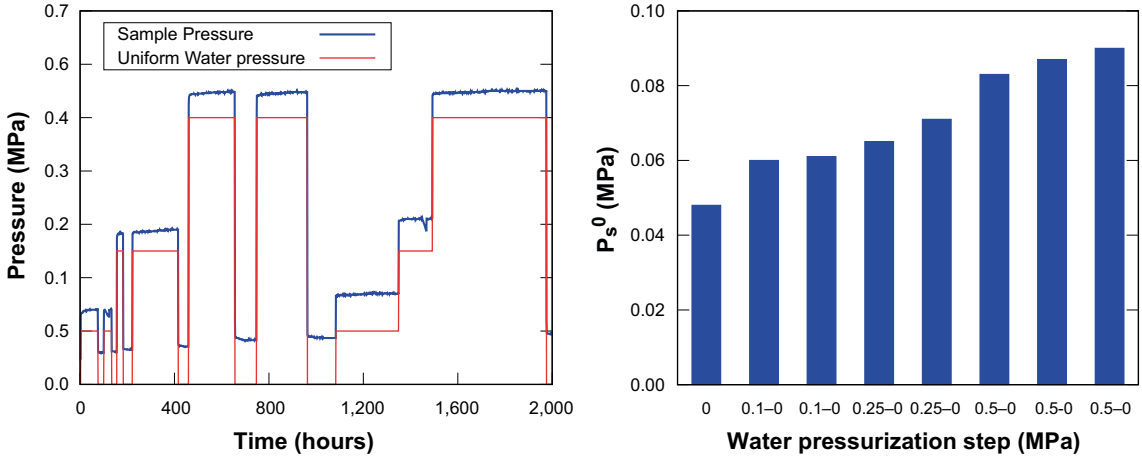

Figure 4-12. *Left External water (red) and sample (blue) pressure history in sample GenCh23 at nominal density 893 kg/m³. Right:Sample pressure after returning to zero water pressure (P_s^0) after each pressurization pulse.*

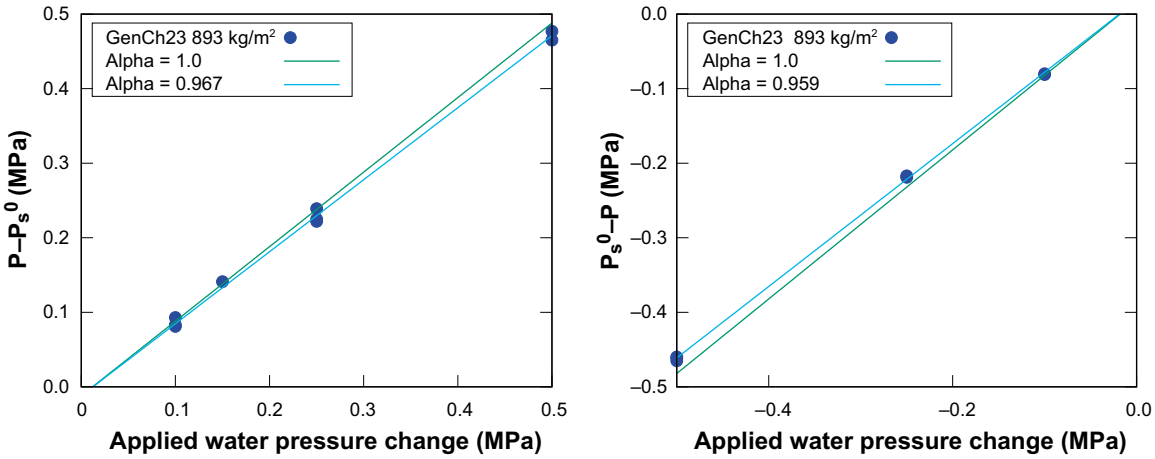

Figure 4-13. *Regression analysis performed on sample pressure response data of sample GenCh23, nominal density 893 kg/m³.*

4.2 Injection filter C

4.2.1 Na-montmorillonite

4.2.1.1 PrefPath01

The pressurization history and P_s^0-values for this sample are displayed in Figure 4-15. Initially a pressurization of 0.5 MPa was performed. The pressure was then lowered in steps to 0.25 MPa and 0 MPa. Finally a pressurization sequence of 2.0 MPa, 1.0 MPa, 2.0 MPa and 0 MPa was performed.

The declining trend of the P_s^0-values are associated with a general trend in pressure drop in the sample, which is visible in the pressurization evolution diagram (left diagram in Figure 4-15). This trend is associated with mass loss, signifying that Na-montmorillonite is not fully stable in a deionized water environment (and that the filter pore size was large enough to allow the passage of separate clay particles). The present set-up is thus not fully adequate for evaluating possible hysteresis in P_s^0 in systems of Na-montmorillonite, in particular in samples as thin as the present one.

The α-factor was evaluated to approximately 0.9 (Figure 4-16). Note that this sample has a substantially lower density than even the lowest considered density of the Ca-montmorillonite sample GenCh23 (Section 4.1.2.2). Despite this fact the α-factor here is lower – comparable to values evaluated for MX-80 Bentonite samples and Ca-montmorillonite of densities above 1,000 kg/m^3. This observation suggests that the value of the α-factor is correlated with the value of P_s^0, rather than density.

Table 4-6. Properties of sample PrefPath01.

Material	Nominal density	Post-analysis	Cell type	h
WyNa	ρ_{dry} = 700 kg/m^3 ϕ = 0.745	not determined	C	2 mm

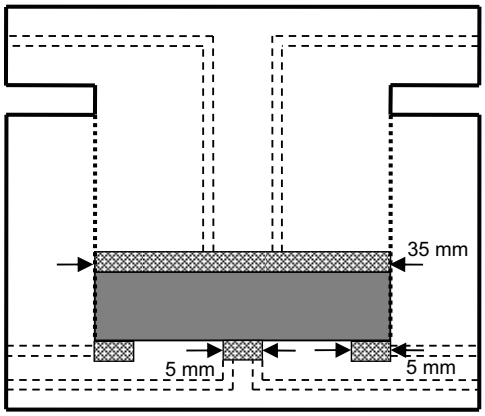

Figure 4-14. *Schematic illustration of filter injection geometry type C.*

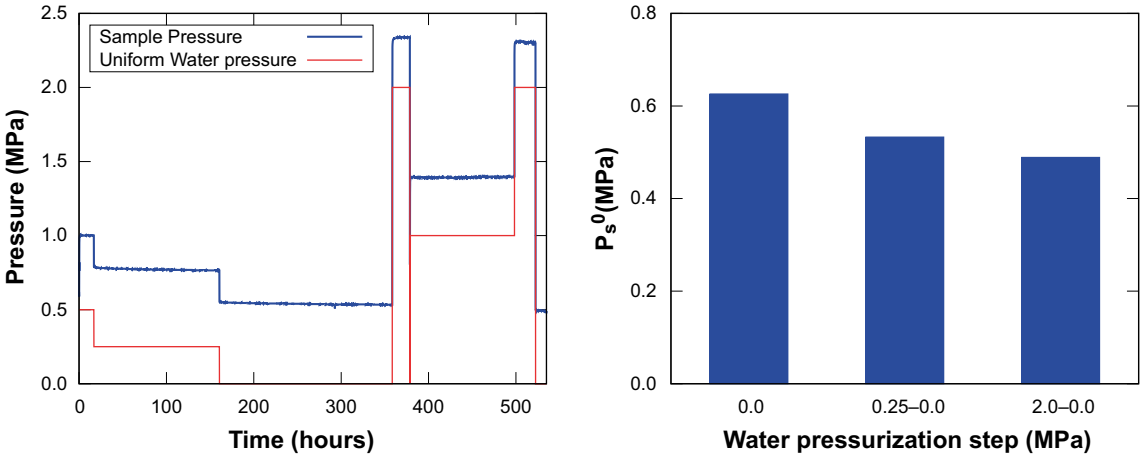

Figure 4-15. *Left: External water (red) and sample (blue) pressure history in sample PrefPath01. Right:Sample pressure after returning to zero water pressure (P_s^0) after each pressurization pulse.*

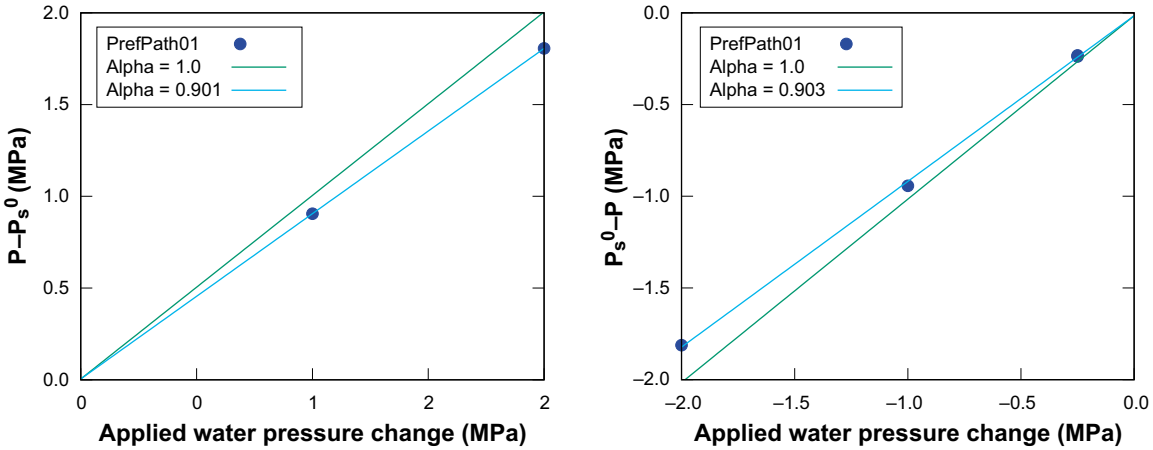

Figure 4-16. *Regression analysis performed on sample pressure response data of sample PrefPath01.*

4.2.2 MX-80 Bentonite

4.2.2.1 GenCh11

This sample was exposed to six pressure pulses: two of magnitude 0.2 MPa, two of 0.5 MPa, and two of 1.0 MPa. The pressurization history and P_s^0-values are shown in Figure 4-17. P_s^0 shows negligible hysteresis, which contrasts the behavior observed in the other MX-80 bentonite systems tested (Section 4.1.1). It should be noticed, however, that the present sample had been tested for response due to both water pressure and gas pressure differences prior to the uniform pressurization tests presented here; when exposed to water pressure differences, substantial hysteresis was observed also in this sample (Section 2.2.2.1).

Figure 4-18 shows the α-factor evaluation, which gave lower values (0.85–0.88) as compared to the same material and similar density in a different pressurization geometry (4.1.1). As the major difference between the present sample and the previous MX-80 samples is injection geometry, it may be speculated that the evaluated α-factor has a geometry dependent component.

Table 4-7. Properties of sample GenCh11.

Material	Nominal density	Post-analysis	Cell type	h
MX-80	ρ_{dry} = 1,179 kg/m^3 ϕ = 0.571	ρ_{dry} = 1,097 kg/m^3 ϕ = 0.601	B	5 mm

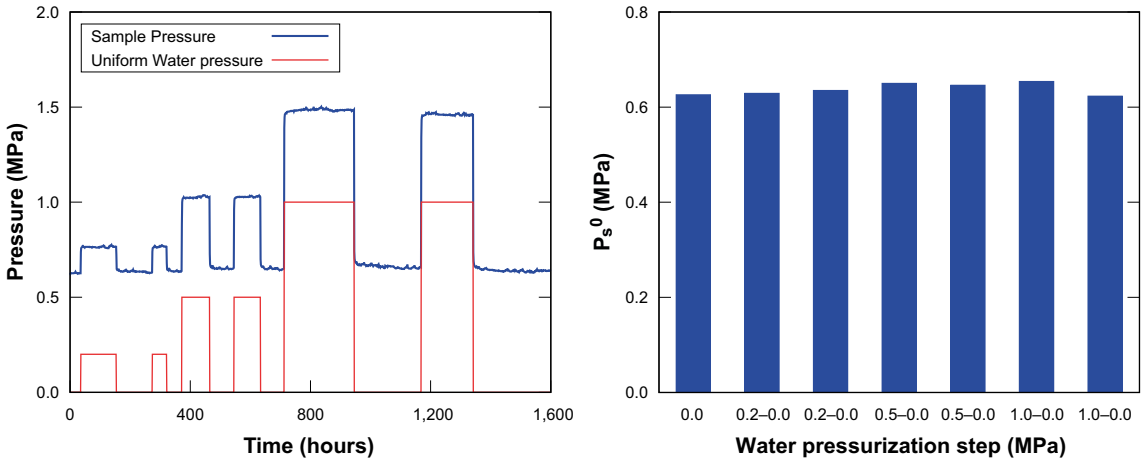

Figure 4-17. *Sample pressure after returning to zero water pressure (P_s^0) after each pressurization pulse GenCh11.*

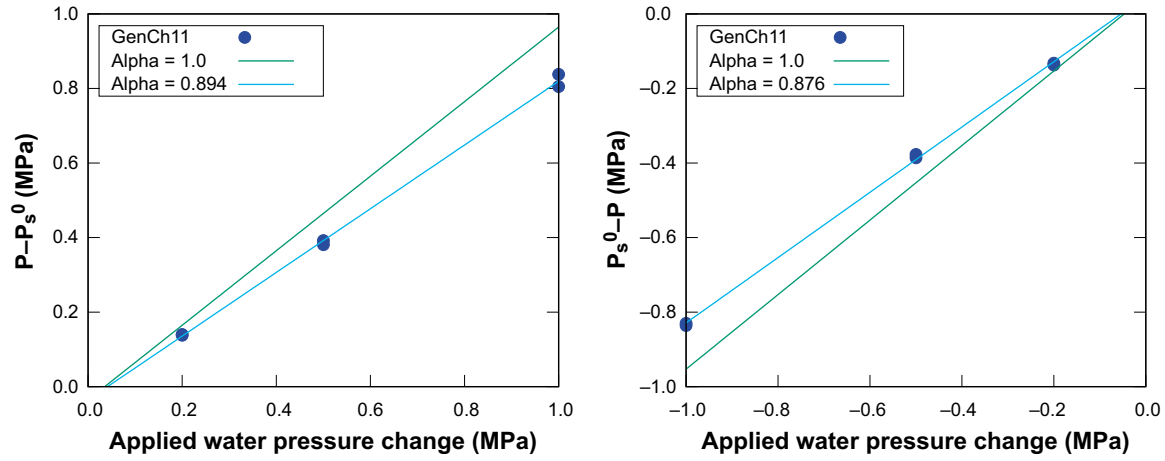

Figure 4-18. *Regression analysis performed on sample pressure response data of sample GenCh11.*

4.3 Summary: uniform water pressurization

The following list summarizes the observed behavior of bentonite/montmorillonite samples exposed to uniform water pressurization.

- Hysteresis in P_s^0.
  - The trend is that P_s^0 increases after exposing samples to pressure pulses (unless mass loss occur). The same trend was seen in some samples exposed to water pressure differences (Chapter 2).
  - After a certain amount of pressure pulses, P_s^0 appear to stabilize. It is however difficult to judge whether "enough" pressure pules has been applied – the path toward a stable P_s^0 can be quite erratic.
  - The hysteresis seems to be larger in MX-80 bentonite samples, as compared to pure montmorillonite. The behavior may therefore be coupled to the presence of accessory minerals.
  - In the sample which was volume expanded (GenCh23), P_s^0 is particularly low just after each expansion.
- α-factor less than unity.
  - In all samples, the observed change in sample pressure was always lower than the change in externally applied water pressure. Measured α-factors was in the range 0.81–0.97.
  - The amount of data is too small to fully evaluate what influences the value of the α-factors, but indicates that it may depend on sample pressure (P_s^0), material (natural bentonite or purified montmorillonite), sample size, pressurization geometry (filter types A or B), as well as on the pressurization history of the sample.

5 External kerosene pressure difference

These tests use the same set-up as the air pressure gradient tests (Chapter 3), with the difference that the air phase is replaced by kerosene in the injection reservoir. Thus, initially the injection reservoir contains water/kerosene/water (compare Figure 3-3), and as the water at the front is pushed through, a kerosene/clay interface is established. Kerosene pressurization testing was only performed on one single sample.

5.1 Injection filter A

5.1.1 MX-80 Bentonite

5.1.1.1 WP3Bench

The pressurization protocol and corresponding sample pressure response of sample WP3Bench is shown in Figure 5-2. Initially, a P_s^0 of 0.58 MPa was measured before an injection pressure of 0.5 MPa was applied. The sample pressure responded by a substantial increase, indicative for pressurization by the residual water at the interface to the clay (5 h). However, as this water flowed through the sample and was replaced in the injection filter by kerosene, the sample pressure dropped back to P_s^0 (25 h – 50 h). This type of pressure response is identical to what has been observed in many samples when air is replacing water at injection pressures below P_s^0 (Section 3.1).

At 144 h, a quick ramping of the injection pressure up to 0.8 MPa was initiated, at a rate of 0.129 MPa/h. This state was then maintained for 53 hours before a kerosene breakthrough event occurred (199 h). In this event, a large kerosene flow was induced through the sample and the reservoir was emptied within an hour. As soon as water from the pressure controlling unit reached the interface, as the kerosene had flowed through, the breakthrough event ceased and the sample pressure response resembled that due to water pressurization. This behavior is also identical to what has been observed in many gas breakthrough events.

Table 5-1. Properties of sample WP3Bench.

Material	Nominal density	Post-analysis	Cell type	h
MX-80	ρ_{dry} = 1,170 kg/m^3 ϕ = 0.575	ρ_{dry} = 1,075 kg/m^3 ϕ = 0.609	A	5 mm

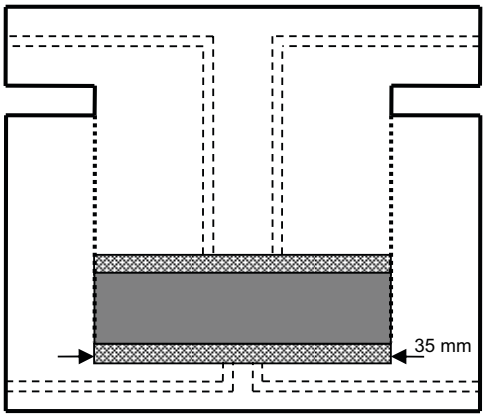

Figure 5-1. *Schematic illustration of filter injection geometry type A.*

At 218 h, the system was refilled with kerosene and the injection pressure was again set to 0.5 MPa. A response in sample pressure, basically identical to the previous 0.5 MPa-pressurization, was observed, with a drop to P_s^0 as the residual water flowed through (218 h – 255 h). This time the state was maintained, without kerosene breakthrough events, for about 200 hours (255 h – 455 h).

The corresponding outflow as a function of time under this pressurization is displayed in the right diagram in Figure 5-2. Initially, when the pressurizing fluid is water, the outflow corresponds to typical hydraulic conductivity of the sample (~ $5 \cdot 10^{-13}$ m/s). As kerosene is replacing the water, however, the flow basically vanishes. This is in contrast to the flow response when air is replacing water, in which case a diffusive flow of dissolved gas is maintained when the residual water has flowed through (Section 3.1.3.1, see specifically Figure 3-13).

Thus, because kerosene is not to any detectable extent soluble in the bentonite, bentonite is completely impermeable for this fluid in states where injection pressure is below P_s^0. Consequently, the only mechanism by which kerosene may be transferred through the clay sample is by induced breakthrough events (for which the injection pressure necessarily is above P_s^0).

The resemblance in response when pressurizing with air and with kerosene demonstrates that it is water pressurization which gives a "special" pressure response in bentonite – any non-polar or weakly polar fluid is expected to give the same type of response as has been demonstrated with air and kerosene (i.e. no mechanical interaction with bentonite at pressures below initial sample pressure).

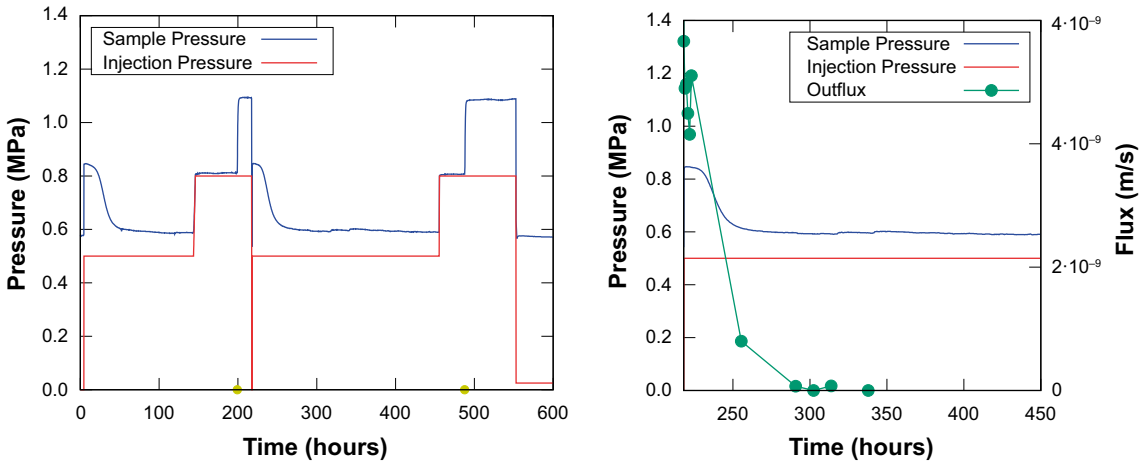

Figure 5-2. *Kerosene injection (red) and sample (blue) pressure history in sample WP3Bench. The right diagram shows a magnification of the period 218–450 h. In this diagram is also plotted corresponding evolution of the volumetric outflow. The yellow dots on the time line indicates breakthrough events. Note that some residual water is the pressurizing fluid at the beginning of the testing, as well as after the injection reservoir was replenished with kerosene (218 h).*

6 Conclusions

For convenience, the conclusions made at the end of each of Chapters 2, 3 and 4 are repeated here.

6.1 External water pressure difference

The following list summarizes the observed behavior of bentonite/montmorillonite samples exposed to external water pressure differences.

- Non-linear response in sample pressure.
  - Using injection filter of type gives a typical sample pressure increase of half the applied injection pressure, when the applied injection pressure is low compared to P_s^0. Using injection filter of type B, the sample pressure response is negligible in the same pressure regime.
  - At injection pressures substantially larger than P_s^0, the sample pressure increase typically equals the increase in injection pressure in both types of injection geometries.
  - In some cases where injection filter type B were used, states could be maintained where the injection pressure was substantially higher than the sample pressure. This was not the case for injection using filter type A.
- Non-linear response in water flow.
  - For filter type A, Darcy's law hold up to applied water pressure of approximately two times P_s^0 (i.e. a linear dependence between steady-state flow and applied water pressure). At higher pressures the flow increase is weaker than linear.
  - In geometry B, the flow response is negligible at low injection pressures (in comparison with P_s^0). At higher pressures (in the samples which can maintain them), the flow increase with increasing injection pressure is stronger than linear.
  - In the samples with guard filters (type C), it can be concluded that this type of flow mainly occurs through top filter.
- Water breakthrough events.
  - Events were induced in several samples, where the system seems to "break". During these events, the flow completely changes characteristics as compared to "normal" flow; in particular the flow rates increase tremendously (a factor 10^4 or more).
  - The events only occur when injection pressure exceeds sample pressure. States have also been maintained, however, with injection pressures significantly larger than sample pressure without induced breakthrough events.
  - In many cases the flow during these events follows the interface between sample holder and clay, in contrast to the "normal" flow which goes through the clay.
  - In the two MX-80 samples tested with point injection (geometry B and C), states with water injection pressures considerably higher than sample pressure could be maintained. In the thinnest sample (2 mm) breakthrough occurred *through* the clay.
  - The process of inducing a breakthrough event has a complex time dependence – by quickly ramping up injection pressure, higher (sample) pressure states could be maintained before breakthrough. Also, in the 2 mm MX-80 sample tested in geometry C, it took 19 hours before the breakthrough occurred after increasing the injection pressure to three times P_s^0.
- Strong density response, i.e. the clay redistributes in an external water pressure gradient, as observed in samples with injection filters of type A.
- Hysteresis in P_s^0.
  - When "coming back" to zero gradient, some of the samples show substantial increase of P_s^0 (up to 60% increase).
- Friction between the clay and the wall of the container was observed in the longer MX-80 samples, which showed lower sample pressure than applied water pressure in geometry A.
- Although the tested samples are small in size, the transient times for the sample pressure response are sometimes long, up to several hundred hours.

6.2 External air pressure difference

The following list summarizes the observed behavior of bentonite/montmorillonite samples exposed to external air pressure differences.

For air pressure below sample pressure:

- There is no response in equilibrium sample pressure when applied gas pressure is below sample pressure.
- In contrast to water pressurization, the (lack of) response due to gas pressure does not depend on injection geometry.
- For applied air pressures below sample pressure, the only transport mechanism is diffusion of dissolved gas.

For air pressure above sample pressure:

- Gas breakthrough events.
  - The flow during a breakthrough event is distinctly different than the diffusive flow. The mechanisms are completely different. At the breakthrough event the flow increases tremendously (a factor 10^4 or more).
  - In many cases the flow path is at the interface between sample holder and clay.
  - In the thinnest samples (2mm) some events occurred *through* the clay.
  - In the looser Na-montmorillonite samples breakthrough occurred when air pressure exceeded sample pressure. States with air injection pressures higher than sample pressure could be maintained in samples with higher density (MX-80 and Ca-montmorillonite).
  - Breakthrough events can be induced either by increasing injection pressure or by lowering sample pressure (e.g. by contacting the sample with a saline solution). The criteria for breakthrough is thus not coupled to a particular pressure (e.g. P_s^0), but is purely mechanical – gas pressure should exceed sample pressure at the point of injection. This behavior directly demonstrates that gas migration in bentonite is not a two-phase flow phenomena, i.e. it is not associated with capillarity.
  - Tailing water from the pressurization unit always followed the air in the less dense Na-montmorillonite samples. In the MX-80 and Ca-montmorillonite samples this was not always the case – sometimes the system shut close when the water reached the clay interface. There are, however, strong similarities between gas and water breakthrough events.
  - The process(es) has a complex time dependence. With fast ramping rather high sample pressures can be achieved. Also transient times on the order of hundred hours were observed.
  - In a few cases, breakthrough events was induced at injection pressures significantly below sample pressure. These events should, however, be viewed as special cases: either the sample height was comparable to the size of the largest accessory mineral grains in the bentonite (sample PrefPath02), or the sample had been preconditioned by extreme water pressurization prior to gas testing (sample GenCh11). It should also be kept in mind that what is here referred to as sample pressure is the average axial stress measured on the top of each sample, while gas is always injected in the bottom.
- Consolidation by gas phase.
  - In some samples states could be maintained where injection pressure exceed the initial sample pressure without inducing gas breakthrough. In these states, sample pressure do respond to the applied air pressure: in some cases sample pressure basically equaled injection pressure, while in others injection pressure could exceed sample pressure quite extensively. This type of behavior is interpreted as consolidation of the clay body (i.e. volume reduction by release of water). In one specific case, consolidation was also confirmed visually.

6.3 Uniform water pressurization

The following list summarizes the observed behavior of bentonite/montmorillonite samples exposed to uniform water pressurization.

- Hysteresis in P_s^0.
  - The trend is that P_s^0 increases after exposing samples to pressure pulses (unless mass loss occur). The same trend was seen in some samples exposed to water pressure differences (Chapter 2).
  - After a certain amount of pressure pulses, P_s^0 appear to stabilize. It is however difficult to judge whether "enough" pressure pules has been applied – the path toward a stable P_s^0 can be quite erratic.
  - The hysteresis seems to be larger in MX-80 bentonite samples, as compared to pure montmorillonite. The behavior may therefore be coupled to the presence of accessory minerals.
  - In the sample which was volume expanded (GenCh23), P_s^0 is particularly low just after each expansion.
- α-factor less than unity.
  - In all samples, the observed change in sample pressure was always lower than the change in externally applied water pressure. Measured α-factors was in the range 0.81–0.97.
  - The amount of data is too small to fully evaluate what influences the value of the α-factors, but indicates that it may depend on sample pressure (P_s^0), material (natural bentonite or purified montmorillonite), sample size, pressurization geometry (filter types A or B), as well as on the pressurization history of the sample.

References

SKB's (Svensk Kärnbränslehantering AB) publications can be found at www.skb.se/publications.

Birgersson M, Börgesson L, Hedström M, Karnland O, Nilsson U, 2009. Bentonite erosion. Final report. SKB TR-09-34, Svensk Kärnbränslehantering AB.

Dueck A, 2004. Hydro-mechanical properties of a water unsaturated sodium bentonite. Laboratory study and theoretical interpretation. PhD thesis. Division of Soil Mechanics and Foundation Engineering, Lund Institute of Technology, Sweden.

Harrington J F, Horseman S T, 2003. Gas migration in KBS-3 buffer bentonite. Sensitivity of test parameters to experimental boundary conditions. SKB TR-03-02, Svensk Kärnbränslehantering AB.

Jacops E, Wouters K, Volckaert G, Moors H, Maes N, Bruggeman C, Swennen R, Littke R J, 2015. Measuring the effective diffusion coefficient of dissolved hydrogen in saturated Boom Clay. Applied Geochemistry 61, 175–184.

Karnland O, Olsson S, Nilsson U, 2006. Mineralogy and sealing properties of various bentonites and smectite-rich clay material. SKB TR-06-30, Svensk Kärnbränslehantering AB.

Sander R, 1999. Compilation of Henry's law constants for inorganic and organic species of potential importance in environmental chemistry. Version 3. Available at: http://www.henrys-law.org/henry-3.0.pdf

SKB, 2011. Long-term safety for the final repository for spent nuclear fuel at Forsmark. Main report of the SR-Site project. SKB TR-11-01, Svensk Kärnbränslehantering AB.